Aus dem Biomedizinischen Centrum

Institut der Ludwig-Maximilians-Universität München

Vorstand: Prof. Dr. Andreas Ladurner

Cryptochromes recruit to laser-induced DNA damage sites through PARP1 activity and promote repair

Dissertation
zum Erwerb des Doktorgrades der Naturwissenschaften
an der Medizinischen Fakultät der
Ludwig-Maximilians-Universität München

vorgelegt von

Tia Tyrsett Kuo

aus

Deinze, Belgien

2023

Mit Genehmigung der Medizinischen Fakultät
der Universität München

Betreuer:	Prof. Dr. Andreas Ladurner
Zweitgutachterin:	PD Dr. Anna Friedl
Dekan:	Prof. Dr. med. Thomas Gudermann
Tag der mündlichen Prüfung:	06. März 2023

Table of content

Table of content 3
Zusammenfassung (Deutsch): 5
Abstract (English): 6
List of figures 7
List of abbreviations 8
1. Introduction 9
1.1 DDR deregulation is a hallmark of cancer 9
1.1.1 The DDR machinery maintains genome integrity 9
1.1.2 DDR is a stepwise event of checkpoint activation, repair, and recovery 10
1.1.3 PARP1-mediated PARylation dynamically regulates DDR 11
1.1.4 DDR factors are current targets for cancer treatment 12
1.2 CRYs are integral components of the molecular clock 13
1.2.1 CRYs share a common evolutionary origin with DNA photolyases 13
1.2.2 CRYs drive oscillatory gene expression through transcription repression 14
1.3 CRYs regulate DDR in *cis* and *trans* 15
1.3.1 CRYs modulate nucleotide excision repair 15
1.3.2 CRY1 regulates DSB repair 16
1.3.3 CRYs interact with DDR factors 16
1.4 Aim of project 17
2. Material and Methods 19
2.1 Cell culture and drug treatments 19
2.1.1 Cell culture 19
2.1.2 Stable cell line generation 19
2.1.3 Drug treatment 19
2.2 Transfection 20
2.2.1 Construct generation 20
2.2.2 Construct and RNA transfection 21
2.3 Biochemical assays 21
2.3.1 Immunoprecipitation 21
2.3.2 Immunoblot 22
2.4 Fluorescence microscopy 23
2.4.1 Live cell imaging 23
2.4.2 Immunofluorescence 23
2.4.2.1 6-4PP staining 23
2.4.2.2 CPD staining 24
2.4.2.3 RNA-Recovery Synthesis assay 24
2.4.2.4 gH2AX, RAD51 and 53BP1 staining 24
2.4.2.5 Fluorescence imaging 24
2.5 Cell based assays 25

2.5.1 Clonogenic assay 25
2.5.2 G2/M checkpoint assay 25
2.5.3 Repair reporter assay 25
2.6 Statistical analyses 26
3. Results 27
3.1 Human CRYs recruit to DNA damage sites 27
3.1.1 Human CRY proteins recruit to laser-induced DNA damage sites 27
3.1.2 CRY recruitment is damage-dependent and enhanced upon stabilization 28
3.1.3 CRY1 colocalizes with γH2AX at DNA breaks 30
3.1.4 The DNA photolyase domain is sufficient for CRY2 recruitment 31
3.2 PARP1 activity is essential for CRY recruitment 33
3.2.1 Pan PARP inhibition abolishes CRY recruitment 33
3.2.2 PARP1 is the key player in CRY recruitment 34
3.3 CRYs modulate DNA strand break repair 36
3.3.1 CRYs regulate IR-induced G2/M checkpoint and gH2AX levels 36
3.3.2 CRY1 promotes homologous recombination 39
3.3.3 CRYs suppress end-joining repair 42
3.4 CRY1 modulates cancer cell survival 46
3.4.1 CRY1 modulates cell survival in response to DSB-induction 46
3.4.2 CRY1 regulates cell survival in response to UV in a cell type specific manner 47
3.4.3 CRY1 regulates UV-Induced transcription recovery 48
4. Discussion 52
4.1 PARP1-mediated PARylation recruits CRYs to damage sites 52
4.2 CRY regulates DSB repair 53
4.3 Potential function of the PARP1/CRY axis in DSB repair 55
4.4 CRY1 may regulate 6-4PP repair 55
4.5 Potential function of the PARP1/CRY axis in NER 56
5. Outlook 58
References 59
Apendix A: 69
Acknowledgements 71
Affidavit 72
Curriculum vitae **Error! Bookmark not defined.**
List of publications 73

Zusammenfassung (Deutsch):

Säugetier-Cryptochrom-Proteine (CRYs) sind Schlüsselkomponenten der circadianen Uhr. Sie sind aus bakteriellen Photolyasen hervorgegangen, Enzymen, die durch UV-Licht verursachte DNA-Schäden reparieren, bei Säugetieren diese Aktivität jedoch verloren zu haben scheinen. Neuere Hinweise deuten darauf hin, dass CRYs eine wichtige Rolle bei der Tumorentstehung und der Reparatur von DNA-Schäden spielen, aber eine direkte Funktion an DNA-Schadensstellen hat sich als schwer fassbar erwiesen. Hier berichte ich, dass CRYs sich durch PARP1-Aktivität schnell an laserinduzierte DNA-Schäden rekrutieren und synchron mit dem PARP1-Enzym auftreten. Konsistent kontrollieren therapeutische PARP- und PARG-Inhibitoren die Assoziation von CRY-Proteinen mit DNA-Schädigungsstellen. Darüber hinaus reguliert CRY1 die Wahl zwischen zwei wichtigen DSB-Reparaturwegen, indem es gleichzeitig die homologe Rekombination mit hoher Genauigkeit fördert und die fehleranfällige nicht homologe Endverbindung unterdrückt. CRY2 hingegen reguliert die Unterwege der DSB-Reparatur, indem es das Glühen einzelner Stränge stimuliert und das Verbinden alternativer Enden unterdrückt. Interessanterweise verleiht die CRY-Aufhebung keine Empfindlichkeit in Osteosarkomzellen, die mit DNA-Schädigungen induzierenden Mitteln behandelt wurden, was darauf hindeutet, dass CRYs DDR und das Zellüberleben unabhängig voneinander regulieren. Darüber hinaus zeigen CRY1-depletierte Zellen nach zellulärer UV-Exposition eine Verzögerung bei der 6-4PP-Reparatur und Transkriptionserholung. Zusammenfassend implizieren meine Daten die durch DNA-Schädigung induzierte PARP1-Aktivität (PARylation) als kritischen Regulator der schnellen und direkten Rekrutierung menschlicher CRY-Proteine an DNA-Schadensstellen und präsentieren CRYs als Mediatoren therapeutisch relevanter DNA-Schadensreaktionen.

Abstract (English):

Mammalian cryptochrome proteins (CRYs) are key components of the circadian clock. They evolved from bacterial photolyases, enzymes that repair DNA damage caused by UV light, but appear to have lost this activity in mammals. Emerging evidence indicates that CRYs play important roles in tumorigenesis and DNA damage repair, but a direct function at DNA damage sites has proved elusive. Here, I report that CRYs rapidly recruit to laser-induced DNA damage sites through PARP1 activity and occur synchronously with the PARP1 enzyme. Consistently, therapeutic PARP and PARG inhibitors control the association of CRY proteins with DNA damage sites. In addition, CRY1 regulates the choice between two major DSB repair pathways by simultaneously promoting high fidelity homologous recombination and suppressing error-prone non homologous end joining. CRY2, on the other hand, regulates DSB repair sub pathways by stimulating single strand annealing and repressing alternative end joining. Intriguingly, CRY abrogation does not confer sensitivity in osteosarcoma cells treated with DNA damage-inducing agents suggesting CRYs regulate DDR and cell survival independently. Moreover, after cellular exposure to UV, CRY1 depleted cells exhibit a delay in 6-4PP repair and transcription recovery. In summary, my data implicates DNA-damage induced PARP1 activity (PARylation) as the critical regulator of the rapid and direct recruitment of human CRY proteins to DNA damage sites and presents CRYs as mediators of therapeutically relevant DNA damage responses.

List of figures

Figure 1. The DDR machinery maintains genome integrity. 10

Figure 2. The PIKK and PARP family members regulate DDR. 11

Figure 3. Mammalian CRYs are highly similar to Drosophila (6-4)photolyases. 14

Figure 4. CRYs drive oscillatory gene expression through transcription repression. 15

Figure 5. CRYs interact with DDR factors. 17

Figure 6. Human CRY proteins recruit to laser-induced DNA damage sites. 28

Figure 7. CRY recruitment is damage-dependent and enhanced upon stabilization. 29

Figure 8. CRY1 colocalizes with γH2AX at DNA breaks. 31

Figure 9. The DNA photolyase domain is sufficient for CRY2 recruitment. 32

Figure 10. Pan PARP inhibition abolishes CRY recruitment. 34

Figure 11. PARP1 is the key player in CRY recruitment. 36

Figure 12. CRYs regulate the G2/M checkpoint. 37

Figure 13. CRYs modulate IR-induced γH2AX levels. 38

Figure 14. CRYs promote homologous recombination. 40

Figure 15. PARP activity does not affect HR. 41

Figure 16. CRYs modulate IR-induced RAD51 levels. 42

Figure 17. CRYs suppress end-joining repair. 43

Figure 18. PARP activity controls end-joining repair. 44

Figure 19. CRYs modulate IR-induced 53BP1 levels. 45

Figure 20. CRY1 modulates cell survival in response to DSB-induction. 46

Figure 21. CRY1 modulates cell survival in response to UV treatment. 47

Figure 22. CRY1 regulates cell survival in response to UV treatment in a cell type dependent manner. 48

Figure 23. CRY1 regulates 6-4PP repair rate. 50

Figure 24. CRY1 regulates UV/NER-induced transcription recovery. 51

List of abbreviations

Cryptochrome 1	CRY1
Cryptochrome 2	CRY2
DNA photolyase	DP
Photolyase homology region	PHR
Coiled-coiled extension	CCE
DNA damage response and repair	DDR
Laser induced damage	LID
Poly (ADP-ribose) polymerase	PARP
Cyclobutane pyrimidine dimer	CPD
6-4 photo product	6-4PP
Nucleotide excision repair	NER
Global genome nucleotide excision repair	GG-NER
Transcription coupled nucleotide excision repair	TC-NER
Phosphatidylinositol 3-kinase protein kinase-like	PIKK
Ataxia telangiectasia and Rad3 related	ATR
Ataxia telangiectasia mutated	ATM
DNA-dependent protein kinase	DNAPK
Homologous recombination	HR
End joining	EJ
Homology directed repair	HDR
Single strand annealing	SSA
Non homologous end joining	NHEJ
Alternative end joining	Alt-EJ
Base excision repair	BER
Single strand break	SSB
Double strand break	DSB

1. Introduction

1.1 DDR deregulation is a hallmark of cancer

1.1.1 The DDR machinery maintains genome integrity

Homeostasis of an organism at the cellular level requires an extensive repertoire of signaling modules to translate and respond to a diverse range of cellular stresses. One such stress, insult to genome integrity, triggers a robust signaling cascade that induces temporal cell cycle arrest (also known as checkpoint control) and repair (Her and Bunting, 2018). However, when damage is excessive, cells either enter permanent cell cycle arrest i.e., senescence or activate programmed cell death i.e., apoptosis to prevent propagation of potentially transformative mutations (Figure 1). To maintain genome integrity, eukaryotic cells have adapted highly conserved and specialized DNA damage response and repair (DDR) pathways to sense and repair a wide range of DNA lesions induced by various sources e.g., ultraviolet (UV) and reactive oxygen species.

Targeting the DDR machinery through IR and antineoplastic agents has been the mainstay of cancer treatment for decades. The general aim is to inflict excessive damage in highly proliferative populations and as a result drive these populations into senescence or cell death. However, in cancer, the integrity of DDR is often compromised through aberrant expression and/or mutations in DDR genes allowing cancer cells to evade such controls (Huang and Zhou, 2021). One example is the tumor suppressor- TP53. TP53 is the master regulator of cell cycle arrest and cell death during the events of DDR and is found to be one of the most mutated genes either through the loss of wildtype function or gain of oncogenic properties in cancer (Muller and Vousden, 2013). As a matter of course, the continuous effort in understanding DDR in cancer has become imperative in advancing cancer treatment.

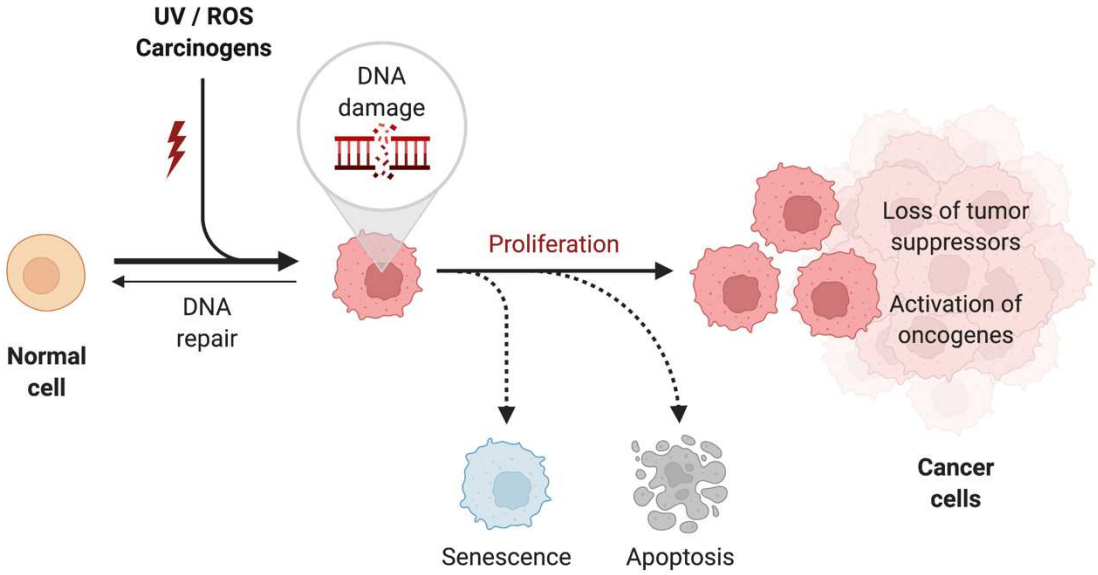

Figure 1. The DDR machinery maintains genome integrity.

When a normal cell is exposed to hazardous carcinogens such as UV and ROS, the cell undergoes temporal cell cycle arrest and executes DNA repair. If DDR is compromised or damage persists, cells either enter senescence or activate apoptosis to prevent propagation of potentially transformative mutations. These mutations include loss of tumor suppressors and/or activation of oncogene expression thereby promoting tumorigenesis. Created with BioRender.com.

1.1.2 DDR is a stepwise event of checkpoint activation, repair, and recovery

While the choice between DDR pathways largely depends on the type of lesion and cell cycle stage, the sequence of events, in general, can be simplified into damage sensing, checkpoint activation, lesion repair followed by recovery and the release from cell cycle arrest. Each step is tightly controlled by the timely recruitment and activation of specific proteins and is mainly regulated by members of the PIKK and PARP families (D'Amours et al., 1999; Yang et al., 2003) (Figure 2).

When damage is present, the PIKK family members ATM, ATR or DNA-PK induce a rapid phosphorylation of the histone variant- H2AX (γ-H2AX) in the proximity of a strand break (Ma et al., 2010). γ-H2AX is a primary event in DBR and is known to form foci to sequester downstream components such as 53BP1 and RAD51 to DNA lesions (Paull et al., 2000; Celeste et al., 2003). While ATR, ATM and DNA-PK of the PIKK family are activated through other sensors e.g., MRN (Lee et al., 2005; Haahr et al., 2016; Chan et al., 2002), PARP1 and PARP2 of the PARP family are activated directly by DNA lesions (Martin-Hernandez et.al., 2016). In parallel to repair induction, the PIKK family regulates checkpoint control by phosphorylating target proteins such as the CHK proteins and TP53 (Bartek and Lukas, 2001). PARPs, on the other hand, catalyze the formation of poly(ADPribose) chains and branches using NAD^+ as substrate in the presence of ssDNA (Matta et al., 2020). PARP1 mediated PARylation is known to not only recruit repair factors but also chromatin remodelers and is important for various DDR pathways such as BER, SSB repair, DSB repair (NHEJ, alt-EJ and HR) as well as GG-NER (Patel et al., 2011; Pines et al., 2012; Reynolds et al., 2015; Xie et al., 2015). Once repair is completed, DDR signaling decreases thereby allowing cells to progress through the cell cycle error-free.

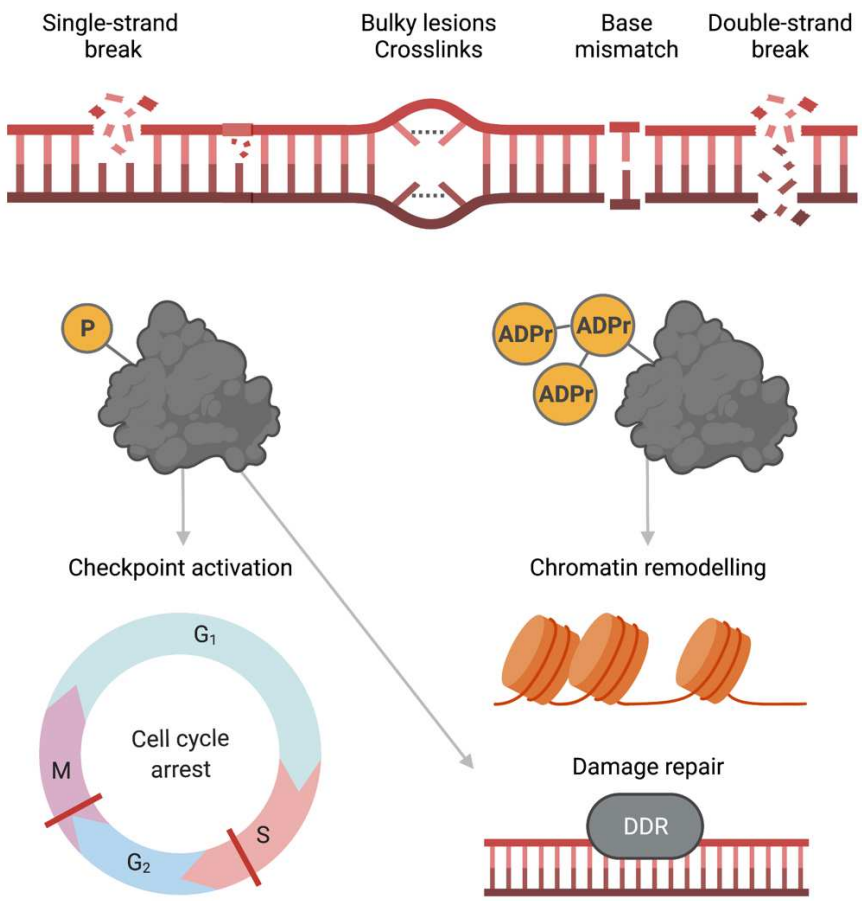

Figure 2. The PIKK and PARP family members regulate DDR.

Various types of DNA damage such as single-strand breaks, bulky lesions, crosslinks, base mismatch, and double-strand breaks trigger a robust signaling cascade through phosphorylation as well as PARylation. These two pivotal post translational modifications have distinct and overlapping functions. Phosphorylation by the PIKK members induces cell cycle arrest and DNA repair, while PARylation by the PARP members induces chromatin remodeling and repair. Created with BioRender.com.

1.1.3 PARP1-mediated PARylation dynamically regulates DDR

PARP1, as previously described, is a major sensor for DNA damage (Kraus, 2015). When damage is present, PARP1 rapidly produces long, branched PAR chains (Wallrodt et al., 2016) and recruits multiple proteins to DNA damage sites (Chaudhuri and Nussenweig, 2017). PARP1 activation and its activity is driven by conformational changes (Eustermann et al., 2015; Dawicki-McKenna et al., 2015) induced by damage recognition and DNA binding by the N-terminal zinc fingers (Ali et al., 2012; Langelier and Pascal, 2013). Once activated, PARP1 modifies a wide and diverse range of proteins (Jungmichel et al., 2013).

PARylation is a dynamic and reversible post-translational modification that adds ADP-ribose onto a variety of substrates. This modification can alter a substrate's chemical property, structure and

ultimately its function. Hundreds of proteins have been identified to recognize distinct features within the PAR polymer. Proteins that recognize and respond to PARylation (Till and Ladurner 2009; Teloni and Altmeyer, 2016) are grouped according to PAR-binding motifs which includes PAR-binding zinc finger, macrodomain, WWE, BRCT, forkhead-associated, OB-fold, PIN, and the RNA recognition motif domain (Zaja et al., 2012).

PAR-binding motifs consist of a sequence of c.a. 20 amino acids enriched in hydrophobic amino acids spaced by basic residues (Pleschke et al., 2000). A computational and proteomic analysis identified c.a. 1,000 proteins containing this motif including proteins involved in DNA replication, repair, and RNA-processing (Gagne et al., 2008). Astonishingly, hundreds of proteins recruit to laser-induced DNA damage sites in a PARP/PAR-dependent manner (Izhar et al., 2015; Buntz et al., 2016). Most of these proteins possess a DNA-binding domain and exhibit a relatively slow recruitment kinetics (Izhar et al., 2015), indicating that their recruitment is likely DNA-dependent, rather than PAR-dependent. The most plausible mechanism by which these DNA-binding proteins recruit is through chromatin decompaction induced by PARP1/PARylation (Sellou et al., 2016; Luijsterburg et al., 2016). Additionally, recent studies have reported proteins lacking globular PAR-binding modules such as CHD2/4 and METTL3/14 recruit to laser-induced DNA damage sites in a PAR-dependent manner *in cellulo* (Chou et al., 2010; Polo et al., 2010; Smeenk et al., 2010; Luijsterburg et al., 2016; Silva et al., 2016; Xiang et al., 2017; Smith et al., 2018). The precise mechanism of how PARP1 activation recruits these proteins lacking PAR-binding motifs remains unclear.

1.1.4 DDR factors are current targets for cancer treatment

As mentioned previously, failure to make timely and precise repairs can lead to cell death, senescence or transformation through the accumulation of DNA damage, mutations, rearrangements, and/or loss of chromosomes (Her and Bunting, 2018). Individuals harboring defects in DDR genes such as *xeroderma pigmentosum* (XP-) (Daya-Grosjean et al., 2008) or *ataxia telangiectasia* (AT-) (Lavin et al., 2008) are prone to developing tumors. While DDR deficiencies serve as a marker for cancer predisposition, they have also, in the recent decade, revealed themselves as selective vulnerabilities in tumors. Thus, many distinct DDR components now count as promising therapeutic targets (Lord and Ashworth, 2012). One of the most promising targets in recent years is the PARP family. Cumulative pre-clinical studies have shown that the catalytic inhibition of PARP impairs several DDR pathways such as BER, NER as well as NHEJ and has been proven to be exceptionally effective in targeting cancer cell populations defective in HR repair. This approach is termed synthetic lethality and exploits the synergistic effect of the *PARP* and *BRCA* genes on DDR which consequently and negatively impacts cell survival (Lord et al., 2015). However, recent studies have reported resistance towards PARP inhibitor treatment. A comprehensive understanding of PARPs and their precise roles in DDR is therefore critical in the successful implementation of PARP inhibitors in various cancer types (Montoni et al., 2013).

1.2 CRYs are integral components of the molecular clock

1.2.1 CRYs share a common evolutionary origin with DNA photolyases

The mammalian proteins CRY1 and CRY2 are flavoproteins present in all three kingdoms of life and belong to the super family of cryptochromes (also known as blue-light receptors) and photolyases (Müller and Carell, 2009). Photolyases are light-driven photo-repair enzymes which repair UV-induced DNA lesions such as CPDs and 6-4PPs by the use of the cofactor FAD to catalyze the cleavage of covalently-linked pyrimidine dimers (Todo et al., 1997; Mees et al., 2004; Maul et al., 2008). Owing to the strikingly high sequence identity to that of the Drosophila (6-4) photolyase (Todo et al., 1996), attempts were made to investigate whether mammalian CRYs retain similar functions (Hsu et al., 1996; Kobayashi et al., 1998; Ozgur and Sancar, 2003). *In vitro*, CRYs bind to both ssDNA and dsDNA as well as the cofactor FAD. In particular, CRY2 displayed an enhanced DNA binding activity in the presence of 6-4PPs. However, light-driven photo-repair activity was absent for both homologs (Hsu et al., 1996; Kobayashi et al., 1998; Ozgur and Sancar, 2003). Recent structural studies showed that despite adopting the canonical photolyase fold, mammalian CRY PHRs present a more open conformation and possess low affinity towards FAD (Czarna et al., 2013, Xing et al., 2013)(Figure 3). In summary, mammalian CRYs therefore are thought to no longer possess the intrinsic ability to repair UV-induced DNA lesions and have instead diverged and have become transcriptional co-regulators of the molecular clock.

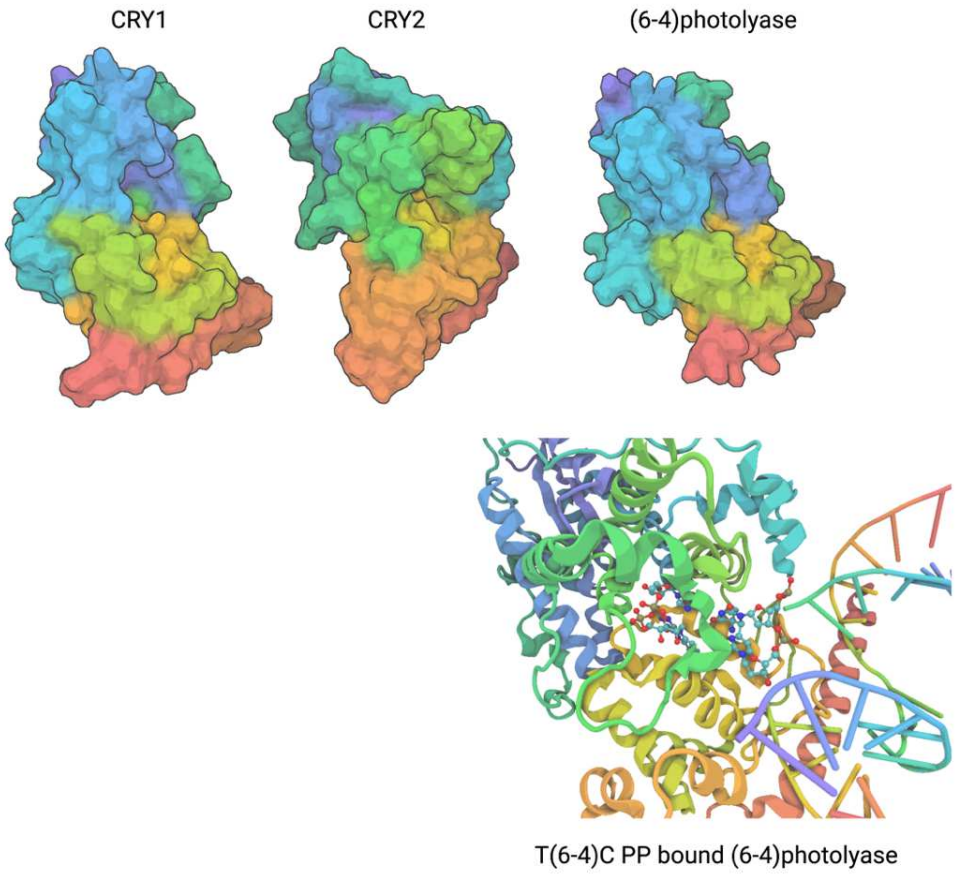

Figure 3. Mammalian CRYs are highly similar to *Drosophila* (6-4)photolyases.

The *Mus Musculus* CRY1 (6KX4), CRY2 (7D0N) and the *Drosophila Melanogaster* (6-4)photolyase (upper: 7AZT, lower: 2WB2) share a common evolutionary origin (Miller et al., 2020; Miller et al., 2021; Cellini et al., 2021; Glas et al., 2009). The mammalian CRYs contain the highly conserved PHR (blue/green/yellow) necessary to bind FAD and repair 6-4PPs. However, mammalian PHR, in comparison to the (6-4)photolyase, presents a much shallow cleft. Solvent-excluded surface. Color coded according to sequence. Created with BioRender.com.

1.2.2 CRYs drive oscillatory gene expression through transcription repression

The molecular clock is a transcription-translational feedback loop (TTFL) driven by the core clock components- CLOCK, BMAL1, CRYs and PERs (Figure 4). These core clock components regulate multiple cellular processes including replication and cell cycle in a time-dependent manner (Koike et al., 2012; Takahashi, 2017). While the transcription activators- CLOCK and BMAL1 are essential for driving oscillation of the molecular clock, the repressors- CRYs and PERs control periodicity. The exact mechanism of how CRYs repress CLOCK/BMAL1 remains unclear. Based on structural analysis, the current theory is that CRYs repress CLOCK/BMAL1 directly on DNA while PERs displace the complex thereby achieving full transcription repression (Ye et al., 2014; Chiou et al., 2016). The two homologs CRY1 and CRY2 have been shown to bind over a

thousand sites in the genome. Intriguingly, despite the high (c.a. 70%) sequence identity, both CRYs were found to bind, in addition to overlapping sites with other core clock components, several thousands of unique loci (Koike et al., 2012). Such a diverse binding profile may be explained by exclusive modifications as well as interactions suggesting that CRY1 and CRY2 play distinctive regulatory roles.

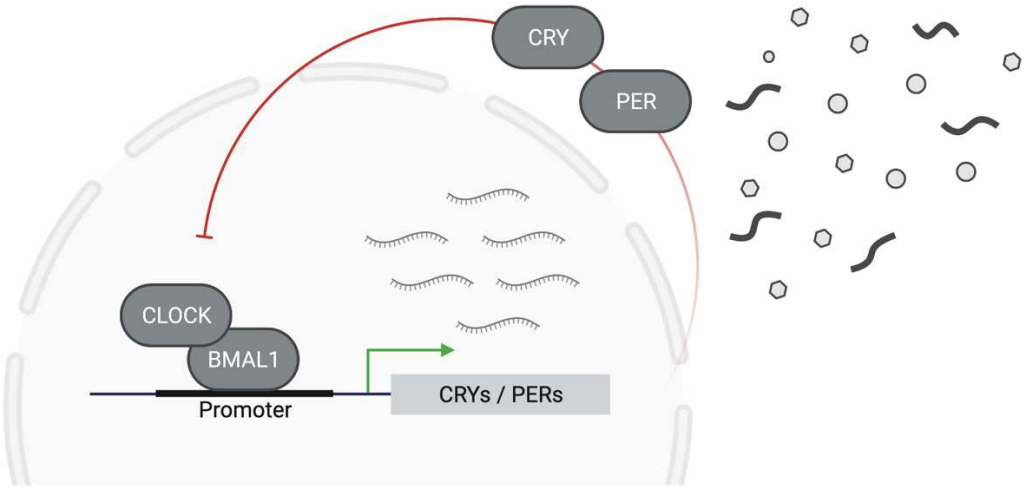

Figure 4. CRYs drive oscillatory gene expression through transcription repression.

The molecular clock is driven by a transcription-translation feedback loop. The transcription activators CLOCK and BMAL1 induce the expression of the transcription repressors CRYs and PERs. CRYs and PERs, in a timely manner, relocate to the nucleus to inhibit CLOCK and BMAL1 thereby forming a c.a. 24-hour feedback loop. This temporal transcription regulation governed by the clock components drives the oscillation of thousands of transcripts and molecules. Created with BioRender.com.

1.3 CRYs regulate DDR in *cis* and *trans*

1.3.1 CRYs modulate nucleotide excision repair

One of the first DDR pathways thought to be gated by the molecular clock is NER. NER is the primary error-free DDR pathway responsible for removing UV-induced as well as platinum-based drug-induced DNA lesions. Indeed, *in vivo*, XPA, one of the rate-limiting factors in NER, displays a circadian oscillation both on a mRNA and protein level (Kang et al., 2009). This circadian regulation of XPA levels and consequently NER capacity was later found to be CRY-dependent (Kang et al., 2010). In concert, the pharmacological inhibition of CRYs led to fewer cisplatin-DNA adducts rendering cells less sensitive towards the treatment (Anabtawi et al., 2021). The role of CRYs in NER, however, extends beyond repair by promoting cancer cell (RAS-transformed TP53-/-) survival through P73 repression in response to UV and oxaliplatin treatment (Ozturk et al., 2009; Lee et al., 2011; Lee et al., 2013). In addition to their roles in repair and cell survival, CRYs

promote cell cycle progression through regulating WEE1 and P21 expression levels (Anabtawi et al., 2021) implying a potential antagonistic role in maintaining genome integrity.

1.3.2 CRY1 regulates DSB repair

While both CRY homologs seem to modulate NER, CRY1 in particular was found to possess an additional regulatory function in DSB repair (Papp et al., 2015; Shafi et al., 2021). Upon DSB-induction by IR, CRY1 is stabilized (Shafi et al., 2021) through de-ubiquitination mediated by USP7 as well as phosphorylation (Papp et al., 2015). Genomic deletion of CRY1 de-represses temporal expression of several pivotal DDR factors such as P21, MDM2, PUMA, RAD51, GADD45a and XRCC1 (Papp et al., 2015). While CRY1 was proposed as a negative regulator of DSB repair (Papp et al., 2015), a later genome-wide study pins CRY1 as a major positive regulator that governs several DDR pathways including MMR, NER, HR, NHEJ and the G2M checkpoint (Shafi et al., 2021). In this study, they showed that CRY1 depletion through shRNA-mediated silencing reduced HR capacity while pharmacological activation of CRY1 enhanced HR through promoting DDR gene expression such as ATM, CHK2, BRCA1/2, RAD51, P21 and many others and is critical for HR-mediated repair at full capacity (Shafi et al., 2021). These contradicting observations can be potentially explained by permanent versus temporary removal of CRY1 and/or normal versus cancerous cell lines. Although a role for CRY2 in DDR was not observed in these studies, CRY2 deficient cells accumulate DSBs (increase 53BP1 foci formation) in the absence of DNA damage-induction (Papp et al., 2015) suggesting CRY2 may play a role in maintaining genome integrity independent of DDBR.

1.3.3 CRYs interact with DDR factors

The speculation of CRYs playing a role apart from transcriptional regulation in DDR continues as CRYs have been identified to interact with several critical DDR factors such as USP7, DDB1, PRKDC, XRCC5, XRCC6 and TIMELESS (Engelen et al., 2013; Papp et al., 2015; Hirano et al., 2016). Based on the known functions of these DDR factors, CRYs may have a more direct function in NER, NHEJ as well as HR (Figure 5). For example, USP7 interacts with UVSSA to promote TC-NER through stabilizing the repair factor- ERCC6 (Schwertman et al., 2013). USP7 has also been reported to regulate MDM2 and TP53 stability thereby impacting TP53-dependent transcription regulation, cell growth repression and apoptosis (Wang et al., 2019). DDB1, on the other hand, is part of the UV-DDB complex which acts as a sensor of UV-induced DNA damage (Fei et al., 2011). Secondly and in the context of DSB repair, PRKDC is the catalytic subunit of DNAPK which phosphorylates target proteins such as TP53, XRCC5 (KU70), XRCC6 (KU80) and H2AX (Yue et al., 2020). PRKDC (DNAPK) recruits to damage sites through the helicases-XRCC5 (KU70) and XRCC6 (KU80) and plays a pivotal role in fostering NHEJ by protecting DNA breaks from further resection (Yue et al., 2020). While TIMELESS, in earlier studies, is described to associate with the replication fork and coordinate the Intra-S checkpoint in response to UV

exposure (Uensal-Kacmaz et al., 2007; Leman et al., 2010), it was later shown to form a stable complex with PARP1 and is crucial for promoting HR (Young et al., 2015; Xie et al, 2015). Whether these CRY interactions bear any biological and/or functional significance in cancer cell survival and DDR remains to be investigated.

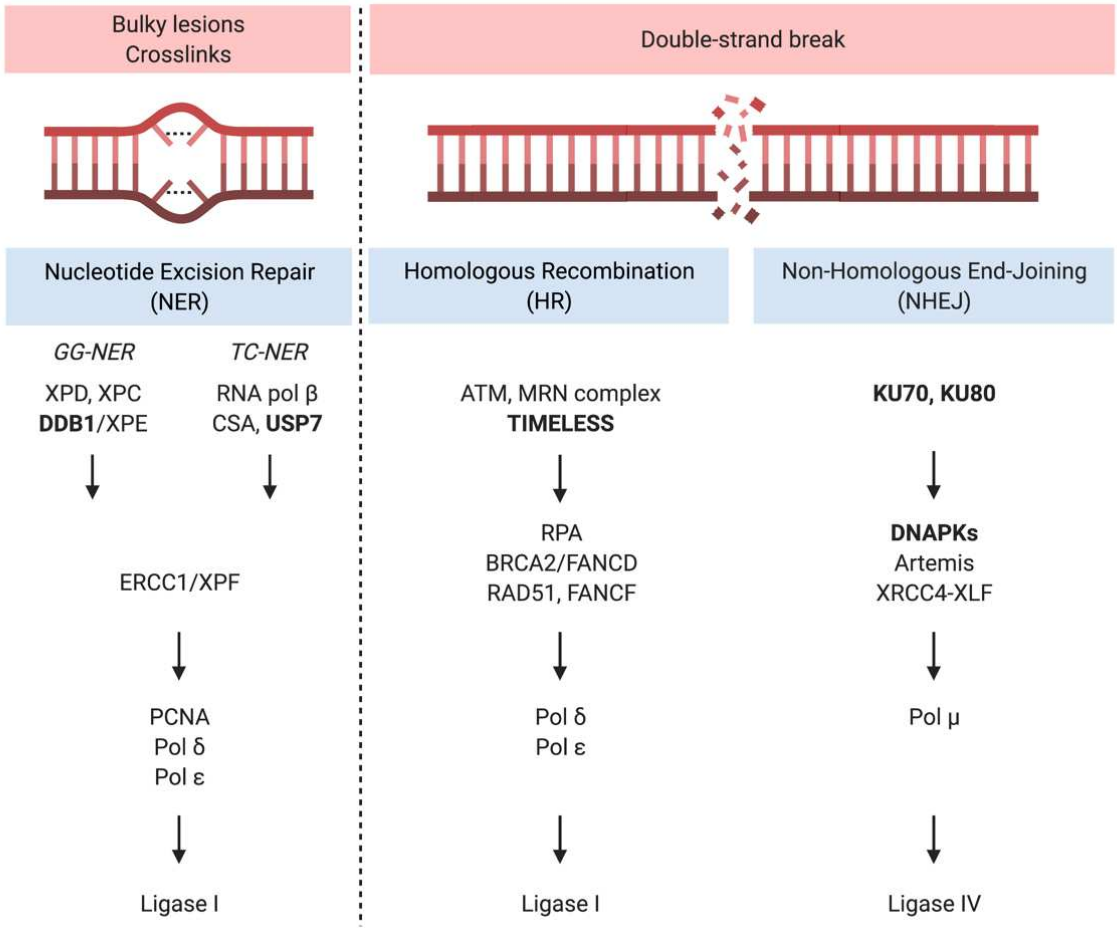

Figure 5. CRYs interact with DDR factors.

CRYs have been identified to interact with several critical DDR factors such as DDB1, USP7, TIMELESS, PRKDC (DNAPK), XRCC5 (KU70), and XRCC6 (KU80). These DDR factors are known to participate and regulate various DDR pathways such as NER of bulky lesions as well as HR and NHEJ repair of double-strand breaks. In addition, these factors are all involved in the initial steps of their respective DDR pathways i.e., damage sensing and signaling. Created with BioRender.com.

1.4 Aim of project

In this study, I sought to investigate the potential role of human CRY proteins in DDR by returning to their primordial function as DNA binding proteins with a preference for damaged DNA. I aim to test this in the context of a chromatinized genome in a living cell using recently published knockin and knockout cell lines, small molecule activators/inhibitors and fluorescence based live cell

imaging. Given the promising success of PARP inhibitors in targeting HR-deficient tumors and emerging evidence linking CRY1 to the regulation of HR, I was inspired to examine CRYs' potential functions using repair reporter cell lines as well as the checkpoint assay with the aim of identifying and dissecting CRYs' more imminent and direct roles in the cellular response to induced DNA damage and their potential impact on DDR-induced cancer cell death.

2. Material and Methods

2.1 Cell culture and drug treatments

2.1.1 Cell culture

U-2 OS and HeLa cell lines purchased from ATCC were maintained in Dulbecco's modified Eagle's medium (Gibco, 31885049X) and HCT-116 cell line in McCoy's medium (Sigma Aldrich, M8403) containing 10% fetal bovine serum (Thermo Fisher Scientific, 10270106) and 1% penicillin/streptomycin (Gibco, 15140122). Cells were passaged at 10% confluence every 5 days for no more than 15 passages. U-2 OS wild-type, ΔCRY1, ΔCRY2 and ΔCRY1/2 were a kind gift from Dr. Achim Kramer and were maintained as described above. U-2 OS wild-type, ΔPARP1, ΔPARP2 and ΔPARP1/2 were a kind gift from Dr. Nicholas Lakin and were maintained as described above. Stable cell lines expressing mEGFP-CRY1, mCherry-CRY2 and PARP1-mCherry clones were maintained in Dulbecco's modified Eagle's medium containing 10% fetal bovine serum, 1% penicillin/streptomycin and 700 µg/mL G-418 (Sigma, A1720-5G). All cell lines were incubated in 5% CO_2 at 37°C.

2.1.2 Stable cell line generation

U-2 OS wild-type cells were seeded at 50% confluency and transfected the next day using the constructs pmEGFP-CRY1, pmCherry-CRY2 and pmCherry-PARP1. 24 hours post transfection, selection medium containing G-418 was added. 24-72 hours post selection, cells were trypsinized and suspended in fluorescence activated cell sorting buffer on ice. Single cells within the top 2% fluorescence signal were sorted into single wells on a 96-well plate and left to recover and expand. Single clones which survived and successfully expanded were seeded into larger well formats for further expansion. After expansion, whole cell lysates were made for each clone for immunoblotting to verify expression.

2.1.3 Drug treatment

Cells were pretreated with inhibitors against ATM (Tocris, 4176), ATR (Tocris, 5198), DNA-PK (Tocris, 3712), PARP (Sellekchem, S1060) and PARG (Sigma, PD00017273) for a duration of 1 hour prior to micro-irradiation and imaging. Cells were pretreated with CRY stabilizer- KL001 (Tocris, 4685) for a duration of 6 hours prior to micro-irradiation and imaging.

2.2 Transfection

2.2.1 Construct generation

CRY1 (cDNA, TCH1003-GVO-TRI, BioCat) along with CRY2 (kind gift from Dr. Eva Wolf) were amplified by PCR and subcloned per manufacturer's instructions using the NEBuilder HiFi DNA assembly cloning kit (NEB, E5520S) into pmEGFP-C1 and pmCherry-N1 respectively using the primers listed below. CRY truncation mutants were generated by inverse PCR using primers listed below. pmCherry-N1-PARP1, pmEGFP-C1-PARP1, pmCherry-N1-PARP1_E988K and pmEGFP-N1-PARP1_E988K were generated as described in Sellou et al., 2016.

Primer	Sequence
CRY1.F	GCTGTACAAGTCCGGAATGGGGGTGAACGCCGTG
CRY1.R	TGGCTGATTATGATCAGCTAATTAGTGCTCTGTCTCTGGACTTTAGG
mEGFP.F	CTGATCATAATCAGCCATACCACATTTGTAG
mEGFP.R	TCCGGACTTGTACAGCTC
CRY2.F	GGACGAGCTGTACAAGTCCGGAATGGCGGCGACTGTGGCG
CRY2.R	CTAGAGTCGCGGCCGTCAGGCATCCTTGCTCGGC
mCherry.F	CGGCCGCGACTCTAGATC
mCherry.R	TCCGGACTTGTACAGCTCGTCCATGC
CRY1_DP.F	TAGCTGATCATAATCAGCCATA
CRY1_DP.R	TAATGTATGTGAAATTCTTACAATGA
**Note: CRY1_DP was cloned from CRY1_DPloop and not CRY1_FL*	
CRY1_DPloop.F	TAGCTGATCATAATCAGCCATA
CRY1_DPloop.R	TAATGTATGTGAAATTCTTACAATG
CRY1_FAD.F	TGGCCAGGCGGAGAA
CRY1_FAD.R	CTGATAGATCTGTTTCATCCTTTCG
CRY1_CE.F	CAGCTTTCACGATATAGAGGACT
CRY1_CE.R	TCCGGACTTGTACAGCTC
CRY2_DP.F	TGACGGCCGCGA
CRY2_DP.R	GGTATGAGAATTCTCCGTC

CRY2_DPloop.F	TGACGGCCGCGA
CRY2_DPloop.R	TCCTCCCTGCCAGAC
CRY2_PHR.F	GGAGAGACAGAAGCTCT
CRY2_PHR.R	CTGATAGATCTGTTTCATCCTTTCG
CRY2_FAD.F	GGAGAGACAGAAGCTCT
CRY2_FAD.R	AAGCTGCTGGTAAATCTG
CRY2_CE.F	CTTTCGCGCTACCG
CRY2_CE.R	TCCGGACTTGTACAGC

2.2.2 Construct and RNA transfection

Construct transfection was performed per manufacturer's instructions using Xfect transfection reagent (Takarobio, 631317). Cells were incubated for 48 hours up until use. siRNA (Thermo Fisher Scientific, please see below for Cat Nº) transfection was performed per manufacturer's instructions with lipofectamine RNAiMAX transfection reagent (Thermo Fisher Scientific, 13778100). Cells were incubated for 48 hours up until use.

siRNA	Catalog Nº
Control (UNC)	AM4611
CRY1 #1	AM16708A/146308
CRY1 #2	AM16708A/146309
CRY2 #1	AM16708A/146763
CRY2 #3	AM16708A/146765
XPA	AM16708A/138727
Artemis	AM16708A/30041

2.3 Biochemical assays

2.3.1 Immunoprecipitation

Routine cell lysis was performed on ice with 50 mM Tris buffer, pH 7.5 containing 250 mM NaCl, 10% glycerol, 0.25% Triton X-100, 1 mM EDTA, 20 mM β-glycerophosphate and a cocktail of protease and phosphatase inhibitors: PMSF, NaF, leupeptin and aprotinin. Cell lysate were centrifuged at 20,000g for 10 minutes at 4°C. The resulting supernatant was transferred to new

tubes and stored at -20°C for use within a week or -80°C for use over a week. Immunoprecipitations were carried out using GFPtrap (Chromotek, gta-20) and RFPtrap (Chromotek, rta-10) following manufacturer's protocol.

2.3.2 Immunoblot

Routine cell lysis was performed as described above. Sample protein concentrations were measured using the Pierce protein BCA kit (Thermo Fisher Scientific, 23227) following manufacturer's protocol. SDS-Page samples were made to contain 25 - 35 µg of protein from whole cell lysates. SDS-Page gel running settings were 150V for one to one and a half hours. Wet transfer settings were 400mA for two hours on ice using PVDF membrane (Roth, T830.1). Membranes were shortly incubated with Ponceau S for transfer verification then washed one time with either TBS-T or PBS-T (depending on the desired antibody) and incubated in blocking milk (5% skim milk in either TBS-T or PBS-T) for one hour at room temperature on rotation. Following blocking, membranes were incubated overnight at 4°C in blocking milk containing desired antibodies as listed below on rotation. Prior to secondary antibody incubation, membranes were washed three times for 10 minutes on rotation with either TBS-Tween or PBS-Tween. Secondary antibody incubation was one hour at room temperature on rotation. Another wash cycle after incubation then one-minute incubation with ECL substrates (Millipore, WBKLS0500). Exposure and development were performed on Super RX-N films (FujiFilm, 47410 19284) with an AGFA Curix 60 film processor.

Antibody	Manufacturer and Cat Nº	Dilution
CRY1	Biomol, A302-614	1:500
CRY2	Biomol, A302-615	1:500
GFP	Cell Signaling Tech, 2955S	1:1000
mCherry	Abcam, ab167453	1:2500
α tubulin	Sigma, T3526	1:10000
XPA	Thermo Fisher Scientific, MA5-13835	1:1000
Artemis	Biomol, A304-902A-M	1:1000

2.4 Fluorescence microscopy

2.4.1 Live cell imaging

Cells were plated at a density of 20,000 cells per well in an 8-well Lab-Tek II chamber (Thermo Fisher Scientific) and incubated overnight before live-cell imaging. Cell culture medium was exchanged for Leibovitz L-15 (Gibco) supplemented with 10% FBS and 1% PS on the day of data collection. Imaging was performed using a confocal spinning-disk microscope system (Zeiss AxioObserver Z1), using a C-Apo 63X water immersion objective (Olympus). The system is equipped with an sCMOS ORCA Flash 4.0 camera (Hamamatsu) and Zen Blue imaging software version 2.0. DNA damage was induced with 20% (unless stated otherwise) 355 nm laser, which operated through a single-point scanning head (UGA-42 firefly, Rapp OptoElectronics). The total number of frames and intervals was 70 frames and c.a. 1.21 seconds per frame including more than one pre-laser images were recorded in all experiments (unless stated otherwise). Prior to analysis, all stacks were registered with the StackReg plugin (Thevenaz et al., 1998). Regions of interest for recruitment intensity were selected manually based on fluorophore-bleaching. The ratio of intensity of a circumscribed laser spot *A* to the adjacent area *B* such that an RFI for each data collection point was calculated by the equation RFI=(*A*–*C*)/(*B*–*C*), where *C* is the background intensity of an unpopulated area of the image. In cases in which recruitment was not detectable, *A* was determined by use of laser coordinates recorded in the data log file.

2.4.2 Immunofluorescence

Cells were plated at a density of 100,000 cells per well on coverslips (Fisher Scientific, 11846933) in a 12-well dish (Greiner Bio-One) and let adhere overnight.

2.4.2.1 6-4PP staining

Following recovery, cells were fixed with 4% paraformaldehyde for 10 minutes at room temperature, washed 3 times with PBS and permeabilized with 0.5% Triton TX-100/PBS for 5 minutes on ice. Permeabilized cells were washed 3 times with PBS treated Denature with 2M HCL for 30 minutes at room temperature, then washed 5 times with PBS. Samples were then blocked with 20% FBS/PBS for 1 hour at temperature on gentle tilt. Cells were washed 5 times with PBS before incubating with 6-4PP antibody (COSMO BIO USA, NMDND002) 1:300 in 5% FBS/PBS for 1 hour at room temperature on gentle tilt. Cells were washed 5 times with PBS before incubating with a secondary Alexa Fluor conjugated fluorescent antibody (Thermo Fisher Scientific, A-11001) 1:2000 in 5% FBS/PBS for 1 hour at room temperature on gentle tilt. Finally, cells were washed 5 times with PBS and mounted with Fluoroshield with DAPI (Sigma Aldrich, F6057).

2.4.2.2 CPD staining

Following recovery, cells were fixed with 2% PFA in 0.1% Triton TX-100/PBS for 15 minutes at room temperature and permeabilized with 0.1% Triton TX-100/PBS for 30 minutes at room temperature. Cells were next treated with 0.07M NaOH for 5 minutes, then washed with 0.1% Triton TX-100/PBS. All samples were then blocked with PBS+ (0.5% BSA/0.15% glycine/PBS). Cells were incubated at 4°C overnight with the CPD antibody (Hölzel Diagnostica, CAC-NM-DND-001) 1:1000 in PBS+. Unspecific antibody staining was removed by washing the cells in 0.1% Triton TX-100/PBS. Cells were then stained with Alexa Fluor conjugated fluorescent secondary antibody (Thermo Fisher Scientific, A-11001) 1:2000 in the blocking solution for 1 hour at room temperature. Finally, cells were washed 3 times with 0.1% Triton TX-100/PBS and mounted with Fluoroshield with DAPI (Sigma Aldrich, F6057).

2.4.2.3 RNA-Recovery Synthesis assay

Following recovery, both NT and 16h samples were washed with PBS and incubated with DMEM 10% dialyzed FBS 10mM HEPES 1mM EU for 2 hours. Cells were fixed with 3.7% PFA for 10 minutes at room temperature followed by 20 minutes of 0.5% Triton-TX100/PBS. Click-iT reaction was performed according to manufacturer's instructions (ThermoFisher Scientific, C10330). Coverslips were washed two times 2 minutes each with 3% BSA/PBS and two times 2 minutes each with PBS before mounting with Fluoroshield with DAPI (Sigma Aldrich, F6057).

2.4.2.4 gH2AX, RAD51 and 53BP1 staining

Cells were fixed with 4% PFA for 10 minutes at room temperature followed by 10 minutes of 0.25% Triton-TX100/PBS. Coverslips were blocked with 3% BSA/PBS for 1 hour at room temperature followed by an overnight incubation with either gH2AX antibody (NOVUS, NB100-78356), RAD51 antibody (Abcam, ab133534) or 53BP1 antibody (NOVUS, NB100-304) 1:1000 in blocking solution at 4°C. The next day, coverslips were washed 3 times 2 minutes each with PBS. Cells were then stained with Alexa Fluor conjugated fluorescent secondary antibody (Thermo Fisher Scientific, A-11001) 1:2000 in the blocking solution for 1 hour at room temperature. Finally, the coverslips were washed 3 times 2 minutes each with PBS before mounting with Fluoroshield with DAPI (Sigma Aldrich, F6057).

2.4.2.5 Fluorescence imaging

All fluorescence imaging experiments were performed on a Zeiss AxioObserver Z1 confocal spinning-disk microscope equipped with a sCMOS ORCA Flash 4.0 camera (Hamamatsu). Fixed cells stained by immunofluorescence were imaged with a C-Apochromat 40x/1.20 W Korr objective.

2.5 Cell based assays

2.5.1 Clonogenic assay

Cells were seeded at 50% confluency and left to adhere for 16 hours followed by transfection with 55 pmol siRNA using Lipofectamine RNAiMAX (Invitrogen, 13778150). 24 hours post transfection, 1,000 cells were seeded in 3 technical replicates per well per sample. 24 hours post seeding, cells were washed one time in warm PBS prior to UV-C exposure. 2mL of warm normal culturing medium was added to the cells after treatment and let incubate for 8 days. After incubation, cells were washed once in warm PBS then fixed and stained with 50% methanol, 7% acetic acid and 0.1% Brilliant Blue R for one hour at room temperature. Stained cells were then washed three times with room temperature ddH2O and let dry upside down overnight. The resulting stainings were scanned and further analyzed using the ColonyArea plugin (Guzman et al., 2014) and macro developed by a fellow colleague, Charlotte Blessing.

2.5.2 G2/M checkpoint assay

Cells were plated at 1,200,000 cells per dish in a 60mm dish and left to adhere for 16 hours followed by transfection with 55 pmol siRNA using Lipofectamine RNAiMAX (Invitrogen, 13778150). 24 hours post RNA transfection, cells were seeded at 600,000 cells per well in a 6-well plate and left to adhere for 16 hours. 24 hours post seeding, cells were irradiated with X-ray (ACCELA, CellRad) and left to recover for 24 hours. After recovery, 40 ng/mL nocodazole (Sigma Aldrich, 487928) was added to each sample and incubated for 6 hours. Following incubation, cells were harvested, washed, and fixed with 1.5mL ice-cold EtOH on mild vortex and stored in -20°C overnight. Fixed cells were washed once with 1%FBS/PBS and permeabilized with 0.25% Triton-TX100/PBS for 10 minutes at room temperature. After permeabilization, cells were washed and incubated with H3S10p antibody (Merck Millipore, 06-570) 1:500 in 1% FBS/PBS at 4°C overnight. The following day, cells were washed and stained with Alexa Fluor conjugated fluorescent secondary antibody (Thermo Fisher Scientific, A-11001) 1:2000 in 1% FBS/PBS for 1 hour at room temperature. After which, the samples were washed and treated with 1 µg propidium iodide (Sigma Aldrich, P4170) and 25 µg RNase A (Thermo Fisher, 12091021) in PBS for 16 hours. All samples were analyzed on the BD LSRFortessa and data analysis was performed using the Flowing software (Turku Bioscience).

2.5.3 Repair reporter assay

U-2 OS DR, SA, EJ5 and EJ2 cells were plated at 1,000,000 cells per well in a 6-well dish and left to adhere for 16 hours followed by transfection with 30 pmol siRNA using Lipofectamine RNAiMAX (Invitrogen, 13778150). 24 hours post RNA transfection, cells were transfected with the 2.4 µg pCBASCE-I plasmid (kind gift from Dr. Stefan Zahler) using Xfect transfection reagent

(Takarobio, 631317). 48 hours post DNA transfection, cells were harvested and kept on ice. Samples were washed and centrifuged at 2000rpm for 5 minutes at 4°C twice before re-suspension in 500 µL of 1% FBS/2mM EDTA/PBS and divided with a cell strainer. 15µL of Hoechst Ready Flow (Thermo Fisher Scientific, 33342) was added to each sample. The samples were vortexed shortly and incubated for 30 minutes at 37°C. All samples were analyzed on the BD LSRFortessa and data analysis was performed using the Flowing software (Turku Bioscience).

2.6 Statistical analyses

All graphs and statistical analyses were plotted and performed using Prism9 (GraphPad software).

3. Results

3.1 Human CRYs recruit to DNA damage sites

3.1.1 Human CRY proteins recruit to laser-induced DNA damage sites

Previous reports have shown CRYs bind to DNA with the preference of 6-4PPs but exhibit no light-induced repair activity (Hsu et al., 1996; Kobayashi et al., 1998; Ozgur and Sancar, 2003). Based on sequence alignment, human CRYs retained the photolyase homology region. I thus hypothesized human CRYs partially preserve their roles in UV-induced DDR. To test this, I generated stable clones expressing mEGFP-CRY1 and mCherry-CRY2 fusion proteins. mEGFP-CRY1 clone G5 (here on abbreviated as C1G5) and mCherry-CRY2 clone C12 (here on abbreviated as C2C12) were chosen based on expression levels for further analyses. Both CRYs rapidly sequestered to DNA damage sites inflicted with the 355 nm laser (Figure 6A). CRY1 and CRY2 demonstrated a c.a. 0.4 and 0.25 fold increase respectively in fluorescence intensity at laser-induced damage (LID) sites (Figure 6B). To verify this finding, I tested the endogenous CRY1 by using a newly generated knockin cell line from a recent study (Gabriel et al., 2020). The endogenously tagged CRY1 (here on abbreviated as C1C) displayed a c.a. 0.5 fold increase (Figure 6C) thereby confirming that CRYs actively recruit to 355 nm LID sites.

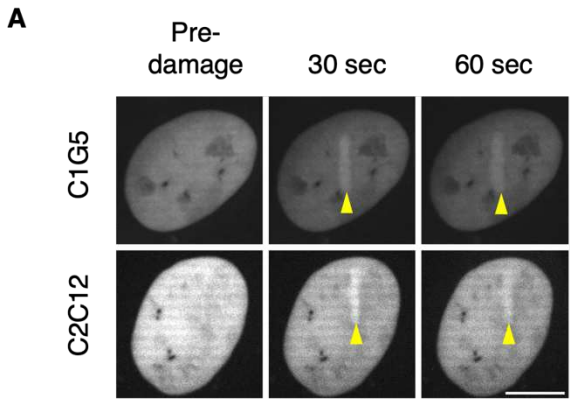

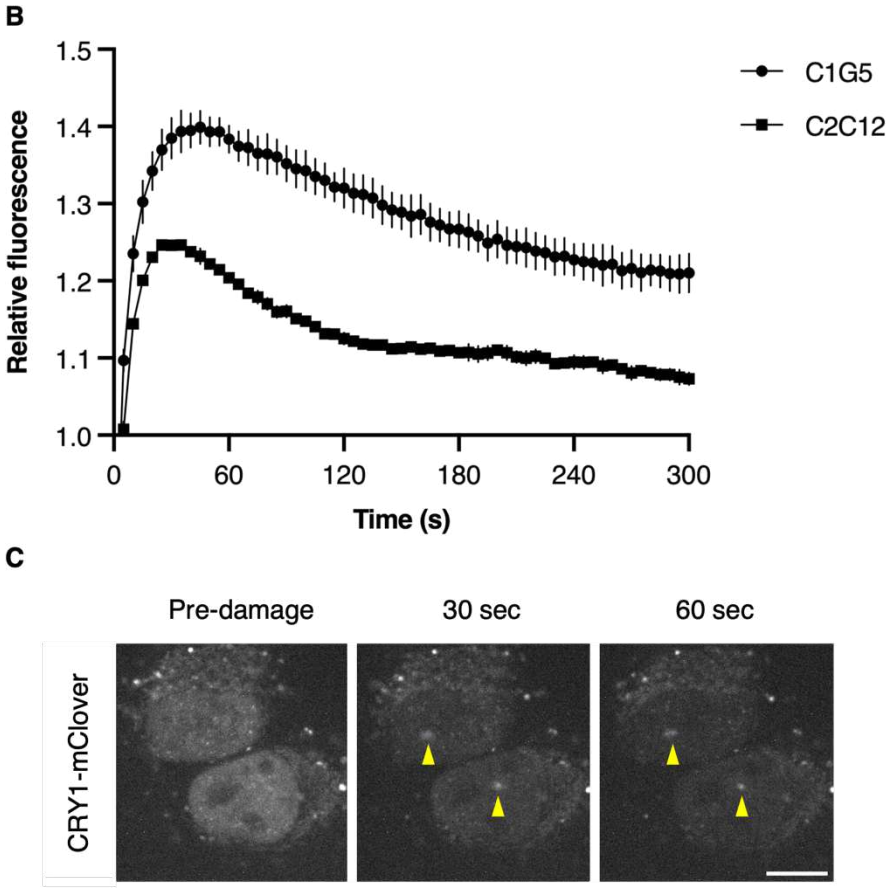

Figure 6. Human CRY proteins recruit to laser-induced DNA damage sites.

A) CRYs enrich at DNA damage sites. 355 nm LID (indicated by arrow head) inflicted on U-2 OS cells stably expressing mEGFP-CRY1 (upper panel) and mCherry-CRY2 (lower panel). Scale bar, 10 µm. B) CRYs display similar recruitment kinetics. quantification of A) mEGFP-CRY1 (solid circle) and mCherry-CRY2 (solid square) intensity at LID relative to pre-damage intensity using live-cell confocal imaging and Fiji ImageJ (N = 3, n ≥ 15-30 cells, mean ± s.e.m.). C) endoCRY1 recruits to LID sites (indicated by arrow head) (N = 3, n ≥ 15-30 cells).

3.1.2 CRY recruitment is damage-dependent and enhanced upon stabilization

CRYs are known to interact with each other. To eliminate the possibility of 'piggy backing', I next addressed whether CRYs require their respective homologs to recruit by transiently expressing both fusion proteins in the four genetic backgrounds i.e., wild-type, ΔCRY1, ΔCRY2 and ΔCRY1/2 (Börding et al., 2019). Neither of the tagged CRYs were affected with the exception of a non-significant increase in ΔCRY2 cells (Figure 7A) suggesting both CRYs recruit independently. Given that the CRY homologs actively recruit to damage sites and that this recruitment occurs independently, I asked whether CRY recruitment is damage dependent. I addressed this by assessing the recruitment amplitude of CRYs using varying laser power. Indeed, I observed a positive correlation between CRY recruitment and the laser power (Figure 7B). Furthermore, IR-

induced DDR stabilizes CRY1 and destabilizes CRY2 independently (Papp et al., 2015; Shafi et al., 2021). So I asked whether CRY stabilization by a carbazole-based stabilizer- KL001 (Hirota et al., 2012) would affect their association with DNA damage sites. Intriguingly, CRY2 association with DNA damage sites occurs earlier upon stabilization; whereas CRY1 recruitment was not affected (Figure 7C). Taken together, CRY1 and CRY2 independently recruit to LID sites in a damage dependent manner and that the stabilization of CRY2 affects its recruitment kinetics.

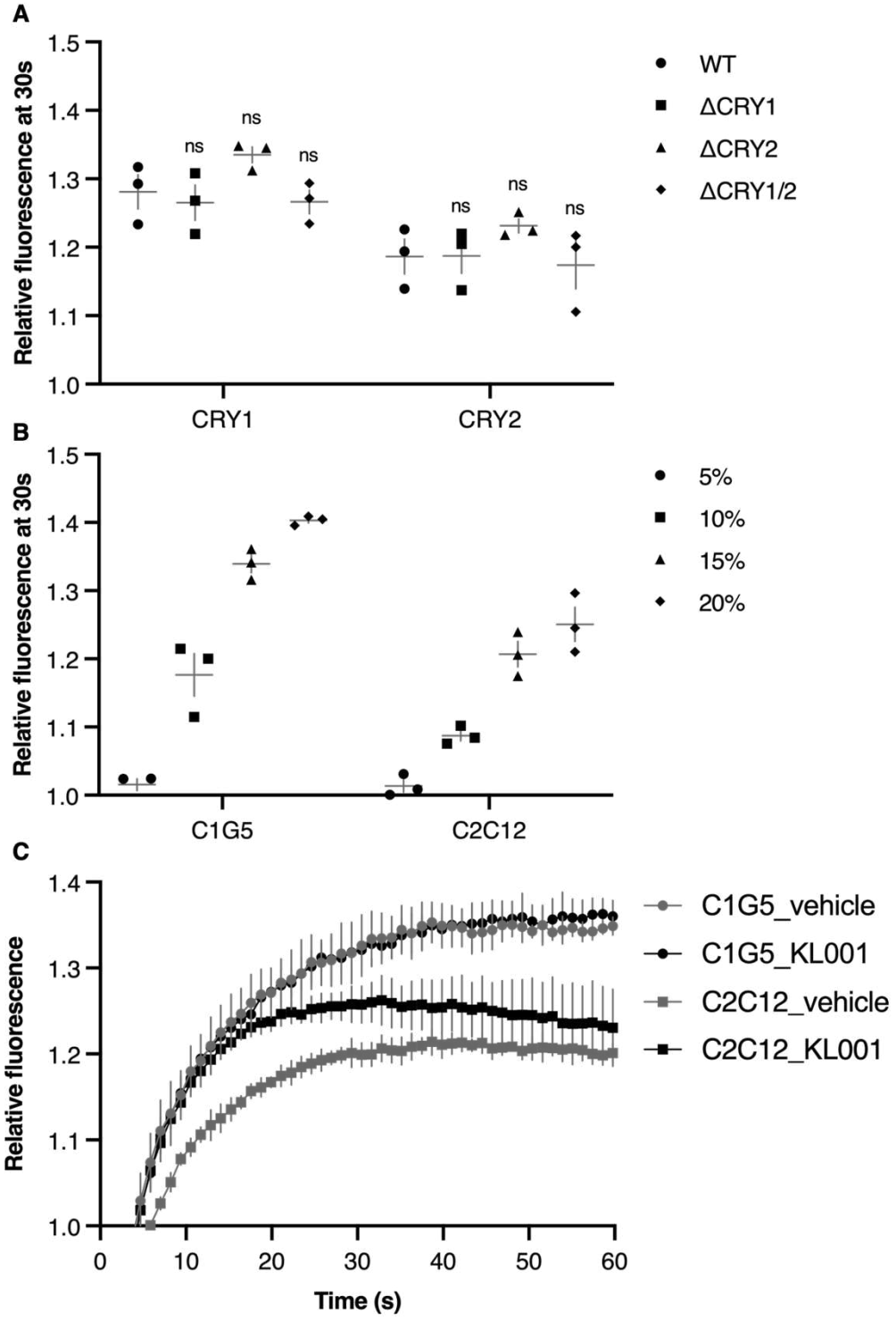

Figure 7. CRY recruitment is damage-dependent and enhanced upon stabilization.

A) CRYs recruit independently. U-2 OS wild-type, ΔCRY1, ΔCRY2 and ΔCRY1/2 cells transiently expressing mEGFP-CRY1 and mCherry-CRY2 were subjected to 355 nm LID infliction. mEGFP-CRY1 and mCherry-CRY2 intensity in indicated genetic backgrounds at LID relative to pre-damage intensity 30 seconds post LID using live-cell confocal imaging (N = 3, n ≥ 15-30 cells, mean ± s.e.m.). Significance by two-way ANOVA. B) CRY recruitment is damage dependent. C1G5 and C2C12 were subjected to 355 nm LID infliction. mEGFP-CRY1 and mCherry-CRY2 intensity at indicated laser doses at LID relative to pre-damage intensity 30 seconds post LID using live-cell confocal imaging (N = 3, n ≥ 15-30 cells, mean ± s.e.m.). Significance by two-way ANOVA. C) CRY2 recruitment is enhanced upon stabilization. C1G5 and C2C12 were subjected to 355 nm LID infliction after 6 hours of vehicle (DMSO) and 10 µM KL001 treatment. mEGFP-CRY1 and mCherry-CRY2 intensity at LID relative to pre-damage intensity 30 seconds post LID using live-cell confocal imaging (N = 2, n ≥ 15-30 cells, mean ± s.e.m.).

3.1.3 CRY1 colocalizes with γH2AX at DNA breaks

The 355 nm laser system generates not only UV-associated lesions such as CPDs and 6-4PPs, but also causes DNA strand breaks as well as oxidized bases (Kong et al., 2009; Muster et al., 2017; Holton et al., 2017). Bearing in mind that CRY2 has been shown to preferentially bind DNA containing 6-4PPs (Ozgur and Sancar, 2003), I asked whether CRY recruitment is damage specific. To approach this, I induced DNA strand breaks by 1) LID using the 405nm laser on nuclei pre-sensitized with Hoechst and 2) global damage using IR. With the first approach, I observed CRY1 enrichment and colocalization with γH2AX at damage sites while CRY2 was scarcely detectable at 1 minute after micro-irradiation (Figure 8A). This implies that CRY1 and CRY2 recruitment may be damage specific. I further tested CRY1 localization using pan IR treatment. Both exoCRY1 and endoCRY1 were enriched at IR-induced γH2AX foci furthering confirming CRY1 association with DNA strand breaks (Figure 8B). In line with previous reports (Papp et al., 2015; Shafi et al., 2021), I observed an overall increase in endoCRY1 as well as γH2AX nuclear after exposure to IR (Figure 8C). Collectively, CRY1 strongly associated with DNA strand breaks while CRY2 did not and raises an interesting question whether structural variation plays a part in the observed damage specific recruitment of CRYs.

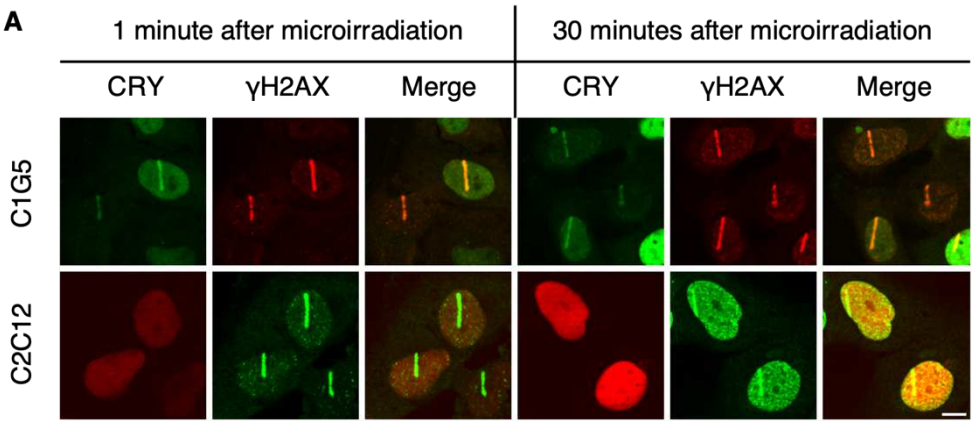

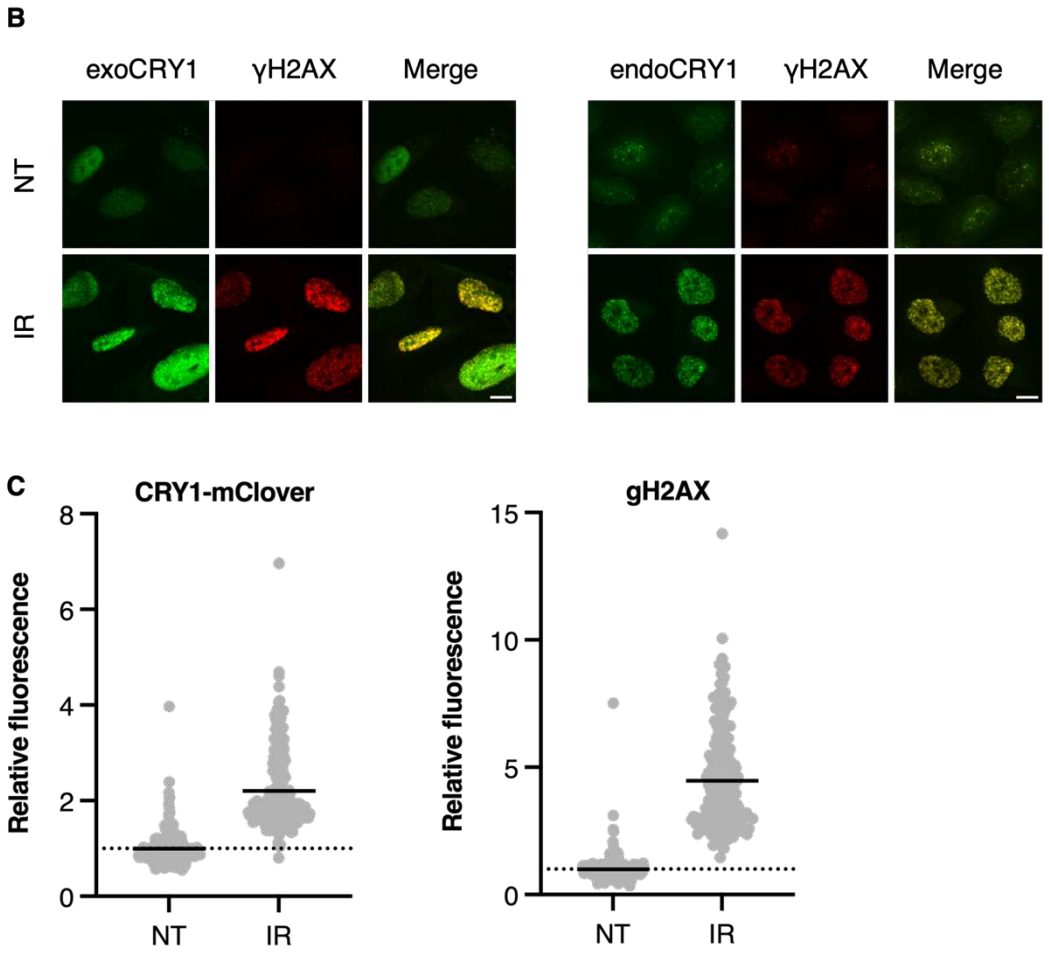

Figure 8. CRY1 colocalizes with γH2AX at DNA breaks.

A) CRY1 enriches at DNA strand breaks. C1G5 and C2C12 were pre-sensitized with hoechst for 15 minutes. After which, the clones were subjected to 405nm LID for the indicated time points then fixed and stained for γH2AX. mEGFP-CRY1 (upper panel) and mCherry-CRY2 (lower panel). Scale bar, 10 µm. (N = 3, n ≥ 20 cells). B) endoCRY1 colocalizes with gH2AX. C1G5 and C1C were subjected to 10 Gy IR and let recover for 30 minutes. After which, cells were fixed and stained for γH2AX. mEGFP-CRY1 (left panel) and CRY1-mClover (right panel). Scale bar, 10 µm. (N = 3, n ≥ 20 cells). C) CRY1 is stabilized upon IR-induced DDR. Nuclear CRY1-mClover (left panel) and γH2AX (right panel) intensity 30 minutes post-IR (10 Gy) treatment using fluorescence confocal imaging. (N = 3, n ≥ 50 cells, mean).

3.1.4 The DNA photolyase domain is sufficient for CRY2 recruitment

To address whether structural variation (c.a. 70% homology) is a factor in the damage specific recruitment of CRYs, I sought to map the domain which is required for the recruitment. CRYs contain two functional domains i.e. DNA photolyase (DP) and FAD-binding (FAD), and the highly unstructured C-terminal coiled-coiled extension (CCE) (Figure 9A). I generated three truncated mutants according to these functional domains based on sequence alignment to the murine CRYs. All constructs expressed and were detectable by immunoblotting with the exception of CRY1 FAD (Figure 9B). This may be explained by targeted degradation through increased

interaction with the E3 ligase- FBXL3 (Xing et al., 2013) (Figure 9B left). All truncated CRY1 mutants exhibited a decrease in recruitment amplitude (Figure 9C). Intriguingly, CRY2 DP and DPloop domains displayed enhanced recruitment (Figure 9C). This suggests that the FAD and CCE domains are non-essential and potentially hinder CRY2 recruitment to LID sites; whereas the full length CRY1 protein may be required for full recruitment. The observed differences between the truncated CRYs supports the notion of damage specific recruitment of CRYs.

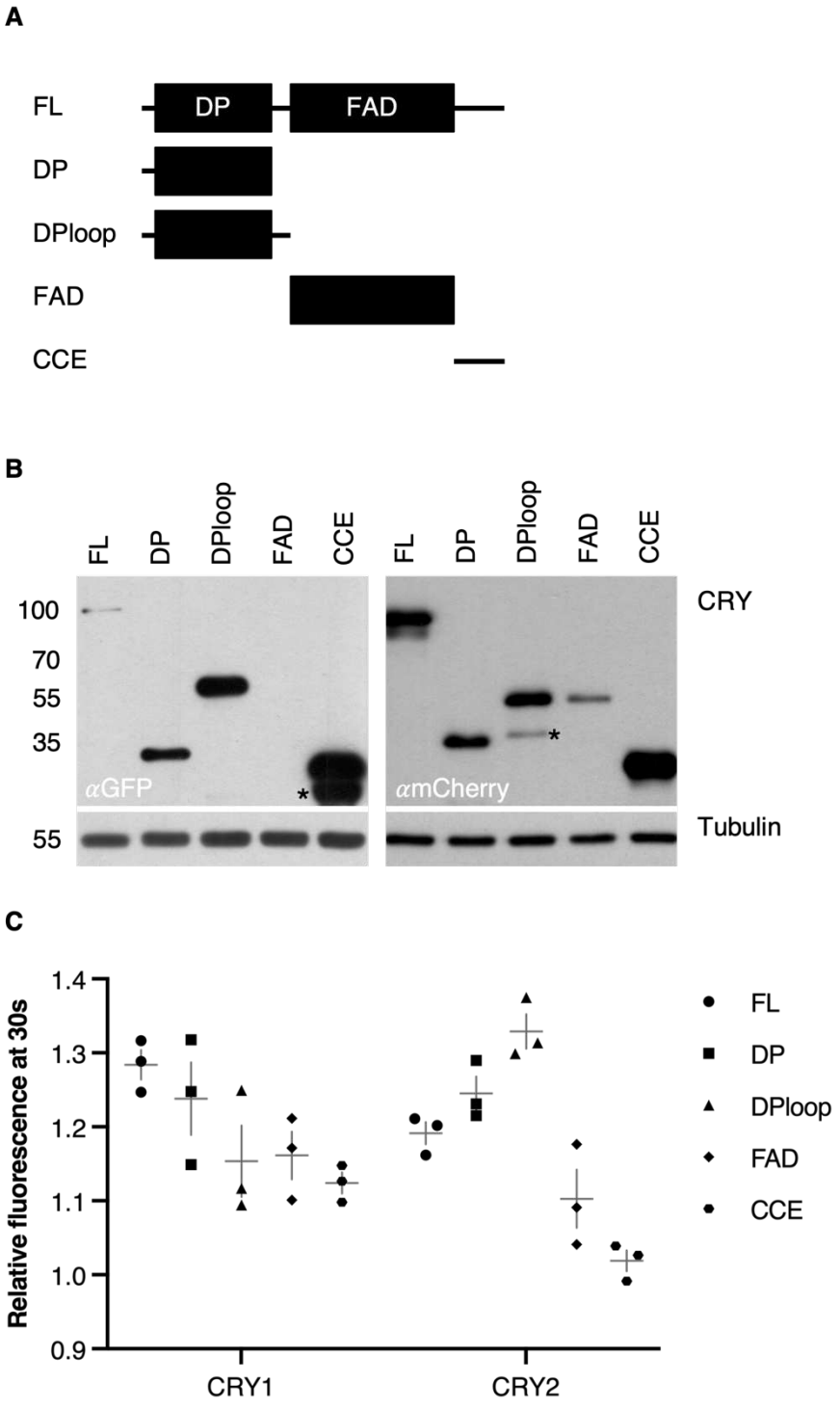

Figure 9. The DNA photolyase domain is sufficient for CRY2 recruitment.

A) Illustration of the functional domains of CRYs and the truncation mutants. FL: full length; DP: DNA photolyase; DPloop: DNA photolyase and loop; FAD: FAD-binding domain; CCE: coiled-coiled extension. B) Protein levels of indicated truncation mutants. Asterisk marks unspecific bands. C) U-2 OS cells transfected with indicated truncation mutants and were subjected to 355 nm LID. mEGFP-CRY1 and mCherry-CRY2 intensity of the indicated truncated proteins at LID relative to pre-damage intensity 30 seconds post LID using live-cell confocal imaging. (N = 3, n ≥ 15-30 cells, mean ± s.e.m.).

3.2 PARP1 activity is essential for CRY recruitment

3.2.1 Pan PARP inhibition abolishes CRY recruitment

The possible damage specific association of CRYs led me to question whether other DNA damage sensors are involved in CRY recruitment. As described previously, the two families- PIKK and PARP are at the frontline of DDR. While ATM, ATR, and DNAPK, through phosphorylation, initiate a rapid signaling cascade to induce downstream checkpoint and repair processes, PARPs generate PARylation to induce chromatin decompaction and recruit DDR factors. To test whether these major DDR signaling pathways regulate CRY recruitment to damage sites, I subjected the stable CRY clones to various inhibitor treatments. In the case of ATR, ATM and DNAPK inhibitor treatment, no significant changes were observed for both homologs with the exception of ATRi treated CRY1 (Figure 10A). However, the pan-PARP inhibitor- olaparib abolished the recruitment of both CRYs (Figure 10A&B). To verify this finding, I tested other PARP inhibitors i.e. talazoparib and veliparib which have an EC50 lower and higher than olaparib respectively (for in vitro EC50 determination method, please refer to https://www.selleckchem.com/PARP.html). Treatment with either inhibitors at the same concentration displayed the same degree of decrease in comparison to that of olaparib (Figure 10C) concluding that PARylation critically regulates CRY recruitment.

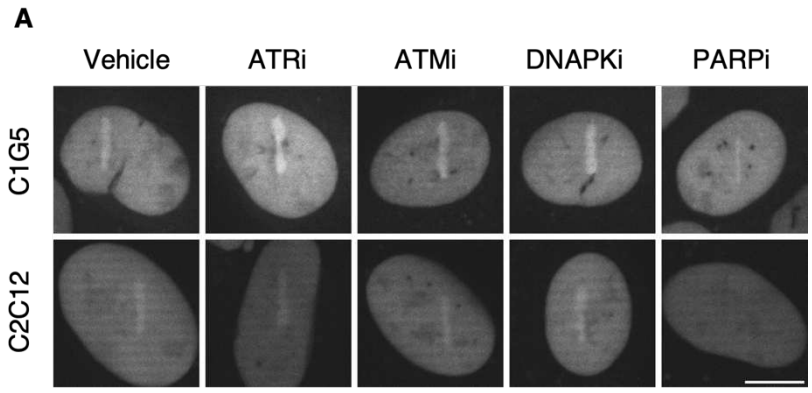

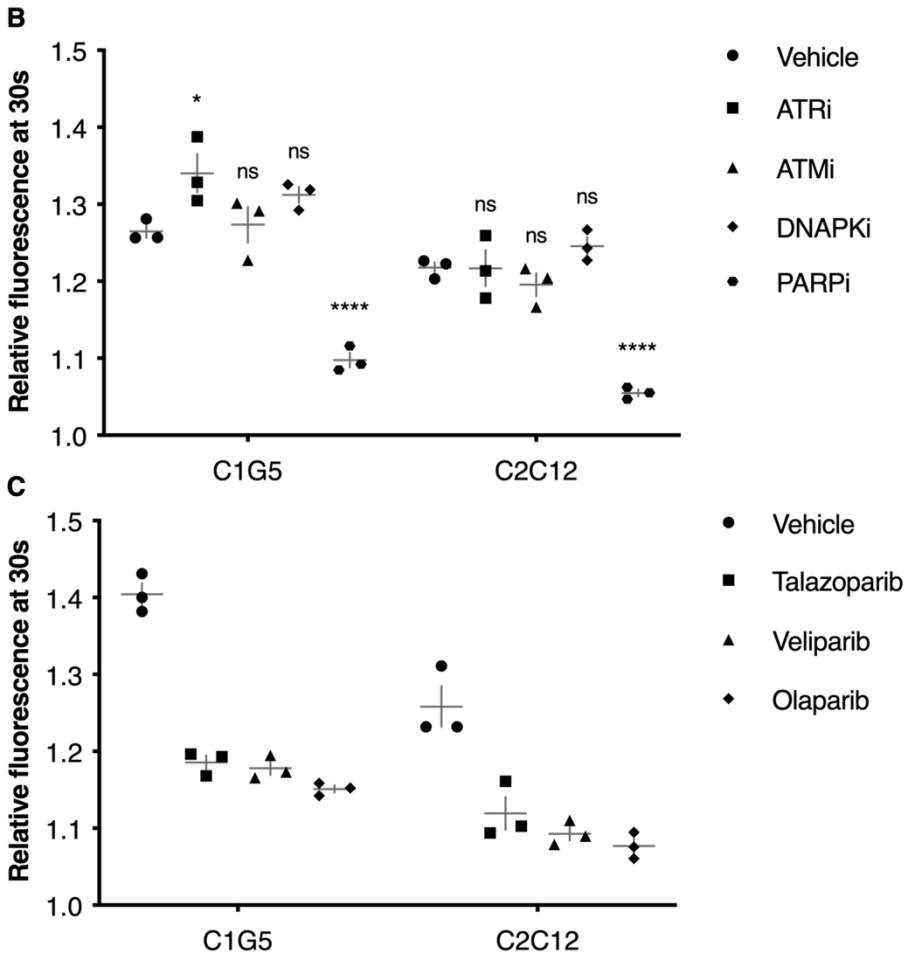

Figure 10. Pan PARP inhibition abolishes CRY recruitment.

A) Olaparib treatment abolishes CRY recruitment. C1G5 (upper panel) and C2C12 (lower panel) cells were treated with indicated inhibitors at 10 µM for one hour and subsequently subjected to 355 nm LID infliction. Scale bar, 10 µm. B) Quantification of A). mEGFP-CRY1 and mCherry-CRY2 intensity of indicated treatments at LID relative to pre-damage intensity 30 seconds post LID using live-cell confocal imaging. (N = 3, n ≥ 15-30 cells, mean ± s.e.m.). Significance by two-way ANOVA. C) PARylation is critical for CRY recruitment. C1G5 and C2C1 cells were treated with indicated inhibitors at 2.5 µM for one hour and subsequently subjected to 355 nm LID infliction. Quantification of mEGFP-CRY1 and mCherry-CRY2 intensity of indicated treatments at LID relative to pre-damage intensity 30 seconds post LID using live-cell confocal imaging. (N = 3, n ≥ 15-30 cells, mean ± s.e.m.). Significance by two-way ANOVA.

3.2.2 PARP1 is the key player in CRY recruitment

Since PAR synthesis critically regulates CRY recruitment, I next asked whether PAR hydrolysis also affects CRY association to damage sites. When PARG, a PAR glycohydrolase, was inhibited, I observed a significant increase in CRY recruitment amplitude (Figure 11A). This suggests that CRY recruitment is regulated by the dynamics of PAR. DDR-induced PARylation is mainly generated by PARP1 and PARP2 (Wei and Yu, 2016). To test whether CRY recruitment is specific to one of the two PARPs, I transiently expressed the CRY constructs in four genetic backgrounds

i.e. wild-type, ΔPARP1, ΔPARP2 and ΔPARP1/2 (Ronson et al., 2018). Both CRY1 and CRY2 did not recruit in the ΔPARP1 background. However, the absence of PARP2 did not affect the recruitment of CRY in comparison to wild-type (Figure 11B) suggesting that PARP1 is essential for CRY recruitment whereas PARP2 is dispensable. To confirm PARP1-mediated PARylation is critical for the recruitment of CRYs, I transiently co-expressed the CRY constructs with either the empty vector, $PARP1_{WT}$ or $PARP1_{PD}$ (E988K) in the ΔPARP1 cells. As expected, cells expressing $PARP1_{WT}$ successfully restored CRY recruitment whereas cells expressing the $PARP1_{PD}$ did not (Figure 11C). Taken together, I concluded that the catalytic activity of PARP1 is critical for the recruitment of CRYs to LID sites.

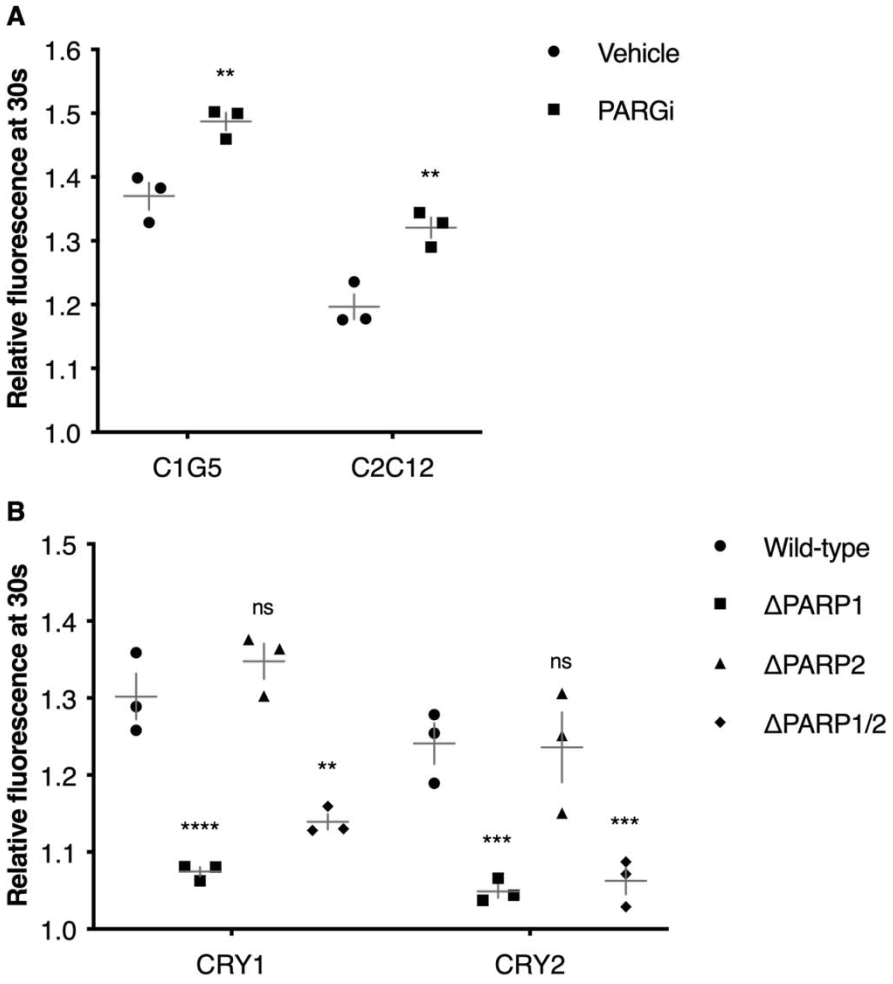

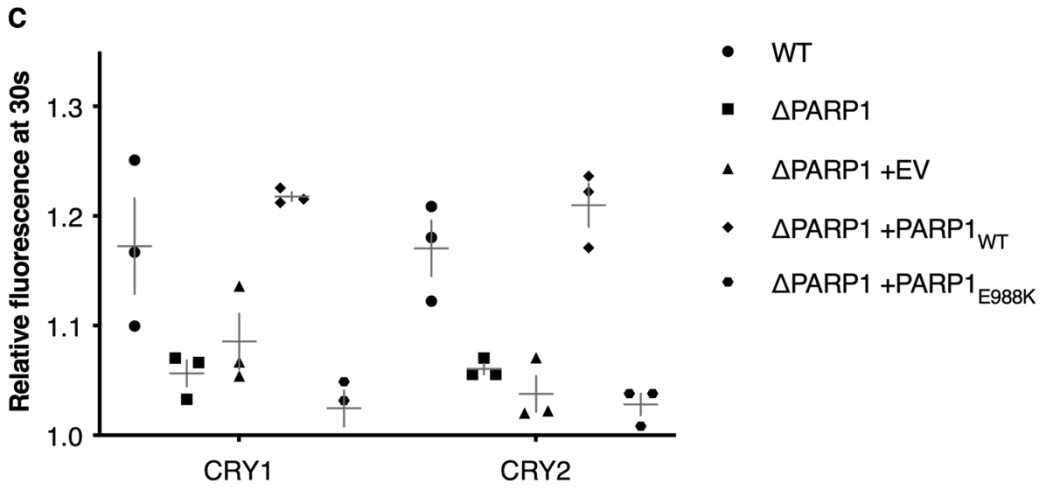

Figure 11. PARP1 is the key player in CRY recruitment.

A) PARG inhibition enhances CRY recruitment. C1G5 and C2C12 cells were treated with 10 µM PARGi for 1 hour and subsequently subjected to 355 nm LID infliction. Quantification of mEGFP-CRY1 and mCherry-CRY2 intensity of indicated treatments at LID relative to pre-damage intensity 30 seconds post LID using live-cell confocal imaging. (N = 3, n ≥ 15-30 cells, mean ± s.e.m.). Significance by two-way ANOVA. B) PARP1 regulates CRY recruitment. U-2 OS wild-type, ΔPARP1, ΔPARP2 and ΔPARP1/2 cells transiently expressing mEGFP-CRY1 and mCherry-CRY2 were subjected to 355 nm LID infliction. Quantification of mEGFP-CRY1 and mCherry-CRY2 intensity in indicated genetic backgrounds at LID relative to pre-damage intensity 30 seconds post LID using live-cell confocal imaging. (N = 3, n ≥ 15-30 cells, mean ± s.e.m.). Significance by two-way ANOVA. C) PARP1 (natural variant 1) rescues CRY recruitment in PARP1 knockout cells. mEGFP-CRY1 and mCherry-CRY2 were co-transfected with indicated constructs in indicated genetic backgrounds and subjected to 355 nm LID. Quantification of mEGFP-CRY1 and mCherry-CRY2 intensity of the respective proteins at LID relative to pre-damage intensity 30 seconds post LID using live-cell confocal imaging. (N = 3, n ≥ 15-30 cells, mean ± s.e.m.). Significance by two-way ANOVA.

3.3 CRYs modulate DNA strand break repair

3.3.1 CRYs regulate IR-induced G2/M checkpoint and gH2AX levels

Thus far, my data has demonstrated a PARylation driven physical association of CRYs with DNA damage sites. Whether this recruitment event bears a functional consequence remains to be tested. Intriguingly, CRY1 was previously shown to regulate genes involved in the G2/M checkpoint (Shafi et al., 2021). I thus hypothesize that CRY1 depletion would negatively impact the G2/M checkpoint integrity in U-2 OS sarcoma cells. To approach this, I sought to assess checkpoint integrity using the G2/M checkpoint assay. If the G2/M checkpoint is compromised, more cells accumulate in mitosis (Figure 12A). Unexpectedly, when CRY1 alone was depleted, I observed a non-significant increase in the mitotic population implying that the checkpoint remained relatively intact. Instead, CRY2 and double CRY depletion resulted in significant

increases of mitotic cells (Figure 12B). This, conversely, indicates that CRY2, less so CRY1, mediates IR-induced G2/M checkpoint response.

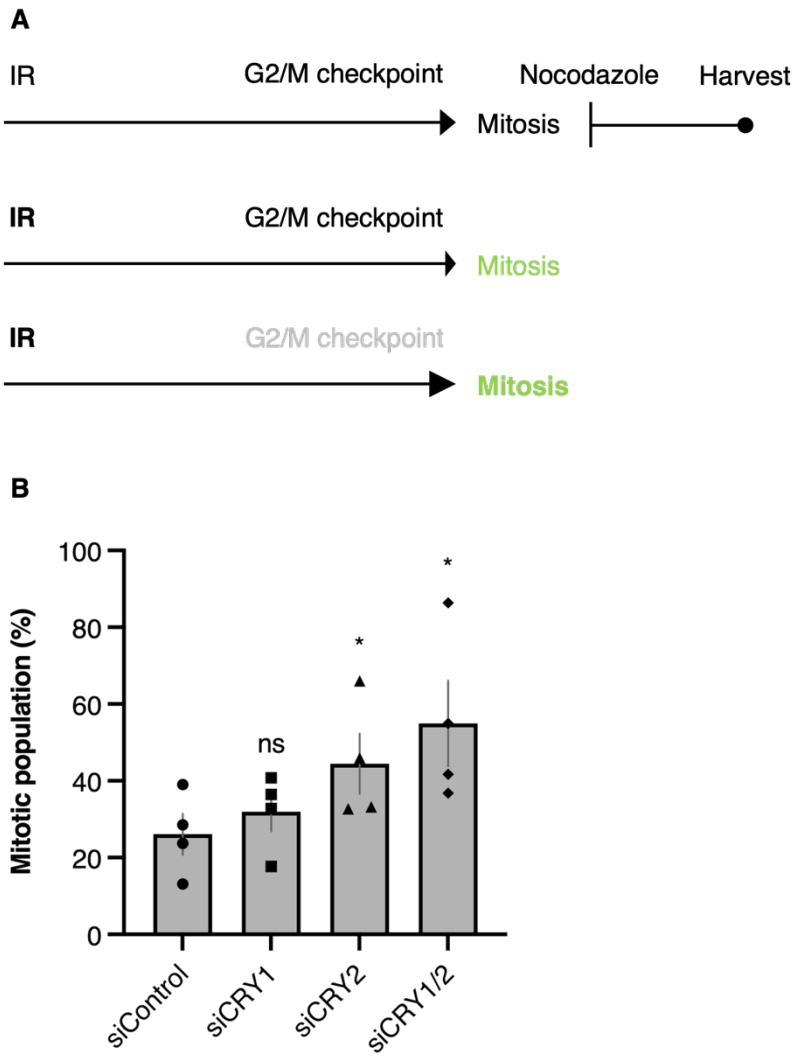

Figure 12. CRYs regulate the G2/M checkpoint.

A) Illustration of the experimental set up for the G2/M checkpoint assay. When cells are exposed to IR, the G2/M checkpoint is activated to halt cell cycle progression causing a delay in mitotic entry. If the G2/M checkpoint is functional, less cells will accumulate in mitosis. When compromised, the result is an accumulation of mitotic cells due to nocodazole-induced mitotic arrest. B) CRYs promote the G2/M checkpoint. Cells were transfected with indicated siRNA for 48 hours followed by 10 Gy IR treatment. 24 hours post treatment, cells were incubated with 40 ng/mL nocodazole for 6 hours to induce mitotic arrest. Cells were then fixed and stained for H3S10p and PI. H3S10p and PI signals were recorded using flow cytometry. (N = 4, n ≥ 10000 cells, mean ± s.e.m.). Significance by one-way ANOVA.

On the account of CRYs impact on the G2/M checkpoint, I next asked whether CRYs affect DSB repair by using γH2AX as a marker for DNA damage (Mah et al., 2010). Although it has already been shown that CRY1 silencing results in an accumulation of IR-induced γH2AX foci in carcinoma cells (Shafi et al., 2021), the authors urged for future studies on the effect of CRYs on

DSB repair in sarcoma cells. In U-2 OS cells, I observed an accumulation of γH2AX in siCRY1 cells 16 hours after IR treatment (Figure 13A). This accumulation of damage was similar to that of Artemis, a well-established NHEJ factor, suggesting CRY1 may play a functional role in DSB repair. Surprisingly, CRY knockout cell lines exhibited an overall and consistent decrease in γH2AX signal both 1 hour and 16 hours after IR exposure (Figure 13B). Further assays are needed to determine the variation between knockdown and knockout.

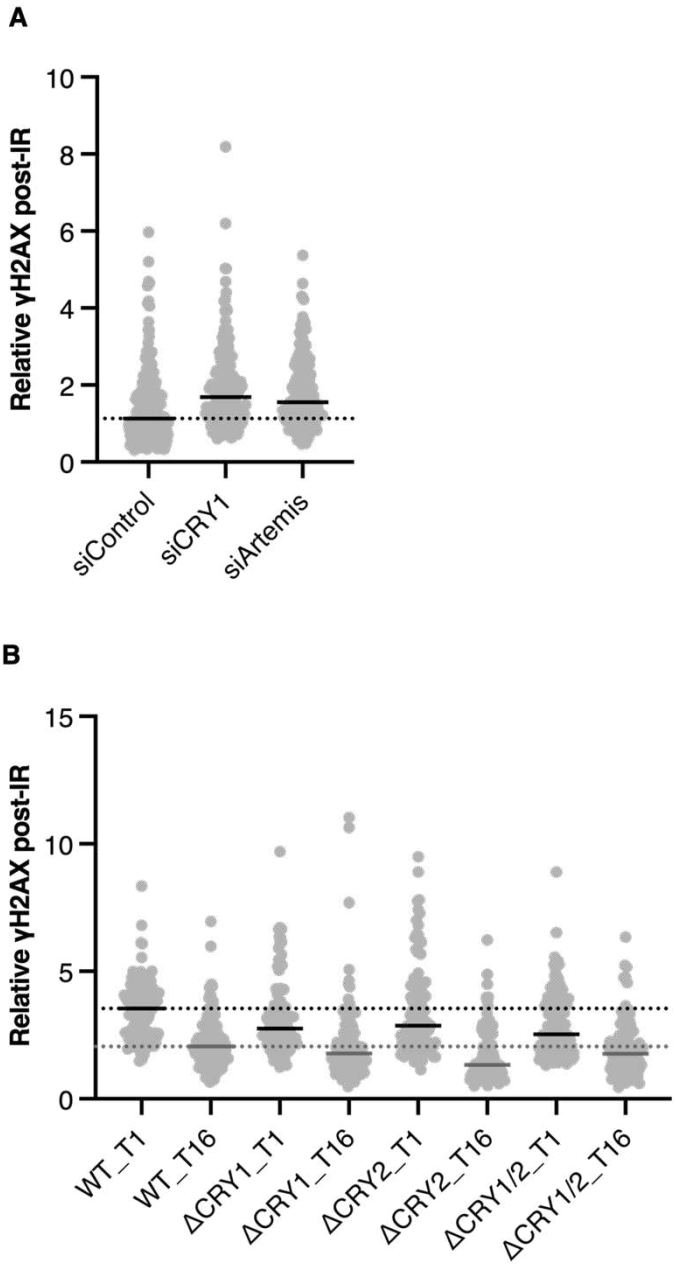

Figure 13. CRYs modulate IR-induced γH2AX levels.

A) CRY1 depleted cells accumulate DSB. Nuclear γH2AX intensity of siRNA-mediated knockdown of indicated factors 16 hours post-IR (10 Gy) treatment. After which, cells were fixed and stained for γH2AX and imaged using fluorescence confocal imaging. (N = 3, n ≥ 50 cells, median) B) CRYs deficient cells have less DSB. Nuclear γH2AX intensity of indicated knockout

cell lines 1 and 16 hours post-IR (10 Gy) treatment. After which, cells were fixed and stained for γH2AX and imaged using fluorescence confocal imaging. (N = 2, n ≥ 50 cells, median)

3.3.2 CRY1 promotes homologous recombination

Combining the observations of CRYs effect on the G2/M checkpoint and γH2AX, I hypothesized CRYs possess a functional role in DSB repair. Indeed, CRY1 abrogation has been reported to impair homology-directed repair (Shafi et al., 2021). Therefore, in this section, I addressed the impact of CRYs not only on homology-directed repair (HDR); but single-strand annealing (SSA) as well by using the U-2 OS repair reporter cell lines DR and SA respectively. These cell lines including EJ5 and EJ2 in the later section harbor a cassette containing a SCE-I cut site and GFP. When repair is completed, GFP is expressed and can be detected by flow cytometry (Figure 14A). siRNA-mediated silencing of CRY1 results in a reduction of GFP signal implying reduced HDR activity (Figure 14B). This HR-deficient phenotype was not observed in CRY2-depleted cells but recurred in the CRY1/2-depleted cells suggesting CRY1 independently regulates HR. Unexpectedly, in the case of SSA, I observed a uniformed reduction in the GFP positive population in both single and double CRY knockdowns (Figure 14C) indicating a previously unreported role for both CRY1 and CRY2 in SSA.

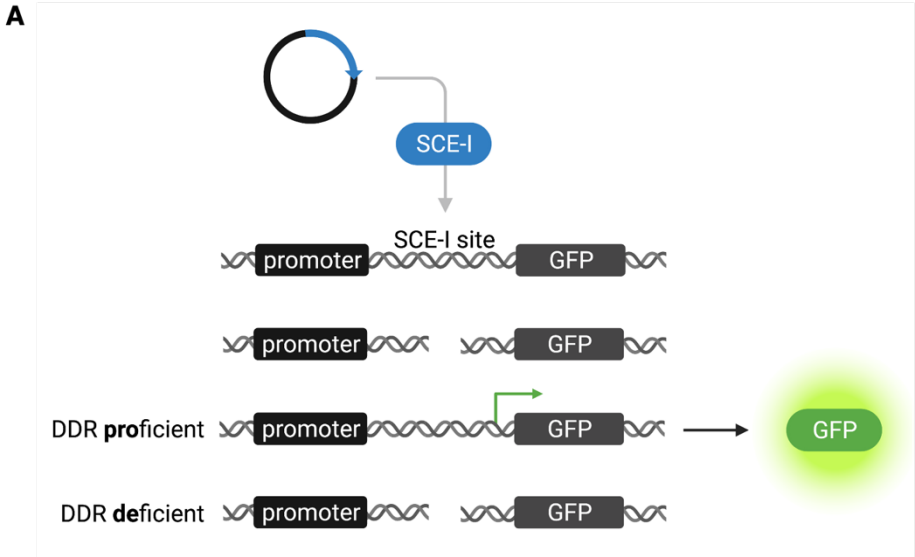

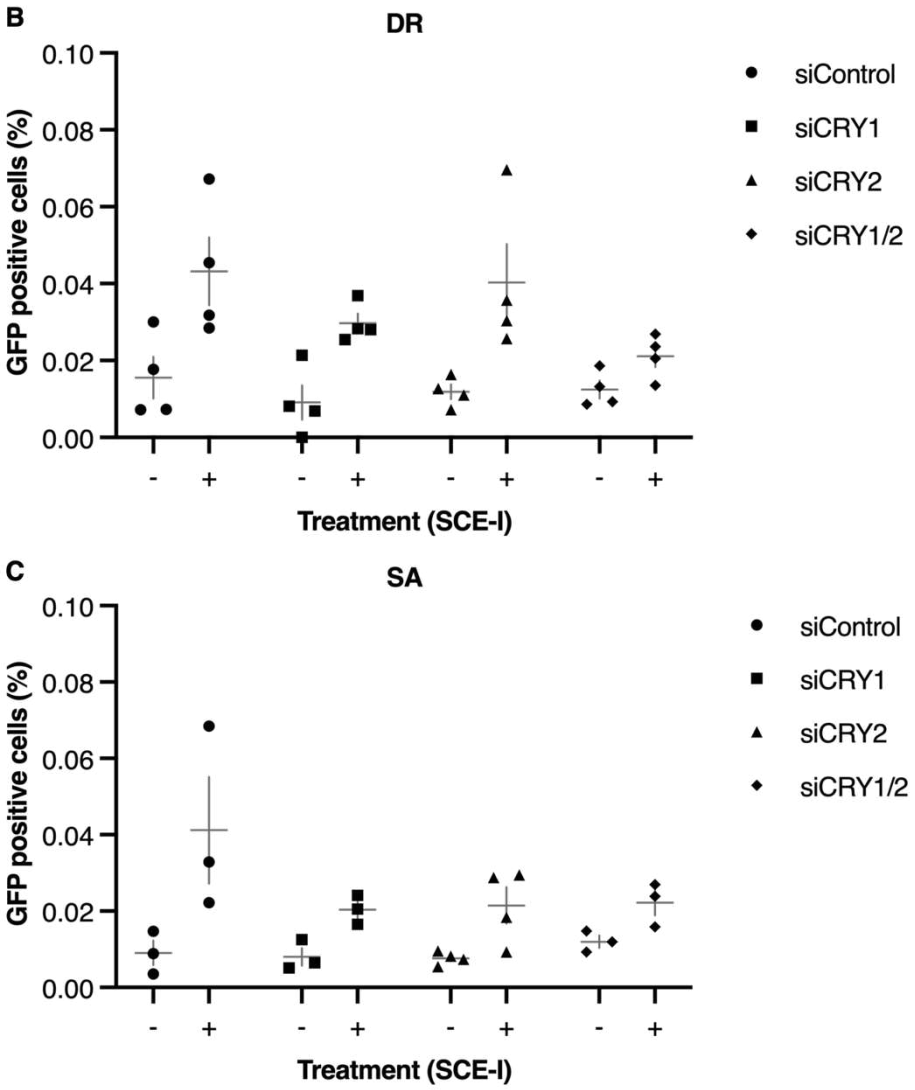

Figure 14. CRYs promote homologous recombination.

A) Simplified schematics of the repair reporter cell lines and the DSB repair assay. These cell lines harbor a cassette containing a SCE-I cut site and the *GFP* gene. In DDR proficient cells, the cut is repaired and GFP is expressed. However, in DDR deficient cells, the cut is left unrepaired thereby prohibiting the expression of GFP. B) CRY1 promotes HDR. DR reporter cells were transfected with indicated siRNA for 48 hours. 24 hours prior to analyses, cells were transfected with pCBASCE-I to induce targeted damage. GFP positive events were recorded using flow cytometry. (N = 3-4, n ≥ 50000 cells, mean ± s.e.m.). C) CRYs promote SSA. SA reporter cells were transfected with indicated siRNA for 48 hours. 24 hours prior to analyses, cells were transfected with pCBASCE-I to induce targeted damage. GFP positive events were recorded using flow cytometry. (N = 3-4, n ≥ 50000 cells, mean ± s.e.m.).

Given that CRYs recruit to LID sites through PARP1 activity, I speculated that PARP inhibition may also negatively impact HDR and SSA. Unexpectedly, olaparib treatment did not affect HDR or SSA activity (Figure 15) suggesting that the PARP1/PAR-dependent recruitment of CRYs and CRY/HR phenotypes are likely to be independent events. To be noted, these results are preliminary and require repetition for confirmation.

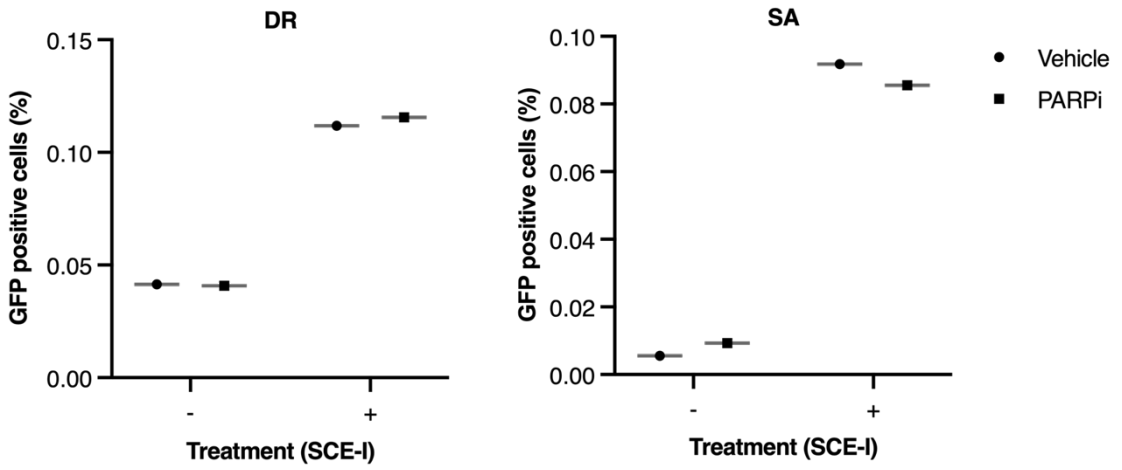

Figure 15. PARP activity does not affect HR.

PARP activity does not affect HDR and SSA. DR and SA reporter cells were transfected with pCBASCE-I to induce targeted damage. 16 hours prior to analyses, cells were treated with 1 µM olaparib. GFP positive events were recorded using flow cytometry. (N = 1, n ≥ 50000 cells, mean).

RAD51 mediates the diverging point for the conservative HDR and the non-conservative SSA (Stark et al., 2004) by catalyzing the recognition of homology and strand exchange to form a joint molecule between a resected DNA end and the repair template (Ameziane et al., 2015). CRY1 was previously shown to regulate HDR through the expression of HDR factors including RAD51 (Shafi et al., 2021). I therefore tested whether the observed CRY1/HDR-deficiency, in this study, was also a consequence of RAD51 downregulation. Intriguingly, RAD51 levels were not affected in both single CRY1 or double CRY depleted cells. Instead, CRY2 depletion resulted in an overall increase of RAD51 levels after IR exposure (Figure 16A). These results imply CRY1 HDR-deficient phenotype may not be a result of RAD51 levels but rather CRY2 promotes SSA possibly through antagonizing RAD51. Conversely, the CRY knockout cell lines displayed an overall and consistent decrease in IR-induced RAD51 levels (Figure 16B). Further assays are needed to determine the variation between knockdown and knockout.

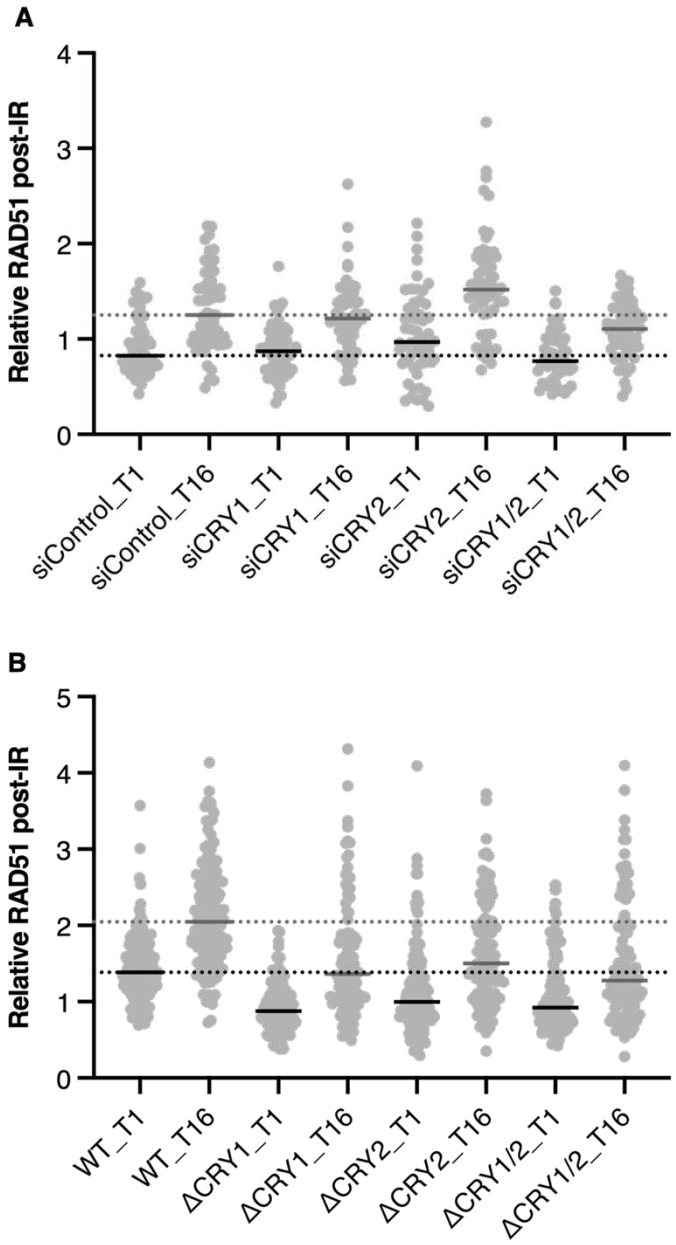

Figure 16. CRYs modulate IR-induced RAD51 levels.

A) CRY2 suppresses IR-induced RAD51. Nuclear RAD51 intensity of siRNA-mediated knockdown of indicated factors 16 hours post-IR (10 Gy) treatment. After which, cells were fixed and stained for RAD51 and imaged using fluorescence confocal imaging. (N = 2, n ≥ 50 cells, median). B) CRYs promote IR-induced RAD51. Nuclear RAD51 intensity of indicated knockout cell lines 1 and 16 hours post-IR (10 Gy) treatment. After which, cells were fixed and stained for RAD51 and imaged using fluorescence confocal imaging. (N = 2, n ≥ 50 cells, median).

3.3.3 CRYs suppress end-joining repair

Repair via end joining (EJ) can occur through two sub pathways: NHEJ and alt-EJ (Frit et al., 2014; Betermier et al., 2014). Given that CRY1 was reported to regulate the expression of NHEJ factors (Shafi et al., 2021), I hypothesized that CRY1 depletion would negatively impact NHEJ

activity. To test this, I used the U-2 OS repair reporter cell lines EJ5 and EJ2 for NHEJ and alt-EJ respectively. In EJ5 cells, I observed an increase in GFP signal suggesting NHEJ repair capacity is enhanced in the absence of CRY1 (Figure 17A). Moreover, all CRY knockdowns affected alt-EJ activity (Figure 17B). Taken together, the data suggests that CRY1 as well as CRY2 negatively regulates alt-EJ but CRY1 alone suppresses NHEJ.

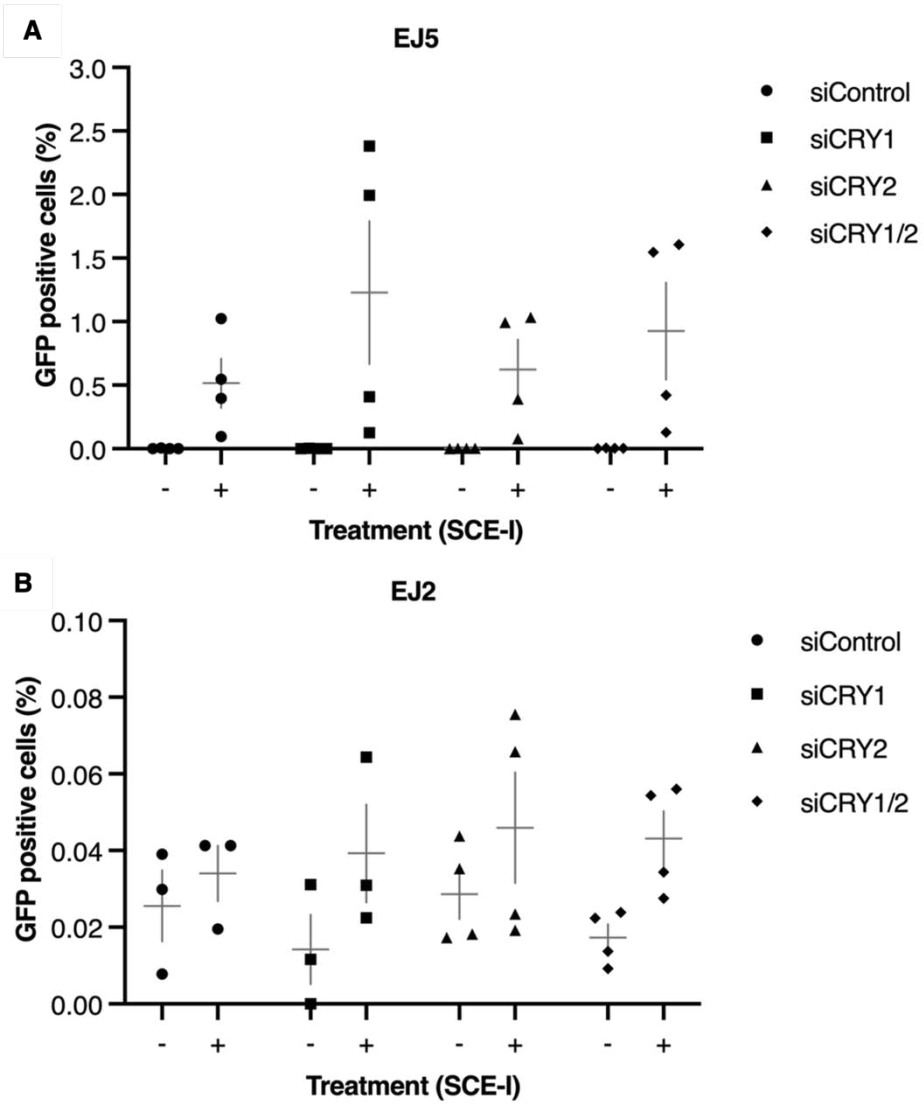

Figure 17. CRYs suppress end-joining repair.

A) CRY1 suppresses NHEJ. EJ5 reporter cells were transfected with indicated siRNA for 48 hours. 24 hours prior to analyses, cells were transfected with pCBASCE-I to induce targeted damage. GFP positive events were recorded using flow cytometry. (N = 3-4, n ≥ 50000 cells, mean ± s.e.m.). B) CRYs suppress alt-EJ. EJ2 reporter cells were transfected with indicated siRNA for 48 hours. 24 hours prior to analyses, cells were transfected with pCBASCE-I to induce targeted damage. GFP positive events were recorded using flow cytometry. (N = 3-4, n ≥ 50000 cells, mean ± s.e.m.).

The role of PARP/PARylation in NHEJ and alt-EJ to this date remains controversial (Isabelle et al., 2010; Mansour et al., 2010; Howard et al., 2015; Caron et al., 2019). PARP1/PAR has been

shown to promote NHEJ while suppressing alt-EJ (Isabelle et al., 2010; Caron et al., 2019). Nevertheless, PARP1/PAR has also been shown to promote alt-EJ (Mansour et al., 2010; Howard et al., 2015). Given that CRYs appear to altogether suppress repair via EJ, I next asked whether PARP inhibition also affects the activity of NHEJ and alt-EJ. Indeed, olaparib treatment abolished NHEJ and promoted alt-EJ activity (Figure 18) suggesting PARylation is critical for the decision between these two EJ pathways. However, these results are preliminary and require repetition for confirmation.

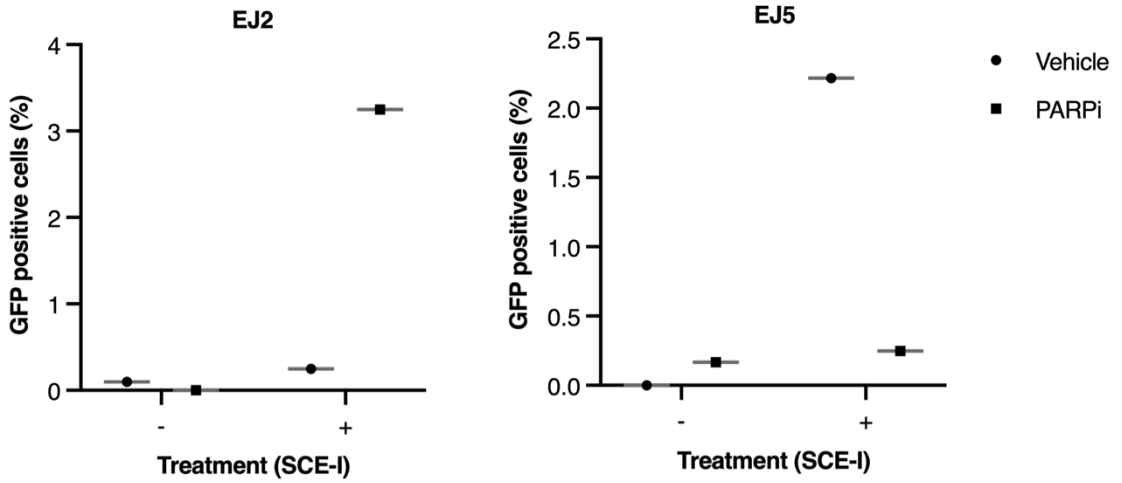

Figure 18. PARP activity controls end-joining repair.

PARP activity affects NHEJ and alt-EJ. EJ2 and EJ5 reporter cells were transfected with pCBASCE-I to induce targeted damage. 16 hours prior to analyses, cells were treated with 1 µM olaparib. GFP positive events were recorded using flow cytometry. (N = 1, n ≥ 50000 cells, mean).

53BP1, also known as TP53-binding protein 1, plays a key role in promoting NHEJ by counteracting BRCA1 and consequently HR. 53BP1 foci formation thus serves as an indicator for NHEJ (Ameziane et al., 2015). Based on the EJ repair assays, I next asked whether 53BP1 levels were also affected by CRY. Unexpectedly, siRNA-mediated silencing of CRYs resulted in a reduction of 53BP1 levels after IR treatment (Figure 19A) suggesting CRYs positively regulates IR-induced 53BP1 levels. On the other hand, CRY1 knockout led to an increase in 53BP1 level 16 hours after treatment; whereas CRY2 knockout displayed an overall decrease both 1 and 16 hours after exposure (Figure 19B). While CRY1 data was contradicting (knockdown versus knockout), CRY2 depletion consistently decreased IR-induced 53BP1 levels suggesting CRY2 plays a critical role in promoting 53BP1 in response to IR. Further assays are needed to determine the variation between knockdown and knockout.

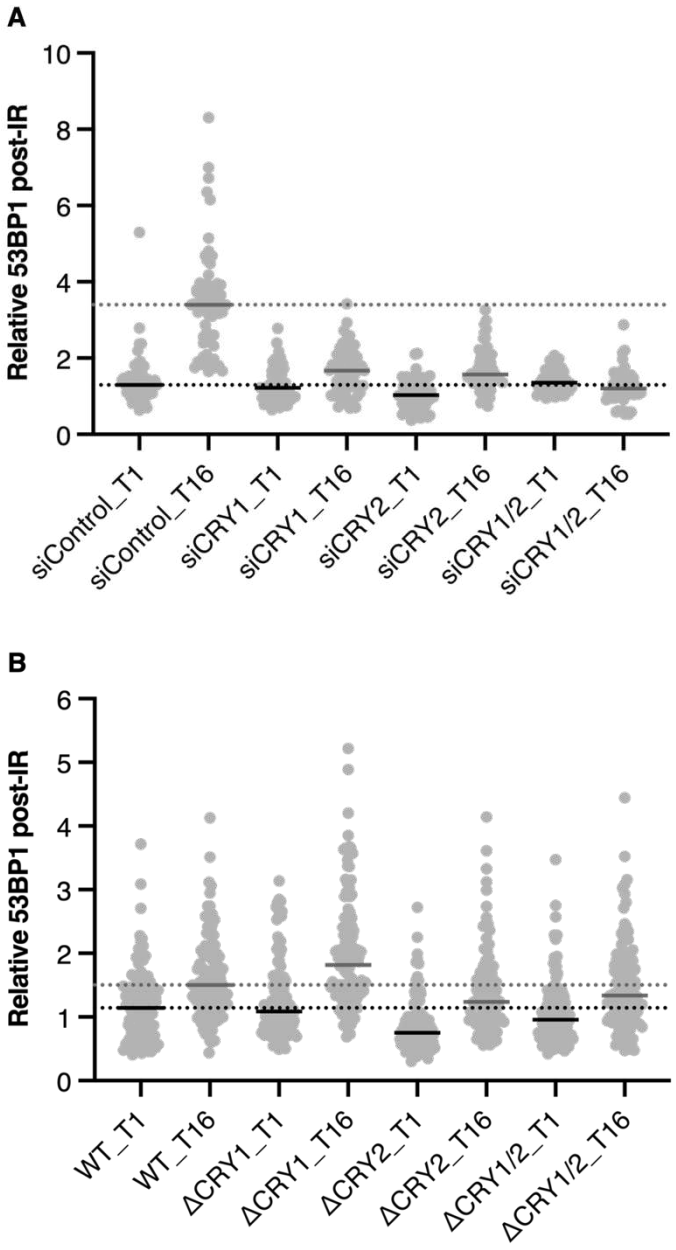

Figure 19. CRYs modulate IR-induced 53BP1 levels.

A) CRY2 promotes IR-induced 53BP1. Nuclear 53BP1 intensity of siRNA-mediated knockdown of indicated factors 16 hours post-IR (10 Gy) treatment. After which, cells were fixed and stained for 53BP1 and imaged using fluorescence confocal imaging. (N = 2, n ≥ 50 cells, median). B) CRY2 modulates IR-induced 53BP1. Nuclear 53BP1 intensity of indicated knockout cell lines 1 and 16 hours post-IR (10 Gy) treatment. After which, cells were fixed and stained for 53BP1 and imaged using fluorescence confocal imaging. (N = 2, n ≥ 50 cells, median).

3.4 CRY1 modulates cancer cell survival

3.4.1 CRY1 modulates cell survival in response to DSB-induction

In the last section, I sought to address whether the observed recruitment and repair phenotypes impact cell survival in response to genomic insults. I induced CRY1 knockdown and assessed whether CRY1 is required for clonogenic capacity in response to DSB-induction by IR and bleomycin (Figure 20B). After IR exposure, cells depleted of CRY1 exhibited a similar proliferation profile to that of siControl cells with an overall mild increase (Figure 20A, left panel). In agreement, Bleomycin treatment induced similar results (Figure 20A, right panel) suggesting that CRY1 depletion does not sensitize cells to DSB induction but instead renders cells more resilient. Unexpectedly, CRY1 knockout cells exhibited an opposite phenotype (Figure 20C). This phenotype was not present in either CRY2 or the double CRY knockout cells (Figure 20C) suggesting a long-term deletion of CRY1 sensitizes cancer cells to IR treatment.

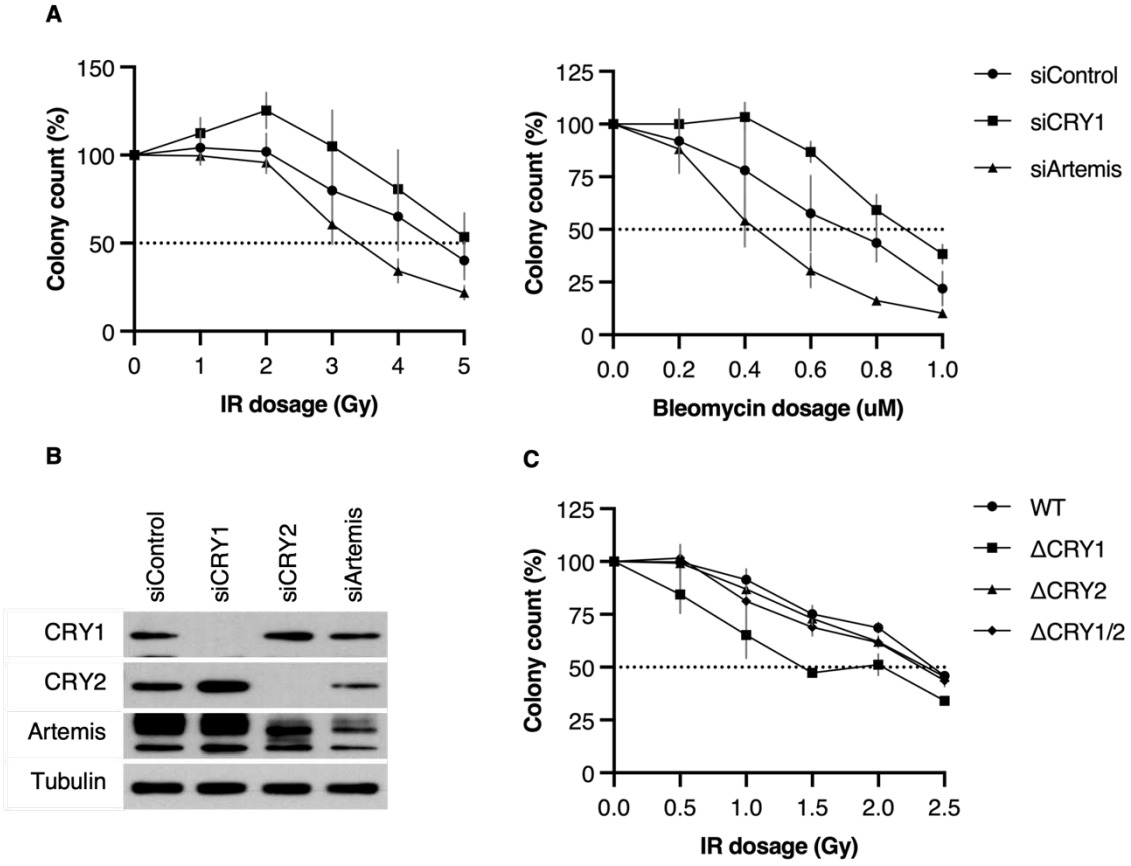

Figure 20. CRY1 modulates cell survival in response to DSB-induction.

A) CRY1 suppresses osteosarcoma survival in response to IR and bleomycin. siRNA-mediated knockdown of indicated factors were treated with titrated IR (left panel) and bleomycin (right panel) dosages and left to recover for 8 days. Cells were stained and imaged to assess the formation of colonies using Fiji ImageJ. (N = 3, n = 3, mean ± s.e.m.). B) Expression levels of the indicated factors 48 hours post transfection. C) CRY1 promotes osteosarcoma survival in response to IR. Knockout cell lines were treated with titrated IR dosages and left to recover for 8

days. Cells were stained and imaged to assess the formation of colonies using Fiji ImageJ. (N = 3, n = 3, mean ± s.e.m.).

3.4.2 CRY1 regulates cell survival in response to UV in a cell type specific manner

Previous studies have shown that CRYs regulate NER activity through XPA expression levels and potentially other repair factors (Kang et al., 2010; Anabtawi et al., 2021; Shafi et al., 2021). In combination with the data in this study, I hypothesized that CRY1 knockdown negatively impacts clonogenic capacity of U-2 OS cells in response to NER-induction. Surprisingly, at higher UV-C dosages, siCRY1 cells were less sensitive to the treatment (Figure 21A&B, left panel). However, cisplatin treatment did not yield the same results (Figure 21A, right panel). I further examined the observed phenotype using the CRY knockout cell lines. Similar to the previous section (DSB treatment), CRY1 knockout showed an overall decrease in clonogenic ability (Figure 21C) suggesting a long-term deletion of CRY1 sensitizes cancer cells to UV-C treatment.

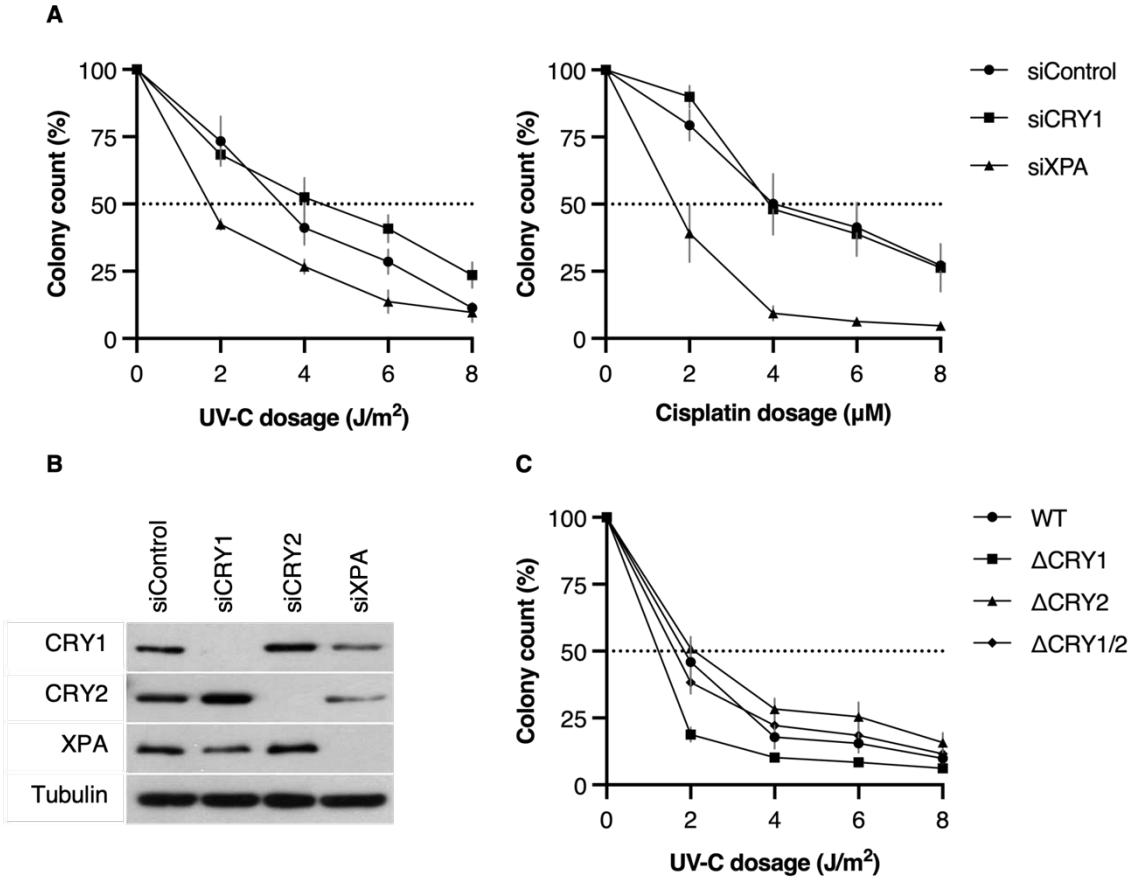

Figure 21. CRY1 modulates cell survival in response to UV treatment.

A) CRY1 suppresses osteosarcoma survival in response to UV. siRNA-mediated knockdown of indicated factors were treated with titrated UV-C (left panel) and cisplatin (right panel) dosages and left to recover for 8 days. Cells were stained and imaged to assess the formation of colonies using Fiji ImageJ. (N = 3, n = 3, mean ± s.e.m.). B) Expression levels of the indicated factors 48

hours post transfection. C) CRY1 promotes osteosarcoma survival in response to UV-C. Knockout cell lines were treated with titrated UV-C dosages and left to recover for 8 days. Cells were stained and imaged to assess the formation of colonies using Fiji ImageJ. (N = 3, n = 3, mean ± s.e.m.).

To test whether this CRY1-mediated desensitization is specific to osteosarcoma cells, I performed the same experiment using the human cervical cancer- HeLa and human colon cancer- HCT116 cell lines. CRY1 silencing sensitized HeLa cells to UV-C treatment whereas HCT116 cells were not affected (Figure 22). Although the findings on temporal and permanent depletion of CRY1 are conflicting, CRY1 seems to regulate cell survival in response to UV-C in a cell type dependent manner.

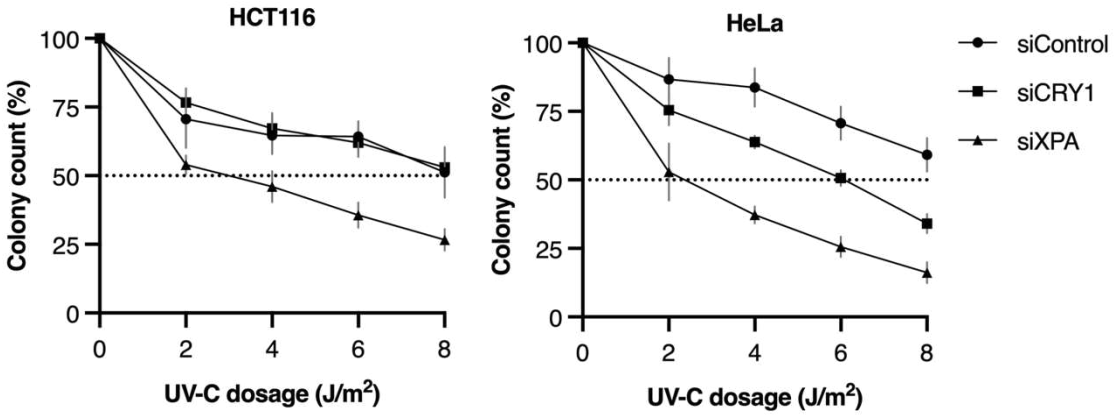

Figure 22. CRY1 regulates cell survival in response to UV treatment in a cell type dependent manner.

CRY1 promotes adenocarcinoma survival in response to UV. siRNA-mediated knockdown of indicated factors in HCT116 (left panel) and HeLa (right panel) were treated with titrated UV-C dosages and left to recover for 8 days. Cells were stained and imaged to assess the formation of colonies using Fiji ImageJ. (N = 4, n = 3, mean ± s.e.m.).

3.4.3 CRY1 regulates UV-Induced transcription recovery

In U-2 OS, CRY1 mildly desensitized cells towards UV-C treatment. The observed phenotype may be a consequence of enhanced repair of 6-4PPs and/or CPDs. These two lesions are structurally distinct. While 6-4PPs cause more distortion in the double helical structure than CPDs, 6-4PPs occur less frequently (Kim et al., 1995; Perdiz et al., 2000) and are much more efficiently repaired by NER (6-4PP: 2 hours; CPD: 33 hours) (Young et al., 1996). If unrepaired, a single 6-4PP lesion is more likely to induce apoptosis than a CPD lesion (Nakajima et al., 2004; Lo et al., 2005) making CPDs a higher risk for mutagenesis. To test whether CRYs impact the resolution of these lesions, I induced siRNA-mediated silencing of CRYs and XPA (NER factor) and measured 6-4PP and CPD signals after UV-C treatment. I observed a mild delay in 6-4PP removal in siCRY1 and siXPA at 1 hour but not 16 hours after UV-C treatment (Figure 23A) suggesting

CRY1 may regulate the speed of which 6-4PPs are repaired. However, CRY depletion and deletion did not affect the overall repair rate of CPD with the exception of the double CRY knockout displaying a non-significant decrease (Figure 23B). In agreement, UV-induced γH2AX was not affected by CRY abrogation (Figure 23C). In summary, CRY1 may regulate the initial repair rate of 6-4PP without impacting the overall repair of 6-4PP and CPD.

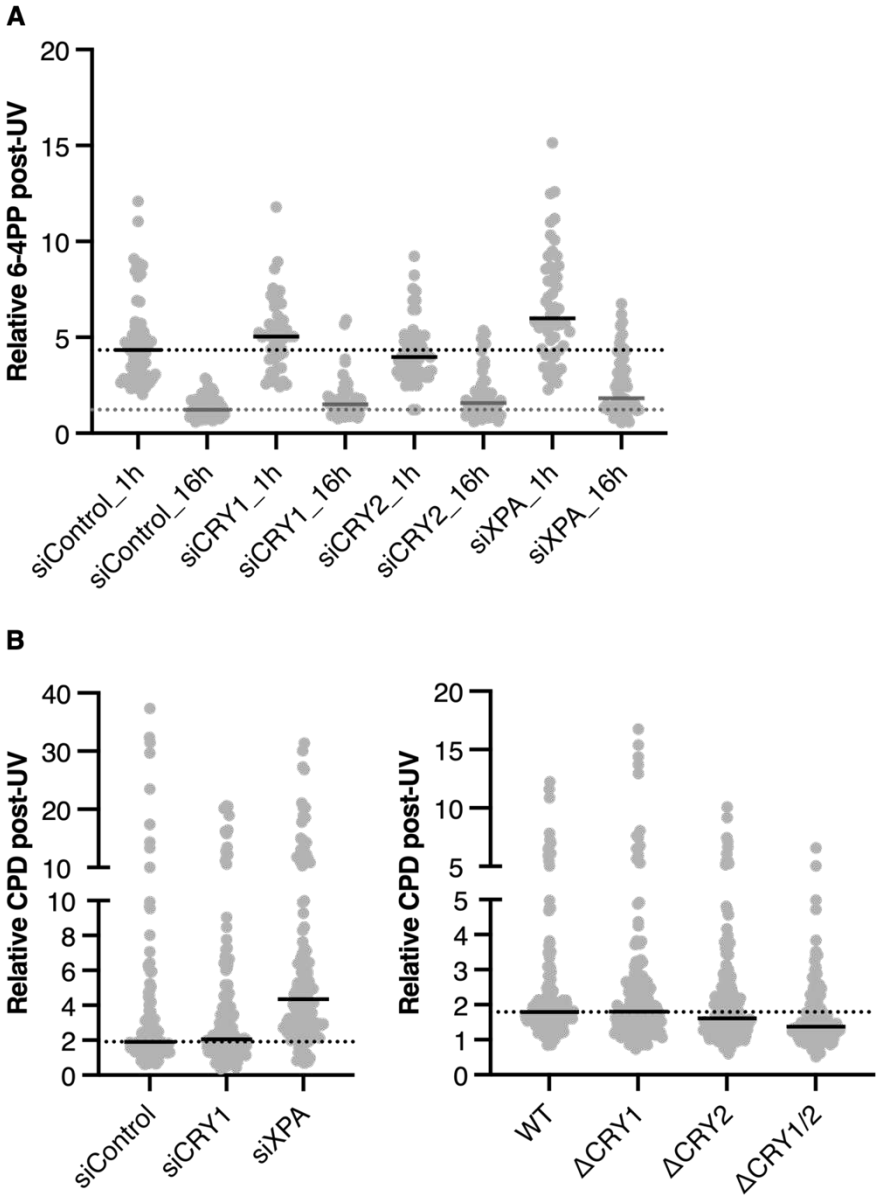

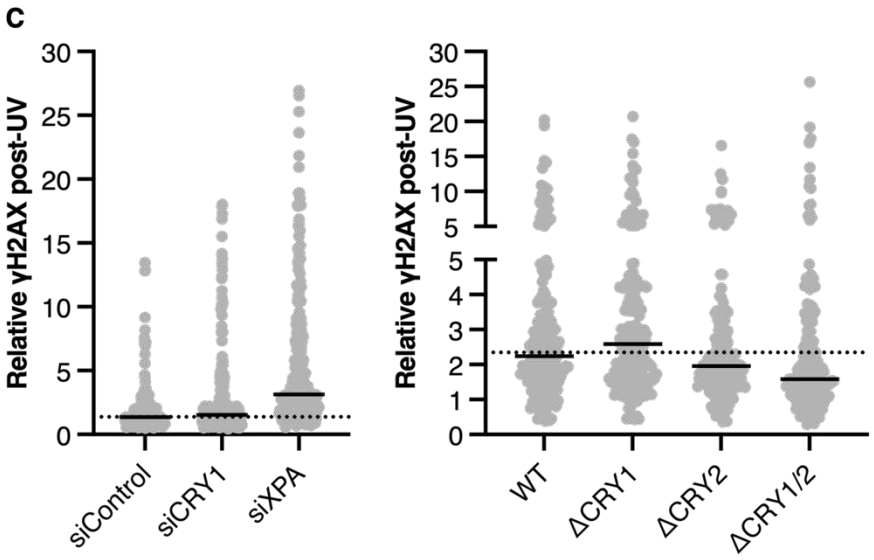

Figure 23. CRY1 regulates 6-4PP repair rate.

A) CRY1 silencing causes a delay in 6-4PP repair. Nuclear 6-4PP intensity of siRNA-mediated knockdown of indicated factors 1 and 16 hours post 4J/m^2 UV-C treatment. Cells were fixed and stained for 6-4PP and imaged using fluorescence confocal imaging. (N = 1, n ≥ 50 cells, median). B) CRYs do not affect CPD resolution. Nuclear CPD intensity of indicated knockdown (left panel) and knockout (right panel) cell lines 16 hours post 4J/m^2 UV-C treatment. Cells were fixed and stained for CPD and imaged using fluorescence confocal imaging. (N = 3, n ≥ 50 cells, median). C) CRYs do not affect UV-C-induced γH2AX signaling. Nuclear γH2AX intensity of indicated knockdown (left panel) and knockout (right panel) cell lines 16 hours post 4J/m^2 UV-C treatment. Cells were fixed and stained for γH2AX and imaged using fluorescence confocal imaging. (N = 3, n ≥ 50 cells, mean)

Thus far, CRYs showed little to no effect on UV-induced NER except for CRY1 in 6-4PP repair rate. However, functional assays in the previous section measure total NER which consists of two subtypes: GG-NER and TC-NER. While GG-NER is responsible for sensing and removing lesions across the genome, TC-NER only occurs at stalled RNAPII (Park et al., 2016). Therefore, to test whether CRYs play a part in TC-NER, I examined transcription recovery of both knockdown and knockout cells in response to UV-C treatment. Upon silencing, CRY1 blunted transcription recovery (Figure 24, left panel). However, CRY1 knockout cells had no effect on transcription recovery after UV exposure (Figure 24, right panel). Further assays are needed to determine the variation between knockdown and knockout.

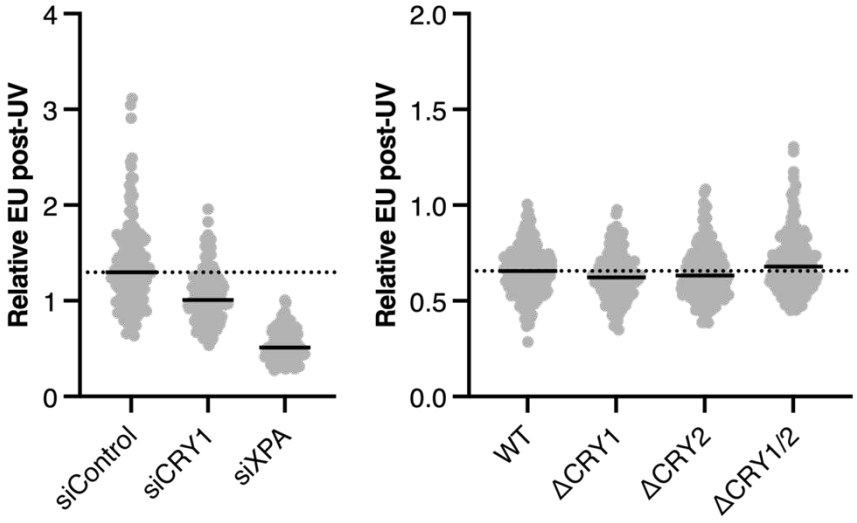

Figure 24. CRY1 regulates UV/NER-induced transcription recovery.

CRY1 promotes transcription recovery. Transcription activity 16 hours after 4 J/m^2 UV-C treatment, followed by 2 hours of pulse labeling with 5-ethynyl uridine (EU) in indicated knockdown (left panel) and knockout (right panel). Transcription activity was assessed by EU labeling and imaged using fluorescence confocal imaging. (N = 3, n ≥ 50 cells, median).

4. Discussion

4.1 PARP1-mediated PARylation recruits CRYs to damage sites

PARylation is a pivotal PTM that appears rapidly at DNA damage sites and is required to recruit DDR proteins and chromatin remodelers (Haince et al., 2008; Izhar et al., 2015; Xie et al., 2015; Sellou et al., 2016; Smith et al., 2018; Caron et al., 2019). Using microirradiation coupled with live-cell imaging, I established that both CRYs rapidly recruit to sites of DNA damage and are dependent on the PARylation activity of the major DNA damage sensor- PARP1 (Figure 6, 10&11). Similar to the majority of PARP1 substrates, CRYs are unable to recruit to LID sites when PARylation is inhibited (Bai et al., 2015; Thomas and Tulin, 2013). PAR-mediated recruitment can occur through two distinct mechanisms: 1) PAR-mediated interaction (Sellou et al., 2016) and 2) PAR-mediated chromatin decompaction (Smith et al., 2018). However, unlike the recruitment of those requiring chromatin decompaction by PARylation, CRYs exhibit similar recruitment kinetics to PARP1 (Appendix A1) prompting the possibility of a direct binding to PARylated PARP1 and/or PAR. On account of the relatively open conformation present in mammalian CRY PHRs (Czarna et al., 2013, Xing et al., 2013), the concept of PAR-binding is conceivable as this structural variation could potentially reduce and/or alter CRY substrate specificity. To determine whether there is an interaction between CRYs, PAR and PARP1, there are several biochemical approaches one can use such as co-IP, dot/slot-blot, thermal shift assay and isothermal titration calorimetry.

Intriguingly and in line with the notion of PAR-binding, I found that several CRY interaction partners (based on MS data from Papp et al., 2015) are targets of PARylation (ADPriboDB 2.0). One of which is USP7. USP7 is implicated in UV-induced TC-NER (Schwertman et al., 2012) as well as IR-induced DDR (Papp et al., 2015). This raises the question whether PARP1/PAR-mediated CRY recruitment to LID sites is achieved through its interaction with PARylated USP7. To test the potential involvement of USP7, one could examine CRY recruitment to DNA damage sites in USP7 deficient cells or induce USP7 inhibition with the small molecule- HBX19818. Additionally, several other CRY interaction partners (Papp et al., 2015) have been shown to interact with PARP1 and/or are PARylated (Based on MS data from Papp et al., 2015 and Isabelle et al., 2010; ADPriboDB 2.0). Three of these are well-established DSB DDR factors: PRKDC, XRCC5 (KU70) and XRCC6 (KU80). These three components form the DNAPK complex and are crucial for promoting NHEJ. Much like CRYs, KU80 recruits to LID sites through PARP1/PARylation (Caron et al., 2019). To determine whether DNAPK is involved in PARP1/PAR-dependent CRY recruitment, one could examine CRY recruitment in cells deficient in PRKDC, XRCC5 and/or XRCC6 to assess the impact of DNAPK. That being said, CRYs do not possess any of the established PAR-binding motifs (Wei and Yu, 2016) nor have they been

found to directly interact with PARP1. The lack of a canonical PAR-binding motif in CRYs leads me to speculate that the PAR-dependent recruitment may be established through interacting with other PAR readers. In conclusion, the precise molecular mechanism of which CRYs recruit to DNA damage remains unclear and calls for further investigation.

4.2 CRY regulates DSB repair

CRYs, in particular CRY1, have been reported to regulate DSB repair through phase-advancement (Engelen et al., 2013; Papp et al., 2015) and transcription regulation as well as the activation of pivotal DNA damage factors such as ATM and CHK2 (Papp et al., 2015; Shafi et al., 2021). Here I showed that CRY1 silencing results in an accumulation of IR-induced γH2AX (Figure 13A). Persistent γH2AX can be a result of impaired DSB repair or impaired dephosphorylation of γH2AX after repair. However, this siCRY1-induced γH2AX accumulation was not observed in CRY1 null cells. In fact, all CRY null cell lines exhibited a decrease in γH2AX levels both at an early (1h) and late (16h) stage in IR-induced DDR (Figure 13B) suggesting either an increased DSB repair capacity or impaired phosphorylation of H2AX at DSB sites. There are three possible ways to explain the contradicting phenotypes between temporal siRNA-mediated silencing and permanent deletion of CRY1. For one, residual CRY1 (though undetectable by immunoblotting) from siRNA-mediated knockdown may be sufficient for the resulting accumulation of γH2AX through either of the aforementioned causations. The second possibility is that the increase in γH2AX is an off-target effect caused by the siRNA. Lastly, as critical transcription regulators, CRY null cells may have undergone clonal selection thereby masking the effects of CRY-depletion in the context of IR-induced γH2AX. One can simultaneously address these three points by transfecting CRY null cells with pooled siRNA to assess the IR-induced γH2AX phenotype. In addition, CRY2 was unfortunately not included in the siRNA/γH2AX and therefore remains to be tested.

In a previous study, it was shown that CRY1 ablation arrest cells in G2/M without damage induction (cell type specific) possibly through derepression of G2/M checkpoint genes (Shafi et al., 2021). That being said, CRY1's role in the DDR-induced G2/M checkpoint was not directly addressed. In this study, I demonstrated that CRY1 silencing does not significantly impair IR-induced G2/M checkpoint activation (Figure 12B). However, and unexpectedly, CRY2 depletion resulted in an impaired G2/M checkpoint (Figure 12B) suggesting a new and imminent role for CRY2 in maintaining genomic integrity. As I previously pointed out in the IR-induced γH2AX experiment, temporal and permanent depletion of the CRY homologs conferred opposite results. Therefore, to confirm CRY2's role in the G2/M checkpoint, further testing with CRY null cells is necessary.

DSB is predominantly repaired through HDR, SSA, alt-EJ and NHEJ (Scully et al., 2019). These DDR pathways are tightly regulated throughout the cell cycle and are mechanistically distinct (Mao et al., 2008). In this study, I found that CRY1 promotes HDR (Shafi et al., 2021) capacity

whereas both CRY homologs are required for a functional SSA (Figure 14C). Moreover, CRY1 impedes NHEJ while both CRY homologs hinder alt-EJ (Figure 17A&B). These results taken together imply that while CRY1 promotes HR and inhibits NHEJ, CRY2 promotes SSA and antagonizes alt-EJ. One of the distinctions between HR and NHEJ is DNA end resection. RAD51 foci formation is a marker for end resection and is a critical mediator between the choices of HDR and SSA (Bhargava et al., 2016). In agreement with CRY2 promoting SSA, CRY2 seems to repress/inhibit RAD51 foci formation (Figure 16A). However, double CRY silencing blunted this inhibitory phenotype. Taken together, I speculate CRY1 promotes HDR over SSA possibly through antagonizing CRY2-mediated RAD51 inhibition.

The choice between HR and EJ pathways often falls upon factors that either promote or inhibit resection. 53BP1, the TP53 binding protein, stimulates NHEJ by antagonizing DNA resection factors (Daley et al., 2014). Since CRY1 abrogation resulted in an enhanced NHEJ activity, the idea that CRY1 negatively regulates 53BP1 was conceivable. Conversely, I found that CRY ablation led to a decrease in 53BP1 levels (Figure 19A) suggesting if anything, CRYs are required for IR-induced 53BP1 foci formation thereby promoting NHEJ. However, it has been reported that RIF1 is the critical effector of 53BP1 in hindering end resection which ensures NHEJ as the dominant DSB repair pathway. ATM-dependent phosphorylation of 53BP1 is essential for RIF1 recruitment to DSB sites (Escribano-Diaz et al., 2013). This raises the question whether CRY1 inhibits NHEJ through regulating 53BP1 phosphorylation thereby affecting RIF1 recruitment rather than directly affecting 53BP1 localization to DSB sites. To address this, one can test IR-induced 53BP1 and RIF1 colocalization in siCRY1 cells treated with ATM or PIKK inhibitor.

In contrast to CRY1, CRY2 appears to possess a specific functional role in regulating the sub pathways- SSA and alt-EJ. While SSA and alt-EJ pathways both involve annealing of flanking homology to bridge a DSB, these events are distinct. In particular, the recombinase- RAD52 mediates synapsis of the annealing intermediate to promote SSA but is dispensable for alt-EJ (Bennardo et al., 2008). Since RAD52, much like RAD51, forms IR-induced foci (Kitao and Yuan, 2002), it is necessary to test CRY2's effect on RAD52 foci formation in order to delineate CRY2's role in promoting SSA while inhibiting alt-EJ.

Lastly, CRY1 depletion desensitizes osteosarcoma cells in response to DSB induction with IR and bleomycin (Figure 20A). On the contrary, permanent deletion of CRY1 sensitizes cells in response to these genomic insults while double CRY knockout blunted this sensitization (Figure 20C). Taking into consideration that human somatic cells predominantly utilize the efficient but error-prone NHEJ as the primary DSB repair pathway at all cell cycle stages (Mao et al., 2008), it is conceivable that the downregulation of HR activity does not affect the overall cell survival in response to DSB induction. Instead the biological significance of CRYs in genomic maintenance is whether cells accumulate potentially hazardous mutations. This requires further testing and comparison of siCRY and HR factors rather than NHEJ factors on DSB-induced cell death as well as examining mutation rate in CRY deficient cells.

4.3 Potential function of the PARP1/CRY axis in DSB repair

In earlier studies, PARP1 was established as a suppressor of HDR through promoting NHEJ (Schultz et al., 2003; Claybon et al., 2010). PARP1 regulation of DSB repair pathways is achieved through blocking resection by interacting with and recruiting the DNAPK complex, 53BP1 and RIF1 to DSB sites (Isabelle et al., 2010; Caron et al., 2019). As a consequence, PARP1 abrogation leads to increased DNA resection and an increase of HR *in cellulo* (Caron et al., 2019). Conversely, PARP1 has also been shown to promote HDR (Xie et al., 2015) via mediating chromatin decondensation (Chen et al., 2019). Furthermore, PARPs have been reported to promote alt-EJ (Mansour et al., 2003; Audebert et al., 2004; Wang et al., 2006; Howard et al., 2015). The precise role of PARPs in alt-EJ, however, has yet to be defined. It is important to point out that with respect to mechanism, PARPi treatment may not be equivalent to the genetic loss of PARP1 and PARP2 for the reason that PARPi not only impairs certain repair pathways but also blocks repair by trapping PARP complexes at DNA damage sites (Murai et al., 2012).

Based on the data present in this study, PARPi treatment had no clear effects on neither HDR nor SSA (Figure 15). However, PARP inhibition significantly reduced NHEJ and enhanced alt-EJ activity respectively (Figure 18) suggesting PARP activity is critical for promoting NHEJ as well as suppressing alt-EJ. That being said, the possibility of PARP1 and/or PARP2's involvement cannot be fully dismissed until one assesses the impact of PARP1 and PARP2 depletion on HDR, SSA, alt-EJ and NHEJ.

Previously I concluded that CRY1 governs the choice between HR (HDR and SSA) and NHEJ; while CRY2 promotes SSA and suppresses alt-EJ. The only overlapping DSB repair phenotype that may suggest an epistatic relationship between PARP1/PAR and CRYs is the suppression of alt-EJ. Therefore, I speculate that PARP1/PAR-mediated CRY1 and CRY2 recruitment to DNA damage sites to actively inhibit alt-EJ activity. To test this, one can inhibit PARP activity in CRY-depleted EJ2 cells to examine whether the derepression of alt-EJ is equivalent to that of siCRY only and PARPi-treated only cells.

4.4 CRY1 may regulate 6-4PP repair

While CPDs and 6-4PPs both contribute to UV-induced sensitization in NER-deficient cells, CPDs are found to be responsible for UV-sensitivity in NER-proficient cells (Lima-Bessa et al., 2007). In combination with my observation that CRYs do not affect CPD removal, it is expected that CRY depletion does not render cells sensitive to UV-C sensitivity (U-2 OS and HCT116 cell lines) (Figure 21A&22). What is rather curious is that CRY1 silencing sensitizes HeLa cells towards UV treatment (Figure 22). Given that CRYs promote TP53 null cancer cell survival by repressing UV-induced P73 expression (Ozturk et al., 2009; Lee et al., 2011; Lee et al., 2013), it is plausible that the cell type specific induction of UV sensitivity (siCRY1 in HeLa) is TP53-dependent. To test

this, one can compare TP53 levels across these cell lines or directly probe for UV-induced P73 levels CRY1 depleted HeLa cells.

Based on functional data, CRY1 and CRY2 silencing does not seem to affect the repair of UV-C-induced 6-4PPs (Figure 23A). However, I observed an increase in protein level of the respective homologs upon single knockdowns (siCRY1 cells exhibit an increase of CRY2 protein level and vice versa) (Figure 21B). To fully exclude the possibility that the CRY homologs can compensate each other in 6-4PP repair, further testing with double knockdown and knockout cell lines is required. On the other hand, CRY1 and CRY2 deficiency (both knockdown and knockout) did not lead to CPD accumulation (Figure 23B) suggesting that neither of the homologs are necessary for the repair of CPDs. Moreover, UV-C-induced γH2AX levels in CRY deficient (both knockdown and knockout) cells were similar to that of siControl and wild-type respectively (Figure 23C). Given that ATR is the major regulator of UV-induced γH2AX (Hanasoge et al., 2007) and has been reported to be negatively regulated by CRY1 in a time-dependent manner (Kang et al., 2014), one would expect siCRY1 to affect UV-induced γH2AX as well. To be noted, a recent study showed that only 6-4PP and not CPD lesions activate the ATR/CHK1 DDR (Hung et al., 2020). Additionally, γH2AX induction is a result of NER (Marti et al., 2006) but can occur in GG-NER-deficient cells as well (Oh et al., 2011). This leads one to question whether γH2AX is an appropriate marker for assessing UV-induced NER capacity. Nonetheless, many questions remain to be answered such as does temporal depletion of CRY2 affect UV-induced γH2AX? Do CRYs influence UV-induced γH2AX at earlier time points? Do CRYs play a role in UV-induced ATR/CHK1 activation in osteosarcoma cells?

In this thesis, I reported that XPA and CRY1 silencing impaired and 'blunted' transcription recovery after UV-C exposure respectively (Figure 24) implying the observed CRY1 phenotype may not be a consequence of NER (GG-NER plus TC-NER) deficiency. Intriguingly, this 'blunting' phenotype was absent in CRY1 null cells (Figure 24). This raises the question whether CRY1 is necessary for full transcription recovery after UV-induced TC-NER. These opposing phenotypes observed in siRNA-mediated silencing will require further testing with CRY1 null cells transfected with the siRNA pool to exclude potential siRNA-induced off-target effects and the possibility of clonal selection. Taken together, it is unlikely that CRY1 and CRY2 play a direct/imminent role in GG-NER and the repair of CPD lesions. Whether CRYs possess a functional role in repairing 6-4PP lesions remains to be determined. Lastly, since XPA plays a vital role in both GG-NER and TC-NER, an additional experiment to compare siCRYs and TC-NER factors is called for in order to either exclude or propose a functional role for CRY1 in TC-NER.

4.5 Potential function of the PARP1/CRY axis in NER

Previous studies have shown that PARP inhibition or PARP1 depletion decreases the efficiency of UV lesions removal in human cells (Pines et al., 2012; Robu et al., 2013; Robu et al., 2017). PARP1/PAR regulates GG-NER through associating with proteins i.e. DDB2 and XPC which are

essential for efficient recognition and subsequent repair (Pines et al., 2012; Robu et al., 2013; Robu et al., 2017). Additionally, DDB2, in turn, has been shown to facilitate PARylation of UV-damaged chromatin thereby increasing the efficiency of lesion recognition (Pines et al., 2012).

My results show that PARP inhibition similar to siXPA leads to accumulation of UV-induced γH2AX (Appendix A2)(Figure 23A). Given that γH2AX occurs both in a NER-dependent (Marti et al., 2006) and independent manner (Oh et al., 2011), it is unclear whether UV-induced PARPi γH2AX accumulation was a result of a defective GG-NER. Moreover, PARP inhibition impaired transcription recovery similar to that of XPA silencing. This transcription impairment was not exacerbated in PARPi treated siXPA cells suggesting an epistatic relationship in NER-induced transcription recovery (Appendix A3). Intriguingly, PARP inhibition led to a mild sensitization towards both UV-C and cisplatin treatment (Appendix A4) implying that impaired repair may not heavily affect cell survival.

Previously I concluded that CRYs are not required for CPD repair; nonetheless CRY1 seems important for the full recovery of transcription (Figure 24). Thus far, the only overlapping UV/NER-associated phenotype of CRYs and PARPs is transcription recovery. This prompts the possibility of epistasis between PARP1/PAR and CRY1 in TC-NER. I therefore speculate PARP1/PAR recruits CRY1 to UV-induced DNA damage sites to promote TC-NER. To test this, one can treat CRY1-depleted cells with PARPi and examine transcription activity after UV exposure. There is also the possibility of a PARP1/CRY1 axis in 6-4PP repair. Unfortunately, I did not acquire data to either support or refute the presence of the PARP1/CRY2 axis in NER and thus remains an intriguing question.

5. Outlook

The connection between the molecular clock and DDR has been a long-standing interest in the field of chrono- and cancer biology (Sancar and Gelder, 2021). In 1965, Colin Pittendrigh presented a model- the escape-from-light hypothesis. His model, in essence, proposes the daily gating of cell division and DNA damage as constraining factors that devised and shaped the molecular clock (Pittendrigh, 1993). Indeed, cumulative evidence underscores the significance of CRYs as transcriptional regulators in various clinically relevant DDR pathways (Papp et al., 2015; Shafi et al., 2021). However, CRYs' more imminent and direct roles in the cellular response to induced DNA damage has proved elusive.

This study provides first hand evidence to support a molecular connection between DNA damage, PARylation and CRY function thereby establishing a newfound link between genome integrity, NAD^+-metabolism and the molecular clock. Functional assays herein indicate CRY1 critically regulates the choice between high-fidelity HR and error-prone NHEJ, whereas CRY2 serves as a crucial node between the sub pathways- SSA and alt-EJ. Unexpectedly, CRYs exhibited no significant impact on UV-induced DDR with the exception of CRY1 in 6-4PP repair rate and transcription recovery. This suggests that human CRYs, in comparison to the closely related photolyases, have adopted alternative functions in order to maintain genome integrity. Taking into consideration that the expression of CRYs, in primates, are tightly regulated and are found most abundant at exclusive phases (Mure et al., 2018), it is conceivable that the PARP1/CRY1 and PARP1/CRY2 axis can only occur at distinct phases consequently creating temporal partitioning of DDR pathways. To summarize, I propose two preliminary models where A) PARP1-mediated PARylation recruits CRYs to DSB sites fostering a competition between NHEJ and HR, and B) PARP1-mediated PARylation recruits CRY1 to UV lesions to facilitate TC-NER. The precise mechanism of how PARP1 and CRYs orchestrates these events remains a compelling option for future studies.

In conclusion, the findings herein solidify a direct link between two major cellular processes and position PARP1 and CRYs at the center of a dynamic crosstalk between the DDR machinery and the molecular clock. The impact of experimental CRY activators and inhibitors on the molecular clock raise the exciting possibility of modulating the efficacy of DDR-targeting therapeutics through novel combinatorial drug treatments. Additional in-depth mechanistic insights will determine how current and future cancer therapies can be adapted and improved by integrating the molecular clock into clinical designs and ultimately facilitating the application of cancer chronotherapy.

References

Ameziane N, May P, Haitjema A, van de Vrugt HJ, van Rossum-Fikkert SE, Ristic D, Williams GJ, Balk J, Rockx D, Li H, Rooimans MA, Oostra AB, Velleuer E, Dietrich R, Bleijerveld OB, Maarten Altelaar AF, Meijers-Heijboer H, Joenje H, Glusman G, Roach J, Hood L, Galas D, Wyman C, Balling R, den Dunnen J, de Winter JP, Kanaar R, Gelinas R, Dorsman JC. A novel Fanconi anaemia subtype associated with a dominant-negative mutation in RAD51. Nat Commun. 2015 Dec 18;6:8829. doi: 10.1038/ncomms9829. PMID: 26681308; PMCID: PMC4703882.

Anabtawi N, Cvammen W, Kemp MG. Pharmacological inhibition of cryptochrome and REV-ERB promotes DNA repair and cell cycle arrest in cisplatin-treated human cells. Sci Rep. 2021 Sep 9;11(1):17997. doi: 10.1038/s41598-021-97603-x. PMID: 34504274; PMCID: PMC8429417.

Audebert M, Salles B, Calsou P. Involvement of poly(ADP-ribose) polymerase-1 and XRCC1/DNA ligase III in an alternative route for DNA double-strand breaks rejoining. J Biol Chem. 2004 Dec 31;279(53):55117-26. doi: 10.1074/jbc.M404524200. Epub 2004 Oct 21. PMID: 15498778.

Bai P. Biology of Poly(ADP-Ribose) Polymerases: The Factotums of Cell Maintenance. Mol Cell. 2015 Jun 18;58(6):947-58. doi: 10.1016/j.molcel.2015.01.034. PMID: 26091343.

Bartek J, Lukas J. Mammalian G1- and S-phase checkpoints in response to DNA damage. Curr Opin Cell Biol. 2001 Dec;13(6):738-47. doi: 10.1016/s0955-0674(00)00280-5. PMID: 11698191.

Bennardo N, Cheng A, Huang N, Stark JM. Alternative-NHEJ is a mechanistically distinct pathway of mammalian chromosome break repair. PLoS Genet. 2008 Jun 27;4(6):e1000110. doi: 10.1371/journal.pgen.1000110. PMID: 18584027; PMCID: PMC2430616.

Bétermier M, Bertrand P, Lopez BS. Is non-homologous end-joining really an inherently error-prone process? PLoS Genet. 2014 Jan;10(1):e1004086. doi: 10.1371/journal.pgen.1004086. Epub 2014 Jan 16. PMID: 24453986; PMCID: PMC3894167.

Bhargava R, Onyango DO, Stark JM. Regulation of Single-Strand Annealing and its Role in Genome Maintenance. Trends Genet. 2016 Sep;32(9):566-575. doi: 10.1016/j.tig.2016.06.007. Epub 2016 Jul 19. PMID: 27450436; PMCID: PMC4992407.

Buntz A, Wallrodt S, Gwosch E, Schmalz M, Beneke S, Ferrando-May E, Marx A, Zumbusch A. Real-Time Cellular Imaging of Protein Poly(ADP-ribos)ylation. Angew Chem Int Ed Engl. 2016 Sep 5;55(37):11256-60. doi: 10.1002/anie.201605282. Epub 2016 Jul 28. PMID: 27468728.

Börding T, Abdo AN, Maier B, Gabriel C, Kramer A. Generation of Human *CRY1* and *CRY2* Knockout Cells Using Duplex CRISPR/Cas9 Technology. Front Physiol. 2019 May 9;10:577. doi: 10.3389/fphys.2019.00577. PMID: 31143130; PMCID: PMC6521593.

Caron MC, Sharma AK, O'Sullivan J, Myler LR, Ferreira MT, Rodrigue A, Coulombe Y, Ethier C, Gagné JP, Langelier MF, Pascal JM, Finkelstein IJ, Hendzel MJ, Poirier GG, Masson JY. Poly(ADP-ribose) polymerase-1 antagonizes DNA resection at double-strand breaks. Nat Commun. 2019 Jul 4;10(1):2954. doi: 10.1038/s41467-019-10741-9. PMID: 31273204; PMCID: PMC6609622.

Celeste A, Fernandez-Capetillo O, Kruhlak MJ, Pilch DR, Staudt DW, Lee A, Bonner RF, Bonner WM, Nussenzweig A. Histone H2AX phosphorylation is dispensable for the initial recognition of DNA breaks. Nat Cell Biol. 2003 Jul;5(7):675-9. doi: 10.1038/ncb1004. PMID: 12792649.

Chen Y, Zhang H, Xu Z, Tang H, Geng A, Cai B, Su T, Shi J, Jiang C, Tian X, Seluanov A, Huang J, Wan X, Jiang Y, Gorbunova V, Mao Z. A PARP1-BRG1-SIRT1 axis promotes HR repair by reducing nucleosome density at DNA damage sites. Nucleic Acids Res. 2019 Sep 19;47(16):8563-8580. doi: 10.1093/nar/gkz592. PMID: 31291457; PMCID: PMC7145522.

Claybon A, Karia B, Bruce C, Bishop AJ. PARP1 suppresses homologous recombination events in mice in vivo. Nucleic Acids Res. 2010 Nov;38(21):7538-45. doi: 10.1093/nar/gkq624. Epub 2010 Jul 21. PMID: 20660013; PMCID: PMC2995050.

Cellini A, Yuan Wahlgren W, Henry L, Pandey S, Ghosh S, Castillon L, Claesson E, Takala H, Kübel J, Nimmrich A, Kuznetsova V, Nango E, Iwata S, Owada S, Stojković EA, Schmidt M, Ihalainen JA, Westenhoff S. The three-dimensional structure of Drosophila melanogaster (6-4) photolyase at room temperature. Acta Crystallogr D Struct Biol. 2021 Aug 1;77(Pt 8):1001-1009. doi: 10.1107/S2059798321005830. Epub 2021 Jul 29. PMID: 34342273; PMCID: PMC8329860.

Chan DW, Chen BP, Prithivirajsingh S, Kurimasa A, Story MD, Qin J, Chen DJ. Autophosphorylation of the DNA-dependent protein kinase catalytic subunit is required for rejoining of DNA double-strand breaks. Genes Dev. 2002 Sep 15;16(18):2333-8. doi: 10.1101/gad.1015202. PMID: 12231622; PMCID: PMC187438.

Chiou YY, Yang Y, Rashid N, Ye R, Selby CP, Sancar A. Mammalian Period represses and de-represses transcription by displacing CLOCK-BMAL1 from promoters in a Cryptochrome-dependent manner. Proc Natl Acad Sci U S A. 2016 Oct 11;113(41):E6072-E6079. doi: 10.1073/pnas.1612917113. Epub 2016 Sep 29. PMID: 27688755; PMCID: PMC5068302.

Chou DM, Adamson B, Dephoure NE, Tan X, Nottke AC, Hurov KE, Gygi SP, Colaiácovo MP, Elledge SJ. A chromatin localization screen reveals poly (ADP ribose)-regulated recruitment of the repressive polycomb and NuRD complexes to sites of DNA damage. Proc Natl Acad Sci U S A. 2010 Oct 26;107(43):18475-80. doi: 10.1073/pnas.1012946107. Epub 2010 Oct 11. PMID: 20937877; PMCID: PMC2972950.

Czarna A, Berndt A, Singh HR, Grudziecki A, Ladurner AG, Timinszky G, Kramer A, Wolf E. Structures of Drosophila cryptochrome and mouse cryptochrome1 provide insight into circadian function. Cell. 2013 Jun 6;153(6):1394-405. doi: 10.1016/j.cell.2013.05.011. PMID: 23746849.

Daley JM, Sung P. 53BP1, BRCA1, and the choice between recombination and end joining at DNA double-strand breaks. Mol Cell Biol. 2014 Apr;34(8):1380-8. doi: 10.1128/MCB.01639-13. Epub 2014 Jan 27. PMID: 24469398; PMCID: PMC3993578.

D'Amours D, Desnoyers S, D'Silva I, Poirier GG. Poly(ADP-ribosyl)ation reactions in the regulation of nuclear functions. Biochem J. 1999 Sep 1;342 (Pt 2)(Pt 2):249-68. PMID: 10455009; PMCID: PMC1220459.

Dawicki-McKenna JM, Langelier MF, DeNizio JE, Riccio AA, Cao CD, Karch KR, McCauley M, Steffen JD, Black BE, Pascal JM. PARP-1 Activation Requires Local Unfolding of an Autoinhibitory Domain. Mol Cell. 2015 Dec 3;60(5):755-768. doi: 10.1016/j.molcel.2015.10.013. Epub 2015 Nov 25. PMID: 26626480; PMCID: PMC4712911.

Daya-Grosjean, L. (2008). Xeroderma Pigmentosum and Skin Cancer. In: Ahmad, S.I., Hanaoka, F. (eds) Molecular Mechanisms of Xeroderma Pigmentosum. Advances in Experimental Medicine and Biology, vol 637. Springer, New York, NY. https://doi.org/10.1007/978-0-387-09599-8_3

de Lima-Bessa KM, Armelini MG, Chiganças V, Jacysyn JF, Amarante-Mendes GP, Sarasin A, Menck CF. CPDs and 6-4PPs play different roles in UV-induced cell death in normal and NER-deficient human cells. DNA Repair (Amst). 2008 Feb 1;7(2):303-12. doi: 10.1016/j.dnarep.2007.11.003. Epub 2007 Dec 21. PMID: 18096446.

Engelen E, Janssens RC, Yagita K, Smits VA, van der Horst GT, Tamanini F. Mammalian TIMELESS is involved in period determination and DNA damage-dependent phase advancing of the circadian clock. PLoS One. 2013;8(2):e56623. doi: 10.1371/journal.pone.0056623. Epub 2013 Feb 13. PMID: 23418588; PMCID: PMC3572085.

Escribano-Díaz C, Orthwein A, Fradet-Turcotte A, Xing M, Young JT, Tkáč J, Cook MA, Rosebrock AP, Munro M, Canny MD, Xu D, Durocher D. A cell cycle-dependent regulatory circuit composed of 53BP1-RIF1 and BRCA1-CtIP controls DNA repair pathway choice. Mol Cell. 2013 Mar 7;49(5):872-83. doi: 10.1016/j.molcel.2013.01.001. Epub 2013 Jan 17. PMID: 23333306.

Eustermann S, Wu WF, Langelier MF, Yang JC, Easton LE, Riccio AA, Pascal JM, Neuhaus D. Structural Basis of Detection and Signaling of DNA Single-Strand Breaks by Human PARP-1. Mol Cell. 2015 Dec 3;60(5):742-754. doi: 10.1016/j.molcel.2015.10.032. Epub 2015 Nov 25. PMID: 26626479; PMCID: PMC4678113.

Fei J, Kaczmarek N, Luch A, Glas A, Carell T, Naegeli H. Regulation of nucleotide excision repair by UV-DDB: prioritization of damage recognition to internucleosomal DNA. PLoS Biol. 2011 Oct;9(10):e1001183. doi: 10.1371/journal.pbio.1001183. Epub 2011 Oct 25. PMID: 22039351; PMCID: PMC3201922.

Frit P, Barboule N, Yuan Y, Gomez D, Calsou P. Alternative end-joining pathway(s): bricolage at DNA breaks. DNA Repair (Amst). 2014 May;17:81-97. doi: 10.1016/j.dnarep.2014.02.007. Epub 2014 Mar 6. PMID: 24613763.

Gabriel CH, Del Olmo M, Zehtabian A, Jäger M, Reischl S, van Dijk H, Ulbricht C, Rakhymzhan A, Korte T, Koller B, Grudziecki A, Maier B, Herrmann A, Niesner R, Zemojtel T, Ewers H, Granada AE, Herzel H, Kramer A. Live-cell imaging of circadian clock protein dynamics in CRISPR-generated knock-in cells. Nat Commun. 2021 Jun 18;12(1):3796. doi: 10.1038/s41467-021-24086-9. PMID: 34145278; PMCID: PMC8213786.

Glas AF, Schneider S, Maul MJ, Hennecke U, Carell T. Crystal structure of the T(6-4)C lesion in complex with a (6-4) DNA photolyase and repair of UV-induced (6-4) and Dewar photolesions. Chemistry. 2009 Oct 12;15(40):10387-96. doi: 10.1002/chem.200901004. PMID: 19722240.

Guzmán C, Bagga M, Kaur A, Westermarck J, Abankwa D. ColonyArea: an ImageJ plugin to automatically quantify colony formation in clonogenic assays. PLoS One. 2014 Mar 19;9(3):e92444. doi: 10.1371/journal.pone.0092444. PMID: 24647355; PMCID: PMC3960247.

Haince JF, McDonald D, Rodrigue A, Déry U, Masson JY, Hendzel MJ, Poirier GG. PARP1-dependent kinetics of recruitment of MRE11 and NBS1 proteins to multiple DNA damage sites. J Biol Chem. 2008 Jan 11;283(2):1197-208. doi: 10.1074/jbc.M706734200. Epub 2007 Nov 19. PMID: 18025084.

Hanasoge S, Ljungman M. H2AX phosphorylation after UV irradiation is triggered by DNA repair intermediates and is mediated by the ATR kinase. Carcinogenesis. 2007 Nov;28(11):2298-304. doi: 10.1093/carcin/bgm157. Epub 2007 Jul 5. PMID: 17615256.

Her J, Bunting SF. How cells ensure correct repair of DNA double-strand breaks. J Biol Chem. 2018 Jul 6;293(27):10502-10511. doi: 10.1074/jbc.TM118.000371. Epub 2018 Feb 5. PMID: 29414795; PMCID: PMC6036189.

Hirano A, Nakagawa T, Yoshitane H, Oyama M, Kozuka-Hata H, Lanjakornsiripan D, Fukada Y. USP7 and TDP-43: Pleiotropic Regulation of Cryptochrome Protein Stability Paces the Oscillation of the Mammalian Circadian Clock. PLoS One. 2016 Apr 28;11(4):e0154263. doi: 10.1371/journal.pone.0154263. PMID: 27123980; PMCID: PMC4849774.

Hirota T, Lee JW, St John PC, Sawa M, Iwaisako K, Noguchi T, Pongsawakul PY, Sonntag T, Welsh DK, Brenner DA, Doyle FJ 3rd, Schultz PG, Kay SA. Identification of small molecule activators of cryptochrome. Science. 2012 Aug 31;337(6098):1094-7. doi: 10.1126/science.1223710. Epub 2012 Jul 12. PMID: 22798407; PMCID: PMC3589997.

Holton NW, Andrews JF, Gassman NR. Application of Laser Micro-irradiation for Examination of Single and Double Strand Break Repair in Mammalian Cells. J Vis Exp. 2017 Sep 5;(127):56265. doi: 10.3791/56265. PMID: 28930988; PMCID: PMC5752190.

Howard SM, Yanez DA, Stark JM. DNA damage response factors from diverse pathways, including DNA crosslink repair, mediate alternative end joining. PLoS Genet. 2015 Jan 28;11(1):e1004943. doi: 10.1371/journal.pgen.1004943. PMID: 25629353; PMCID: PMC4309583.

Hsu DS, Zhao X, Zhao S, Kazantsev A, Wang RP, Todo T, Wei YF, Sancar A. Putative human blue-light photoreceptors hCRY1 and hCRY2 are flavoproteins. Biochemistry. 1996 Nov 5;35(44):13871-7. doi: 10.1021/bi962209o. PMID: 8909283.

Huang R, Zhou PK. DNA damage repair: historical perspectives, mechanistic pathways and clinical translation for targeted cancer therapy. Signal Transduct Target Ther. 2021 Jul 9;6(1):254. doi: 10.1038/s41392-021-00648-7. PMID: 34238917; PMCID: PMC8266832.

Hung KF, Sidorova JM, Nghiem P, Kawasumi M. The 6-4 photoproduct is the trigger of UV-induced replication blockage and ATR activation. Proc Natl Acad Sci U S A. 2020 Jun 9;117(23):12806-12816. doi: 10.1073/pnas.1917196117. Epub 2020 May 22. PMID: 32444488; PMCID: PMC7293618.

Isabelle M, Moreel X, Gagné JP, Rouleau M, Ethier C, Gagné P, Hendzel MJ, Poirier GG. Investigation of PARP-1, PARP-2, and PARG interactomes by affinity-purification mass spectrometry. Proteome Sci. 2010 Apr 13;8:22. doi: 10.1186/1477-5956-8-22. PMID: 20388209; PMCID: PMC2861645.

Izhar L, Adamson B, Ciccia A, Lewis J, Pontano-Vaites L, Leng Y, Liang AC, Westbrook TF, Harper JW, Elledge SJ. A Systematic Analysis of Factors Localized to Damaged Chromatin Reveals PARP-Dependent Recruitment of Transcription Factors. Cell Rep. 2015 Jun 9;11(9):1486-500. doi: 10.1016/j.celrep.2015.04.053. Epub 2015 May 21. PMID: 26004182; PMCID: PMC4464939.

Kang TH, Reardon JT, Kemp M, Sancar A. Circadian oscillation of nucleotide excision repair in mammalian brain. Proc Natl Acad Sci U S A. 2009 Feb 24;106(8):2864-7. doi: 10.1073/pnas.0812638106. Epub 2009 Jan 21. PMID: 19164551; PMCID: PMC2629438.

Kang TH, Lindsey-Boltz LA, Reardon JT, Sancar A. Circadian control of XPA and excision repair of cisplatin-DNA damage by cryptochrome and HERC2 ubiquitin ligase. Proc Natl Acad Sci U S A. 2010 Mar 16;107(11):4890-5. doi: 10.1073/pnas.0915085107. PMID: 20304803; PMCID: PMC2841896.Langelier MF, Pascal JM. PARP-1 mechanism for coupling DNA damage detection to poly(ADP-ribose) synthesis. Curr Opin Struct Biol. 2013 Feb;23(1):134-43. doi: 10.1016/j.sbi.2013.01.003. Epub 2013 Jan 16. PMID: 23333033; PMCID: PMC3572337.

Kang TH, Leem SH. Modulation of ATR-mediated DNA damage checkpoint response by cryptochrome 1. Nucleic Acids Res. 2014 Apr;42(7):4427-34. doi: 10.1093/nar/gku094. Epub 2014 Jan 30. PMID: 24489120; PMCID: PMC3985666.

Kim JK, Patel D, Choi BS. Contrasting structural impacts induced by cis-syn cyclobutane dimer and (6-4) adduct in DNA duplex decamers: implication in mutagenesis and repair activity. Photochem Photobiol. 1995 Jul;62(1):44-50. doi: 10.1111/j.1751-1097.1995.tb05236.x. PMID: 7638271.

Kitao H, Yuan ZM. Regulation of ionizing radiation-induced Rad52 nuclear foci formation by c-Abl-mediated phosphorylation. J Biol Chem. 2002 Dec 13;277(50):48944-8. doi: 10.1074/jbc.M208151200. Epub 2002 Oct 11. PMID: 12379650.

Kobayashi K, Kanno S, Smit B, van der Horst GT, Takao M, Yasui A. Characterization of photolyase/blue-light receptor homologs in mouse and human cells. Nucleic Acids Res. 1998 Nov 15;26(22):5086-92. doi: 10.1093/nar/26.22.5086. PMID: 9801304; PMCID: PMC147960.

Koike N, Yoo SH, Huang HC, Kumar V, Lee C, Kim TK, Takahashi JS. Transcriptional architecture and chromatin landscape of the core circadian clock in mammals. Science. 2012 Oct 19;338(6105):349-54. doi: 10.1126/science.1226339. Epub 2012 Aug 30. PMID: 22936566; PMCID: PMC3694775.

Kraus WL. PARPs and ADP-Ribosylation: 50 Years … and Counting. Mol Cell. 2015 Jun 18;58(6):902-10. doi: 10.1016/j.molcel.2015.06.006. PMID: 26091339; PMCID: PMC4477203.

Kong X, Mohanty SK, Stephens J, Heale JT, Gomez-Godinez V, Shi LZ, Kim JS, Yokomori K, Berns MW. Comparative analysis of different laser systems to study cellular responses to DNA damage in mammalian cells. Nucleic Acids Res. 2009 May;37(9):e68. doi: 10.1093/nar/gkp221. Epub 2009 Apr 7. PMID: 19357094; PMCID: PMC2685111.

Lavin MF. Ataxia-telangiectasia: from a rare disorder to a paradigm for cell signalling and cancer. Nat Rev Mol Cell Biol. 2008 Oct;9(10):759-69. doi: 10.1038/nrm2514. Erratum in: Nat Rev Mol Cell Biol. 2008 Dec;9(12). doi: 10.1038/nrm2514. PMID: 18813293.

Lee JH, Paull TT. ATM activation by DNA double-strand breaks through the Mre11-Rad50-Nbs1 complex. Science. 2005 Apr 22;308(5721):551-4. doi: 10.1126/science.1108297. Epub 2005 Mar 24. Erratum in: Science. 2005 Jun 24;308(5730):1870. PMID: 15790808.

Lee JH, Sancar A. Circadian clock disruption improves the efficacy of chemotherapy through p73-mediated apoptosis. Proc Natl Acad Sci U S A. 2011 Jun 28;108(26):10668-72. doi: 10.1073/pnas.1106284108. Epub 2011 May 31. PMID: 21628572; PMCID: PMC3127903.

Lee JH, Gaddameedhi S, Ozturk N, Ye R, Sancar A. DNA damage-specific control of cell death by cryptochrome in p53-mutant ras-transformed cells. Cancer Res. 2013 Jan 15;73(2):785-91. doi: 10.1158/0008-5472.CAN-12-1994. Epub 2012 Nov 13. PMID: 23149912; PMCID: PMC3548992.

Leman AR, Noguchi C, Lee CY, Noguchi E. Human Timeless and Tipin stabilize replication forks and facilitate sister-chromatid cohesion. J Cell Sci. 2010 Mar 1;123(Pt 5):660-70. doi: 10.1242/jcs.057984. Epub 2010 Feb 2. PMID: 20124417; PMCID: PMC2823575.

Lo HL, Nakajima S, Ma L, Walter B, Yasui A, Ethell DW, Owen LB. Differential biologic effects of CPD and 6-4PP UV-induced DNA damage on the induction of apoptosis and cell-cycle arrest. BMC Cancer. 2005 Oct 19;5:135. doi: 10.1186/1471-2407-5-135. PMID: 16236176; PMCID: PMC1276790.

Lord CJ, Ashworth A. The DNA damage response and cancer therapy. Nature. 2012 Jan 18;481(7381):287-94. doi: 10.1038/nature10760. PMID: 22258607.

Lord CJ, Tutt AN, Ashworth A. Synthetic lethality and cancer therapy: lessons learned from the development of PARP inhibitors. Annu Rev Med. 2015;66:455-70. doi: 10.1146/annurev-med-050913-022545. Epub 2014 Oct 17. PMID: 25341009.

Luijsterburg MS, de Krijger I, Wiegant WW, Shah RG, Smeenk G, de Groot AJL, Pines A, Vertegaal ACO, Jacobs JJL, Shah GM, van Attikum H. PARP1 Links CHD2-Mediated Chromatin Expansion and H3.3 Deposition to DNA Repair by Non-homologous End-Joining. Mol Cell. 2016 Feb 18;61(4):547-562. doi: 10.1016/j.molcel.2016.01.019. PMID: 26895424; PMCID: PMC4769320.

Mah LJ, El-Osta A, Karagiannis TC. gammaH2AX: a sensitive molecular marker of DNA damage and repair. Leukemia. 2010 Apr;24(4):679-86. doi: 10.1038/leu.2010.6. Epub 2010 Feb 4. PMID: 20130602.

Mansour WY, Rhein T, Dahm-Daphi J. The alternative end-joining pathway for repair of DNA double-strand breaks requires PARP1 but is not dependent upon microhomologies. Nucleic Acids Res. 2010 Oct;38(18):6065-77. doi: 10.1093/nar/gkq387. Epub 2010 May 18. PMID: 20483915; PMCID: PMC2952854.

Mao Z, Bozzella M, Seluanov A, Gorbunova V. DNA repair by nonhomologous end joining and homologous recombination during cell cycle in human cells. Cell Cycle. 2008 Sep 15;7(18):2902-6. doi: 10.4161/cc.7.18.6679. PMID: 18769152; PMCID: PMC2754209.

Marti TM, Hefner E, Feeney L, Natale V, Cleaver JE. H2AX phosphorylation within the G1 phase after UV irradiation depends on nucleotide excision repair and not DNA double-strand breaks. Proc Natl Acad Sci U S A. 2006 Jun 27;103(26):9891-6. doi: 10.1073/pnas.0603779103. Epub 2006 Jun 20. PMID: 16788066; PMCID: PMC1502549.

Martin-Hernandez K, Rodriguez-Vargas JM, Schreiber V, Dantzer F. Expanding functions of ADP-ribosylation in the maintenance of genome integrity. Semin Cell Dev Biol. 2017 Mar;63:92-101. doi: 10.1016/j.semcdb.2016.09.009. Epub 2016 Sep 23. PMID: 27670719.

Matta E, Kiribayeva A, Khassenov B, Matkarimov BT, Ishchenko AA. Insight into DNA substrate specificity of PARP1-catalysed DNA poly(ADP-ribosyl)ation. Sci Rep. 2020 Feb 28;10(1):3699. doi: 10.1038/s41598-020-60631-0. PMID: 32111879; PMCID: PMC7048826.

Maul MJ, Barends TR, Glas AF, Cryle MJ, Domratcheva T, Schneider S, Schlichting I, Carell T. Crystal structure and mechanism of a DNA (6-4) photolyase. Angew Chem Int Ed Engl. 2008;47(52):10076-80. doi: 10.1002/anie.200804268. PMID: 18956392.

Mees A, Klar T, Gnau P, Hennecke U, Eker AP, Carell T, Essen LO. Crystal structure of a photolyase bound to a CPD-like DNA lesion after in situ repair. Science. 2004 Dec 3;306(5702):1789-93. doi: 10.1126/science.1101598. PMID: 15576622.

Miller S, Son YL, Aikawa Y, Makino E, Nagai Y, Srivastava A, Oshima T, Sugiyama A, Hara A, Abe K, Hirata K, Oishi S, Hagihara S, Sato A, Tama F, Itami K, Kay SA, Hatori M, Hirota T. Isoform-selective regulation of mammalian cryptochromes. Nat Chem Biol. 2020 Jun;16(6):676-685. doi: 10.1038/s41589-020-0505-1. Epub 2020 Mar 30. PMID: 32231341.

Miller S, Srivastava A, Nagai Y, Aikawa Y, Tama F, Hirota T. Structural differences in the FAD-binding pockets and lid loops of mammalian CRY1 and CRY2 for isoform-selective regulation. Proc Natl Acad Sci U S A. 2021 Jun 29;118(26):e2026191118. doi: 10.1073/pnas.2026191118. PMID: 34172584; PMCID: PMC8255803.

Montoni A, Robu M, Pouliot E, Shah GM. Resistance to PARP-Inhibitors in Cancer Therapy. Front Pharmacol. 2013 Feb 27;4:18. doi: 10.3389/fphar.2013.00018. PMID: 23450678; PMCID: PMC3583007.

Muller PA, Vousden KH. p53 mutations in cancer. Nat Cell Biol. 2013 Jan;15(1):2-8. doi: 10.1038/ncb2641. PMID: 23263379.

Müller M, Carell T. Structural biology of DNA photolyases and cryptochromes. Curr Opin Struct Biol. 2009 Jun;19(3):277-85. doi: 10.1016/j.sbi.2009.05.003. Epub 2009 May 30. PMID: 19487120.

Murai J, Huang SY, Das BB, Renaud A, Zhang Y, Doroshow JH, Ji J, Takeda S, Pommier Y. Trapping of PARP1 and PARP2 by Clinical PARP Inhibitors. Cancer Res. 2012 Nov 1;72(21):5588-99. doi: 10.1158/0008-5472.CAN-12-2753. PMID: 23118055; PMCID: PMC3528345.

Mure LS, Le HD, Benegiamo G, Chang MW, Rios L, Jillani N, Ngotho M, Kariuki T, Dkhissi-Benyahya O, Cooper HM, Panda S. Diurnal transcriptome atlas of a primate across major neural and peripheral tissues. Science. 2018 Mar 16;359(6381):eaao0318. doi: 10.1126/science.aao0318. Epub 2018 Feb 8. PMID: 29439024; PMCID: PMC5924732.

Muster B, Rapp A, Cardoso MC. Systematic analysis of DNA damage induction and DNA repair pathway activation by continuous wave visible light laser micro-irradiation. AIMS Genet. 2017 Feb 21;4(1):47-68. doi: 10.3934/genet.2017.1.47. PMID: 31435503; PMCID: PMC6690239.

Nakajima S, Lan L, Kanno S, Takao M, Yamamoto K, Eker AP, Yasui A. UV light-induced DNA damage and tolerance for the survival of nucleotide excision repair-deficient human cells. J Biol Chem. 2004 Nov 5;279(45):46674-7. doi: 10.1074/jbc.M406070200. Epub 2004 Sep 1. PMID: 15342631.

Oh KS, Bustin M, Mazur SJ, Appella E, Kraemer KH. UV-induced histone H2AX phosphorylation and DNA damage related proteins accumulate and persist in nucleotide excision repair-deficient XP-B cells. DNA Repair (Amst). 2011 Jan 2;10(1):5-15. doi: 10.1016/j.dnarep.2010.09.004. Epub 2010 Oct 13. PMID: 20947453; PMCID: PMC3010519.

Ozgur S, Sancar A. Purification and properties of human blue-light photoreceptor cryptochrome 2. Biochemistry. 2003 Mar 18;42(10):2926-32. doi: 10.1021/bi026963n. PMID: 12627958.

Ozturk N, Lee JH, Gaddameedhi S, Sancar A. Loss of cryptochrome reduces cancer risk in p53 mutant mice. Proc Natl Acad Sci U S A. 2009 Feb 24;106(8):2841-6. doi: 10.1073/pnas.0813028106. Epub 2009 Feb 2. PMID: 19188586; PMCID: PMC2634797.

Papp SJ, Huber AL, Jordan SD, Kriebs A, Nguyen M, Moresco JJ, Yates JR, Lamia KA. DNA damage shifts circadian clock time via Hausp-dependent Cry1 stabilization. Elife. 2015 Mar 10;4:e04883. doi: 10.7554/eLife.04883. PMID: 25756610; PMCID: PMC4352707.

Park JM, Kang TH. Transcriptional and Posttranslational Regulation of Nucleotide Excision Repair: The Guardian of the Genome against Ultraviolet Radiation. Int J Mol Sci. 2016 Nov 4;17(11):1840. doi: 10.3390/ijms17111840. PMID: 27827925; PMCID: PMC5133840.

Patel AG, Sarkaria JN, Kaufmann SH. Nonhomologous end joining drives poly(ADP-ribose) polymerase (PARP) inhibitor lethality in homologous recombination-deficient cells. Proc Natl

Acad Sci U S A. 2011 Feb 22;108(8):3406-11. doi: 10.1073/pnas.1013715108. Epub 2011 Feb 7. PMID: 21300883; PMCID: PMC3044391.

Paull TT, Rogakou EP, Yamazaki V, Kirchgessner CU, Gellert M, Bonner WM. A critical role for histone H2AX in recruitment of repair factors to nuclear foci after DNA damage. Curr Biol. 2000 Jul 27-Aug 10;10(15):886-95. doi: 10.1016/s0960-9822(00)00610-2. PMID: 10959836.

Perdiz D, Grof P, Mezzina M, Nikaido O, Moustacchi E, Sage E. Distribution and repair of bipyrimidine photoproducts in solar UV-irradiated mammalian cells. Possible role of Dewar photoproducts in solar mutagenesis. J Biol Chem. 2000 Sep 1;275(35):26732-42. doi: 10.1074/jbc.M001450200. PMID: 10827179.

Pines A, Vrouwe MG, Marteijn JA, Typas D, Luijsterburg MS, Cansoy M, Hensbergen P, Deelder A, de Groot A, Matsumoto S, Sugasawa K, Thoma N, Vermeulen W, Vrieling H, Mullenders L. PARP1 promotes nucleotide excision repair through DDB2 stabilization and recruitment of ALC1. J Cell Biol. 2012 Oct 15;199(2):235-49. doi: 10.1083/jcb.201112132. Epub 2012 Oct 8. PMID: 23045548; PMCID: PMC3471223.

Pittendrigh CS. Temporal organization: reflections of a Darwinian clock-watcher. Annu Rev Physiol. 1993;55:16-54. doi: 10.1146/annurev.ph.55.030193.000313. PMID: 8466172.

Pleschke JM, Kleczkowska HE, Strohm M, Althaus FR. Poly(ADP-ribose) binds to specific domains in DNA damage checkpoint proteins. J Biol Chem. 2000 Dec 29;275(52):40974-80. doi: 10.1074/jbc.M006520200. PMID: 11016934.

Polo SE, Kaidi A, Baskcomb L, Galanty Y, Jackson SP. Regulation of DNA-damage responses and cell-cycle progression by the chromatin remodelling factor CHD4. EMBO J. 2010 Sep 15;29(18):3130-9. doi: 10.1038/emboj.2010.188. Epub 2010 Aug 6. PMID: 20693977; PMCID: PMC2944064.

Ray Chaudhuri A, Nussenzweig A. The multifaceted roles of PARP1 in DNA repair and chromatin remodelling. Nat Rev Mol Cell Biol. 2017 Oct;18(10):610-621. doi: 10.1038/nrm.2017.53. Epub 2017 Jul 5. PMID: 28676700; PMCID: PMC6591728.

Reynolds P, Cooper S, Lomax M, O'Neill P. Disruption of PARP1 function inhibits base excision repair of a sub-set of DNA lesions. Nucleic Acids Res. 2015 Apr 30;43(8):4028-38. doi: 10.1093/nar/gkv250. Epub 2015 Mar 26. PMID: 25813046; PMCID: PMC4417162.

Robu M, Shah RG, Petitclerc N, Brind'Amour J, Kandan-Kulangara F, Shah GM. Role of poly(ADP-ribose) polymerase-1 in the removal of UV-induced DNA lesions by nucleotide excision repair. Proc Natl Acad Sci U S A. 2013 Jan 29;110(5):1658-63. doi: 10.1073/pnas.1209507110. Epub 2013 Jan 14. PMID: 23319653; PMCID: PMC3562836.

Robu M, Shah RG, Purohit NK, Zhou P, Naegeli H, Shah GM. Poly(ADP-ribose) polymerase 1 escorts XPC to UV-induced DNA lesions during nucleotide excision repair. Proc Natl Acad Sci U S A. 2017 Aug 15;114(33):E6847-E6856. doi: 10.1073/pnas.1706981114. Epub 2017 Jul 31. PMID: 28760956; PMCID: PMC5565455.

Ronson GE, Piberger AL, Higgs MR, Olsen AL, Stewart GS, McHugh PJ, Petermann E, Lakin ND. PARP1 and PARP2 stabilise replication forks at base excision repair intermediates through Fbh1-dependent Rad51 regulation. Nat Commun. 2018 Feb 21;9(1):746. doi: 10.1038/s41467-018-03159-2. PMID: 29467415; PMCID: PMC5821833.

Sancar A, Van Gelder RN. Clocks, cancer, and chronochemotherapy. Science. 2021 Jan 1;371(6524):eabb0738. doi: 10.1126/science.abb0738. PMID: 33384351.

Scully R, Panday A, Elango R, Willis NA. DNA double-strand break repair-pathway choice in somatic mammalian cells. Nat Rev Mol Cell Biol. 2019 Nov;20(11):698-714. doi: 10.1038/s41580-019-0152-0. Epub 2019 Jul 1. PMID: 31263220; PMCID: PMC7315405.

Sellou H, Lebeaupin T, Chapuis C, Smith R, Hegele A, Singh HR, Kozlowski M, Bultmann S, Ladurner AG, Timinszky G, Huet S. The poly(ADP-ribose)-dependent chromatin remodeler Alc1 induces local chromatin relaxation upon DNA damage. Mol Biol Cell. 2016 Dec 1;27(24):3791-3799. doi: 10.1091/mbc.E16-05-0269. Epub 2016 Oct 12. PMID: 27733626; PMCID: PMC5170603.

Schiewer MJ, Brunner M, Feng FY, Zwart W, Knudsen KE. The circadian cryptochrome, CRY1, is a pro-tumorigenic factor that rhythmically modulates DNA repair. Nat Commun. 2021 Jan 15;12(1):401. doi: 10.1038/s41467-020-20513-5. PMID: 33452241; PMCID: PMC7810852.

Schultz N, Lopez E, Saleh-Gohari N, Helleday T. Poly(ADP-ribose) polymerase (PARP-1) has a controlling role in homologous recombination. Nucleic Acids Res. 2003 Sep 1;31(17):4959-64. doi: 10.1093/nar/gkg703. PMID: 12930944; PMCID: PMC212803.

Schwertman P, Vermeulen W, Marteijn JA. UVSSA and USP7, a new couple in transcription-coupled DNA repair. Chromosoma. 2013 Aug;122(4):275-84. doi: 10.1007/s00412-013-0420-2. Epub 2013 Jun 13. PMID: 23760561; PMCID: PMC3714559.

Schwertman P, Lagarou A, Dekkers DH, Raams A, van der Hoek AC, Laffeber C, Hoeijmakers JH, Demmers JA, Fousteri M, Vermeulen W, Marteijn JA. UV-sensitive syndrome protein UVSSA recruits USP7 to regulate transcription-coupled repair. Nat Genet. 2012 May;44(5):598-602. doi: 10.1038/ng.2230. PMID: 22466611.

Shafi AA, McNair CM, McCann JJ, Alshalalfa M, Shostak A, Severson TM, Zhu Y, Bergman A, Gordon N, Mandigo AC, Chand SN, Gallagher P, Dylgjeri E, Laufer TS, Vasilevskaya IA,

Silva AP, Ryan DP, Galanty Y, Low JK, Vandevenne M, Jackson SP, Mackay JP. The N-terminal Region of Chromodomain Helicase DNA-binding Protein 4 (CHD4) Is Essential for Activity and Contains a High Mobility Group (HMG) Box-like-domain That Can Bind Poly(ADP-ribose). J Biol Chem. 2016 Jan 8;291(2):924-38. doi: 10.1074/jbc.M115.683227. Epub 2015 Nov 12. PMID: 26565020; PMCID: PMC4705410.

Smeenk G, Wiegant WW, Vrolijk H, Solari AP, Pastink A, van Attikum H. The NuRD chromatin-remodeling complex regulates signaling and repair of DNA damage. J Cell Biol. 2010 Sep 6;190(5):741-9. doi: 10.1083/jcb.201001048. Epub 2010 Aug 30. PMID: 20805320; PMCID: PMC2935570.

Smith R, Sellou H, Chapuis C, Huet S, Timinszky G. CHD3 and CHD4 recruitment and chromatin remodeling activity at DNA breaks is promoted by early poly(ADP-ribose)-dependent chromatin relaxation. Nucleic Acids Res. 2018 Jul 6;46(12):6087-6098. doi: 10.1093/nar/gky334. PMID: 29733391; PMCID: PMC6158744.

Stark JM, Pierce AJ, Oh J, Pastink A, Jasin M. Genetic steps of mammalian homologous repair with distinct mutagenic consequences. Mol Cell Biol. 2004 Nov;24(21):9305-16. doi: 10.1128/MCB.24.21.9305-9316.2004. PMID: 15485900; PMCID: PMC522275.

Takahashi JS. Transcriptional architecture of the mammalian circadian clock. Nat Rev Genet. 2017 Mar;18(3):164-179. doi: 10.1038/nrg.2016.150. Epub 2016 Dec 19. PMID: 27990019; PMCID: PMC5501165.

Teloni F, Altmeyer M. Readers of poly(ADP-ribose): designed to be fit for purpose. Nucleic Acids Res. 2016 Feb 18;44(3):993-1006. doi: 10.1093/nar/gkv1383. Epub 2015 Dec 15. PMID: 26673700; PMCID: PMC4756826.

Thévenaz P, Ruttimann UE, Unser M. A pyramid approach to subpixel registration based on intensity. IEEE Trans Image Process. 1998;7(1):27-41. doi: 10.1109/83.650848. PMID: 18267377.

Thomas C, Tulin AV. Poly-ADP-ribose polymerase: machinery for nuclear processes. Mol Aspects Med. 2013 Dec;34(6):1124-37. doi: 10.1016/j.mam.2013.04.001. Epub 2013 Apr 25. PMID: 23624145; PMCID: PMC3750069.

Till S, Ladurner AG. Sensing NAD metabolites through macro domains. Front Biosci (Landmark Ed). 2009 Jan 1;14(9):3246-58. doi: 10.2741/3448. PMID: 19273270.

Todo T, Ryo H, Yamamoto K, Toh H, Inui T, Ayaki H, Nomura T, Ikenaga M. Similarity among the Drosophila (6-4)photolyase, a human photolyase homolog, and the DNA photolyase-blue-light photoreceptor family. Science. 1996 Apr 5;272(5258):109-12. doi: 10.1126/science.272.5258.109. PMID: 8600518.

Todo T, Ryo H, Borden A, Lawrence C, Sakaguchi K, Hirata H, Nomura T. Non-mutagenic repair of (6-4)photoproducts by (6-4)photolyase purified from Drosophila melanogaster. Mutat Res. 1997 Nov;385(2):83-93. doi: 10.1016/s0921-8777(97)00045-1. PMID: 9447230.

Unsal-Kaçmaz K, Chastain PD, Qu PP, Minoo P, Cordeiro-Stone M, Sancar A, Kaufmann WK. The human Tim/Tipin complex coordinates an Intra-S checkpoint response to UV that slows replication fork displacement. Mol Cell Biol. 2007 Apr;27(8):3131-42. doi: 10.1128/MCB.02190-06. Epub 2007 Feb 12. PMID: 17296725; PMCID: PMC1899931.

Wallrodt S, Buntz A, Wang Y, Zumbusch A, Marx A. Bioorthogonally Functionalized NAD(+) Analogues for In-Cell Visualization of Poly(ADP-Ribose) Formation. Angew Chem Int Ed Engl. 2016 Jun 27;55(27):7660-4. doi: 10.1002/anie.201600464. Epub 2016 Apr 15. PMID: 27080423.

Wang M, Wu W, Wu W, Rosidi B, Zhang L, Wang H, Iliakis G. PARP-1 and Ku compete for repair of DNA double strand breaks by distinct NHEJ pathways. Nucleic Acids Res. 2006;34(21):6170-82. doi: 10.1093/nar/gkl840. Epub 2006 Nov 6. PMID: 17088286; PMCID: PMC1693894.

Wang Z, Kang W, You Y, Pang J, Ren H, Suo Z, Liu H, Zheng Y. USP7: Novel Drug Target in Cancer Therapy. Front Pharmacol. 2019 Apr 30;10:427. doi: 10.3389/fphar.2019.00427. PMID: 31114498; PMCID: PMC6502913.Xiang Y, Laurent B, Hsu CH, Nachtergaele S, Lu Z, Sheng W, Xu C, Chen H, Ouyang J, Wang S, Ling D, Hsu PH, Zou L, Jambhekar A, He C, Shi Y. RNA m^6A methylation regulates the ultraviolet-induced DNA damage response. Nature. 2017 Mar 23;543(7646):573-576. doi: 10.1038/nature21671. Epub 2017 Mar 15. Erratum in: Nature. 2017 Nov 29;: PMID: 28297716; PMCID: PMC5490984.

Wei H, Yu X. Functions of PARylation in DNA Damage Repair Pathways. Genomics Proteomics Bioinformatics. 2016 Jun;14(3):131-139. doi: 10.1016/j.gpb.2016.05.001. Epub 2016 May 27. PMID: 27240471; PMCID: PMC4936651.

Xie S, Mortusewicz O, Ma HT, Herr P, Poon RY, Helleday T, Qian C. Timeless Interacts with PARP-1 to Promote Homologous Recombination Repair. Mol Cell. 2015 Oct 1;60(1):163-76. doi: 10.1016/j.molcel.2015.07.031. Epub 2015 Sep 3. Erratum in: Mol Cell. 2016 Jan 7;61(1):181. Poon, Randy R Y [Corrected to Poon, Randy Y C]. PMID: 26344098.

Xing W, Busino L, Hinds TR, Marionni ST, Saifee NH, Bush MF, Pagano M, Zheng N. SCF(FBXL3) ubiquitin ligase targets cryptochromes at their cofactor pocket. Nature. 2013 Apr 4;496(7443):64-8. doi: 10.1038/nature11964. Epub 2013 Mar 17. PMID: 23503662; PMCID: PMC3618506.

Yang J, Yu Y, Hamrick HE, Duerksen-Hughes PJ. ATM, ATR and DNA-PK: initiators of the cellular genotoxic stress responses. Carcinogenesis. 2003 Oct;24(10):1571-80. doi: 10.1093/carcin/bgg137. Epub 2003 Aug 14. PMID: 12919958.

Ye R, Selby CP, Chiou YY, Ozkan-Dagliyan I, Gaddameedhi S, Sancar A. Dual modes of CLOCK:BMAL1 inhibition mediated by Cryptochrome and Period proteins in the mammalian circadian clock. Genes Dev. 2014 Sep 15;28(18):1989-98. doi: 10.1101/gad.249417.114. PMID: 25228643; PMCID: PMC4173159.

Young AR, Chadwick CA, Harrison GI, Hawk JL, Nikaido O, Potten CS. The in situ repair kinetics of epidermal thymine dimers and 6-4 photoproducts in human skin types I and II. J Invest Dermatol. 1996 Jun;106(6):1307-13. doi: 10.1111/1523-1747.ep12349031. PMID: 8752675.

Young LM, Marzio A, Perez-Duran P, Reid DA, Meredith DN, Roberti D, Star A, Rothenberg E, Ueberheide B, Pagano M. TIMELESS Forms a Complex with PARP1 Distinct from Its Complex with TIPIN and Plays a Role in the DNA Damage Response. Cell Rep. 2015 Oct 20;13(3):451-459. doi: 10.1016/j.celrep.2015.09.017. Epub 2015 Oct 8. PMID: 26456830; PMCID: PMC4618055.Yue X, Bai C, Xie D, Ma T, Zhou PK. DNA-PKcs: A Multi-Faceted Player in DNA Damage Response. Front Genet. 2020 Dec 23;11:607428. doi: 10.3389/fgene.2020.607428. PMID: 33424929; PMCID: PMC7786053.

Zaja R, Mikoč A, Barkauskaite E, Ahel I. Molecular Insights into Poly(ADP-ribose) Recognition and Processing. Biomolecules. 2012 Dec 21;3(1):1-17. doi: 10.3390/biom3010001. PMID: 24970154; PMCID: PMC4030884.

Apendix A:

1

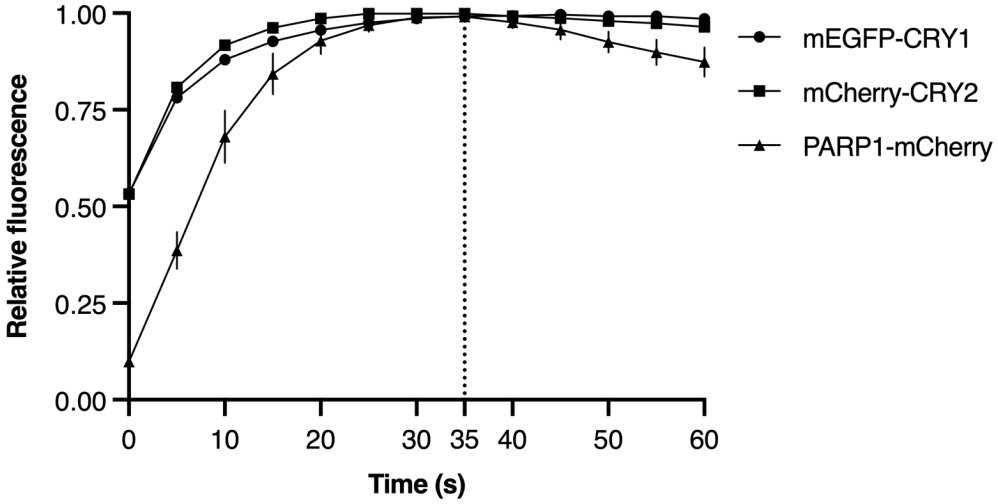

2

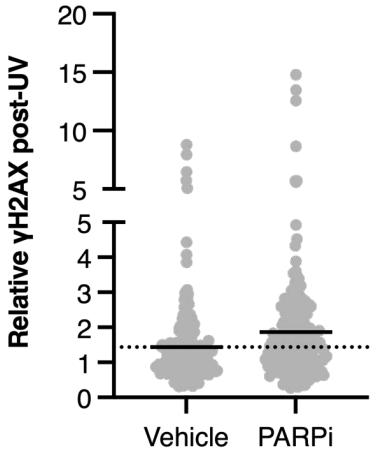

3

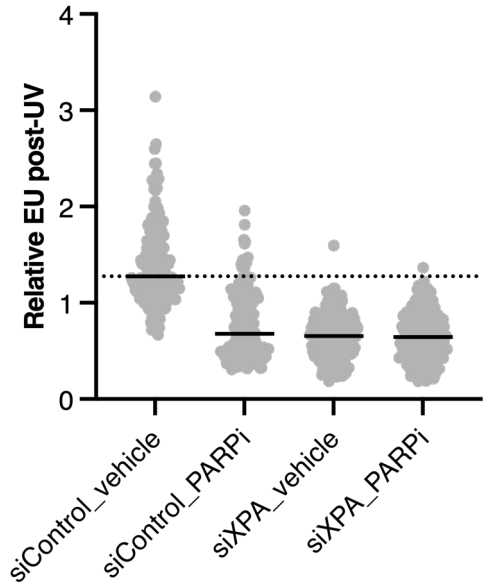

4

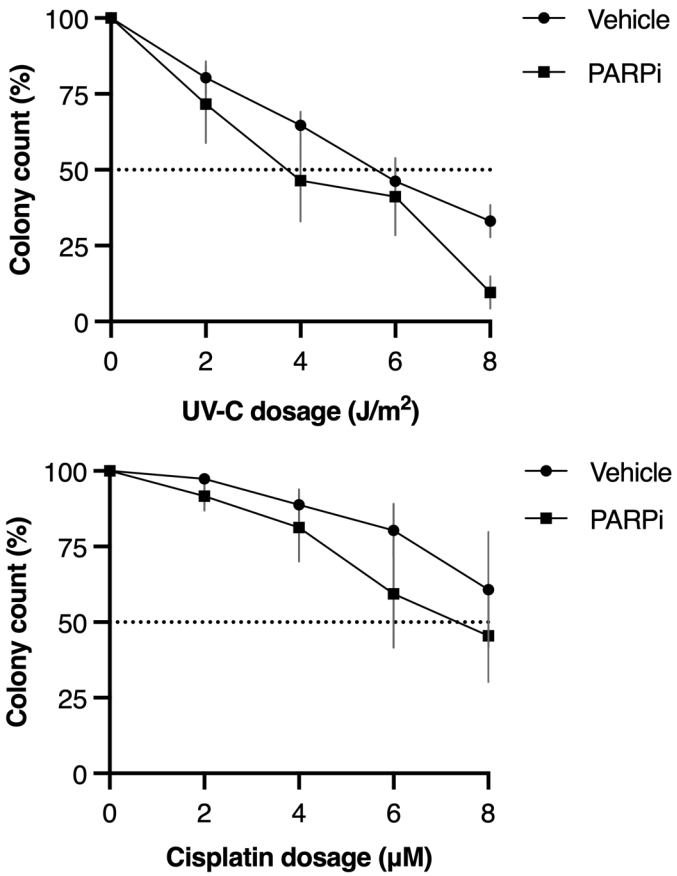
Vehicle
PARPi
Colony count (%)
100
75
50
25
0
0
2
4
6
8
UV-C dosage (J/m2)
Vehicle
PARPi
Colony count (%)
100
75
50
25
0
0
2
4
6
8
Cisplatin dosage (µM)

Acknowledgements

I thank Andreas Ladurner for providing this truly amazing opportunity, his continuous support and guidance for the past 5 years.

I thank Hans-Joerg Schaeffer, Ingrid Wolf and the IMPRS-LS team for the support and memorable moments they created for me and the IMPRS community.

I thank everyone in the ChroMe network for the exchange of science, laughter, and the bitter-sweet moments.

I thank Carla Margulies, Jane Mellor, Maria Robles, Martijn Luijsterburg and Eva Wolf for experimental advice and the Ladurner Lab for support and discussion. I thank the Biophysics, Bioimaging and Flow Cytometry Core Facilities (special thanks to Lisa Richter) of the LMU Biomedical Center for usage of their machines and training. I thank Achim Kramer for kindly providing U-2 OS CRY KO and KI cells, Nicholas Lakin for kindly providing U-2 OS PARP KO cells, Eva Wolf for sharing CRY plasmids and Stefan Zahler for sharing pCBASCE-I plasmid.

Affidavit

Affidavit

Kuo, Tia Tyrsett

Surname, first name

Street

Zip code, town, country

I hereby declare, that the submitted thesis entitled:

Cryptochromes recruit to laser-induced DNA damage sites through PARP1 activity and promote repair

is my own work. I have only used the sources indicated and have not made unauthorized use of services of a third party. Where the work of others has been quoted or reproduced, the source is always given.
I further declare that the submitted thesis or parts thereof have not been presented as part of an examination degree to any other university.

Los Angeles, 18.03.2023
place, date

Tia Tyrsett Kuo
Signature doctoral candidate

List of publications

Kuo TT, Ladurner AG. Exploiting the Circadian Clock for Improved Cancer Therapy: Perspective From a Cell Biologist. Front Genet. 2019 Dec 11;10:1210. doi: 10.3389/fgene.2019.01210. Erratum in: Front Genet. 2020 Jun 19;11:601. PMID: 31921283; PMCID: PMC6927292.

Larsen BD, Benada J, Yung PYK, Bell RAV, Pappas G, Urban V, Ahlskog JK, **Kuo TT**, Janscak P, Megeney LA, Elsässer SJ, Bartek J, Sørensen CS. Cancer cells use self-inflicted DNA breaks to evade growth limits imposed by genotoxic stress. Science. 2022 Apr 29;376(6592):476-483. doi: 10.1126/science.abi6378. Epub 2022 Apr 28. PMID: 35482866.

Blessing C, Apelt K, van den Heuvel D, Gonzalez-Leal C, Rother MB, van der Woude M, González-Prieto R, Yifrach A, Parnas A, Shah RG, **Kuo TT**, Boer DEC, Cai J, Kragten A, Kim HS, Schärer OD, Vertegaal ACO, Shah GM, Adar S, Lans H, van Attikum H, Ladurner AG, Luijsterburg MS. XPC-PARP complexes engage the chromatin remodeler ALC1 to catalyze global genome DNA damage repair. Nat Commun. 2022 Aug 13;13(1):4762. doi: 10.1038/s41467-022-31820-4. PMID: 35963869.